

January 2019

## **An Experimental Study of Fractional Wettability Effects on Gas Assisted Gravity Drainage (GAGD)**

ABDULLAH ABDULRAHMAN A. AL-TAMEEMI

*Louisiana State University and Agricultural and Mechanical College*

Follow this and additional works at: [https://digitalcommons.lsu.edu/gradschool\\_theses](https://digitalcommons.lsu.edu/gradschool_theses)



Part of the [Petroleum Engineering Commons](#)

---

### **Recommended Citation**

AL-TAMEEMI, ABDULLAH ABDULRAHMAN A., "An Experimental Study of Fractional Wettability Effects on Gas Assisted Gravity Drainage (GAGD)" (2019). *LSU Master's Theses*. 4846.  
[https://digitalcommons.lsu.edu/gradschool\\_theses/4846](https://digitalcommons.lsu.edu/gradschool_theses/4846)

This Thesis is brought to you for free and open access by the Graduate School at LSU Digital Commons. It has been accepted for inclusion in LSU Master's Theses by an authorized graduate school editor of LSU Digital Commons. For more information, please contact [gradetd@lsu.edu](mailto:gradetd@lsu.edu).

# **AN EXPERIMENTAL STUDY OF FRACTIONAL WETTABILITY EFFECTS ON GAS ASSISTED GRAVITY DRAINAGE (GAGD)**

A Thesis

Submitted to the Graduate Faculty of the  
Louisiana State University and  
Agricultural and Mechanical College  
in partial fulfillment of the  
requirements for the degree of  
Master of Science in Petroleum Engineering

In

The Craft & Hawkins Department of Petroleum Engineering

by

Abdullah Abdulrahman A. Al-Tameemi  
B.S. (Mechanical Engineering), University of Baghdad, 2012  
May 2019

*For Azhaar my mother,  
& Abdulrahman my father,  
for their endless love and motivation.*

*"If I have seen further than others, it is by standing upon the shoulders of giants."*

*Sir Isaac Newton*

## ACKNOWLEDGMENTS

At the end of this journey, I would like to thank and appreciate everyone who helped or believed in me; I do give my sincere gratitude, your support is essential to finish this work and has made me the proud person who I am today.

I emphasize my great appreciation and respect to my advisor, Dr. Dandina Rao. Working with a world scale patent holder, expert in the profession, and inspiring person like Dr. Rao was always a source of pride and motivation for me. He did help me greatly through many tough endeavors of my study, without him this work would not come to life. It would not be possible without his knowledge, wisdom, and kindness. I do really appreciate his encouragement and advice.

I want to give my thanks to my committee members: Dr. Ipsita Gupta, and Dr. Wesley C. Williams for their support and their valuable comments on my work. In addition to being in my committee, Dr. Gupta did teach me three courses through my studies and so did Dr. Williams with one course. My thanks to Iskandar Dzulkarnain for introducing me to the lab work and for enormous help and advice, his efforts and patience were boundless. Special thanks for Dayo Afekare for revision, I appreciate your enormous efforts.

I want to thank my family and friends for all the support and love I received from them. Especially my Mother and Father whom I owe my life, words cannot express my gratitude for their efforts. My sister Duha for continuous care and Dayna Rodriguez for sharing happy and tough times.

I give my thanks to Dr. Watheq Al-Mudhafar for his great help, advice, and continuous support since the start of my studies at LSU, also, the rest of the Enhanced Oil Recovery team: Dr. Bikash Saikia, Alok Shah, and Muzher Al Musabeh. And James Nielsen for proofreading and support.

And of course, my great thanks and appreciation for the Fulbright U.S. Student Program grant for helping me to pursue my dreams of studying abroad, without this generous opportunity nothing would have been possible, and my appreciation for The Craft & Hawkins Department of Petroleum Engineering for the graduate school award.

# TABLE OF CONTENTS

ACKNOWLEDGMENTS .....	iv
ABSTRACT.....	x
CHAPTER 1. INTRODUCTION .....	1
1.1. Research Background.....	1
1.2. Problem Statement and Motivation.....	2
1.3. Research Objectives and Anticipated Results .....	4
1.4. Study Plan.....	5
CHAPTER 2. LITERATURE REVIEW .....	6
2.1. Fundamentals of Pore-scale Physics .....	6
2.2. Studies of Core-scale.....	37
2.3. Applications on Field-scale .....	43
CHAPTER 3. EXPERIMENTAL MATERIALS, APPARATUS, AND PROCEDURES.....	46
3.1. Materials Used in the Experiments .....	46
3.2. Experimental Apparatus .....	48
3.3. Experimental Procedures.....	54
CHAPTER 4. RESULTS AND DISCUSSION.....	68
4.1. Experimental Results.....	68
4.2. Discussion of Results .....	82
CHAPTER 5. CONCLUSIONS AND RECOMMENDATIONS .....	91
5.1. Conclusions .....	91
5.2. Recommendations .....	94
REFERENCES .....	95
VITA.....	100

## **LIST OF TABLES**

Table 3.1. Physical properties of experiments fluids (at room temperature).....	47
Table 3.2. Experiments systems: interfacial tensions and spreading conditions values.....	48
Table 4.1. Summary of experimental results for procedure (B) .....	69

## LIST OF FIGURES

Figure 1.1. Schematic drawing of the GAGD process.....	2
Figure 2.1. Contact Angle. An oil drop (green) surrounded by water (blue) .....	7
Figure 2.2. Three-phase fluid system with strong wetting conditions .....	9
Figure 2.3. The wettability of pores.....	12
Figure 2.4. Classification of wettability illustrating the difference between mixed and .....	13
Figure 2.5. The difference between (left) fractional wetting and (right) mixed wetting .....	13
Figure 2.6. Effect of capillary pressure on the distribution of two immiscible phases.....	17
Figure 2.7. Effect of capillary pressure on fluids distribution inside the pore body.....	19
Figure 2.8. the spreading phenomnon.....	22
Figure 2.9. Vertical equilibrium of oil, water, and gas .....	25
Figure 2.10. (a) fluid distribution in waterflood; (b) residual oil saturation of waterflood .....	28
Figure 2.11. Distribution of oil, water, and gas in the oil-wet system.....	29
Figure 2.12. The gas interface at the start of the tertiary gas flood .....	29
Figure 2.13. (a) Gas meeting a water-filled pore body; (b , c) invading oil-filled pore throats ....	30
Figure 2.14. Gas (in black) breakthrough in micromodel (oil-wet, positive spreading system) ...	31
Figure 2.15. Differernt configurations of oil, water, and gas on a flat solid surface .....	38
Figure 2.16. Possible static positions of gas, water, and oil .....	41
Figure 2.17. Plot is showing U.S. oil production in barrels per day. ....	45



Figure 3.1. Experiment configuration for water saturation.....	49
Figure 3.2. Experiment configuration for oil saturation .....	50
Figure 3.3. Experiment configuration for gas injection.....	50
Figure 3.4. Picture of the laboratory apparatus used in the experiments.....	51
Figure 3.5. (left): Picture of an empty sand column, (right): a cross-section .....	52
Figure 3.6. HPLC pump (left) schematic frontal view (right) actual view.....	53
Figure 3.7. (left) a drop of water on oil-wet sand analyzes by <i>ImageJ</i> .....	57
Figure 3.8. Procedure (A) sequences of the experiment.....	63
Figure 3.9. Procedure (B) sequences of the experiment .....	64
Figure 3.10. Water-wet sandpacks at different conditions .....	67
Figure 4.1. Summary of ultimate recoveries for procedure (B).....	71
Figure 4.2. Oil and water production during GAGD floods in 100%WW sandpack .....	72
Figure 4.3. Photographs progression of GAGD floods in 100% WW sandpack with Soltrol.....	73
Figure 4.4. Photographs progression of GAGD floods in 100% WW sandpack with Decane.....	73
Figure 4.5. Oil and water production during GAGD floods in 100% OW sandpack .....	74
Figure 4.6. Photographs progression of GAGD floods in 100% OW sandpack with Soltrol .....	75
Figure 4.7. Photographs progression of GAGD floods in 100%OW sandpack with Decane .....	75
Figure 4.8. Oil and water production during GAGD floods in 12.5% OW sandpack .....	76
Figure 4.9. Photographs progression of GAGD floods in 12.5%OW sandpack with Soltrol.....	77

Figure 4.10. Photographs progression of GAGD floods in 12.5%OW sandpack with Decane ....	77
Figure 4.11. Oil and water production during GAGD floods in 25%OW sandpack .....	78
Figure 4.12. Photographs progression of GAGD floods in 25%OW sandpack with Soltrol.....	79
Figure 4.13. Photographs progression of GAGD floods in 25%OW / sandpack with Decane .....	79
Figure 4.14. Oil and water production during GAGD floods in 62.5% OW sandpack .....	80
Figure 4.15. Photographs progression of GAGD floods in 62.5%OW sandpack with Soltrol.....	81
Figure 4.16. Photographs progression of GAGD floods in 62.5%OW sandpack with Decane ....	81
Figure 4.17. Decane (-ve) $S_o$ system recoveries vs. time .....	83
Figure 4.18. Decane (-ve) $S_o$ system recoveries vs. PVI (pore volume injected of gas) .....	84
Figure 4.19. Soltrol (+ve) $S_o$ system recoveries vs. time .....	86
Figure 4.20. Soltrol (+ve) $S_o$ system recoveries vs. PVI (pore volume injected of gas).....	87

## ABSTRACT

Utilizing the power of nature to solve engineering problems has been a time-honored tradition, for example, using the sunlight as a heat and light source. From this principle, the visionary idea of Gas Assisted Gravity Drainage (GAGD) came. The GAGD process utilizes the natural segregation phenomenon of fluids with different densities in order to produce oil efficiently and economically. Waterflooding processes typically do not recover more than 40% of the original oil in place (OOIP), leaving a vast amount of oil behind. A practical and well-planned enhanced oil recovery (EOR) method is needed. However, to plan a successful project, the knowledge of reservoir characteristics and physics that govern these characteristics is required.

Wettability and spreading are critical properties of fluid flow in a porous medium and the recovery of oil. The objective of this work is to study the role that rock-fluid (wettability) and fluid-fluid (spreading) interactions play on GAGD performance. For this purpose, an experimental study has been conducted using sandpacks containing oil-wet sand ratios of 0, 12.5, 25, 62.5, and 100% with different spreading conditions (Decane as non-spreading oil and Soltrol as spreading oil). This core-scale study also described the pore-scale mechanisms to evaluate a reservoir-scale problem.

The results, regarding the recovered oil percent, are as follows: The highest recovery occurred in both complete water-wet sand with the spreading system and complete oil-wet with the non-spreading system. The lowest recovery occurred in both complete water-wet sand with the non-spreading system and complete oil-wet with the spreading system. The second highest recovery was in 12.5% fractional-wet with spreading oil (Soltrol).

The second lowest recovery was in 12.5% fractional-wet with non-spreading oil (Decane). Similar oil recoveries were obtained in 25% fractional-wet and 12.5% fractional-wet, either in spreading conditions or non-spreading conditions. Finally, oil recovery in 62.5% fractional-wet sand in both spreading and the non-spreading system was alike.

The element of innovation in this work is the evaluation of GAGD process in fractional-wettability systems and will help to plan more successful GAGD projects and is considered a step forward in understanding wettability and spreading phenomena and their influence on GAGD performance.

# CHAPTER 1. INTRODUCTION

## 1.1. Research Background

On a pore-scale, first representations of wettability segregate oil reservoirs into either water-wet or oil-wet systems. However, the idea of the existence of a spectrum of wettability conditions goes back to when Brown and Fatt (1956) introduced the definition of fractional wettability. The vital part is that a small difference in wettability influences a noticeable effect on recovery. This novel term was presented to describe the heterogeneous wetting of the pore surfaces in the rock which are scattered arbitrarily, where the favored wetting of surfaces is down to the part of the pore size and no continuous networks of oil and water exists. Substantially, this occurs due to the random allocation of minerals (in the rock) with diverse chemical characteristics (Donaldson and Alam, 2008).

It is worth to notice that fractional-wet is different from mixed-wet concept established by Salathiel (1973) which refers to a system with water filling the small pores and pore crevices are water-wet, while the larger pores are filled with the oil and are oil-wet. Salathiel justified that throughout the original oil accumulation period, in-place oil holds surface-active components that discharge connate water from large pores. Still, oil cannot invade small pores due to the immense capillary pressure required to displace water as scales decrease. The broad neutral wettability term refers to both intermediate wettability which is a homogenous state of wettability.

On a reservoir scale, the GAGD process implemented via use of injection wells to inject CO<sub>2</sub> gas at the top of the reservoir with a group of horizontal producers situated just above the oil/water contact (OWC)(Rao et al., 2004). The gas injected in miscible or immiscible mode (both proven to improve recovery) and due to gravity segregation resultant from separate fluid densities

in the reservoir, the injected gas accumulates at the top and start displacing the oil and drain it down to the horizontal producers (Mahmoud and Rao, 2007). The process schematic drawing is shown in Figure 1.1.

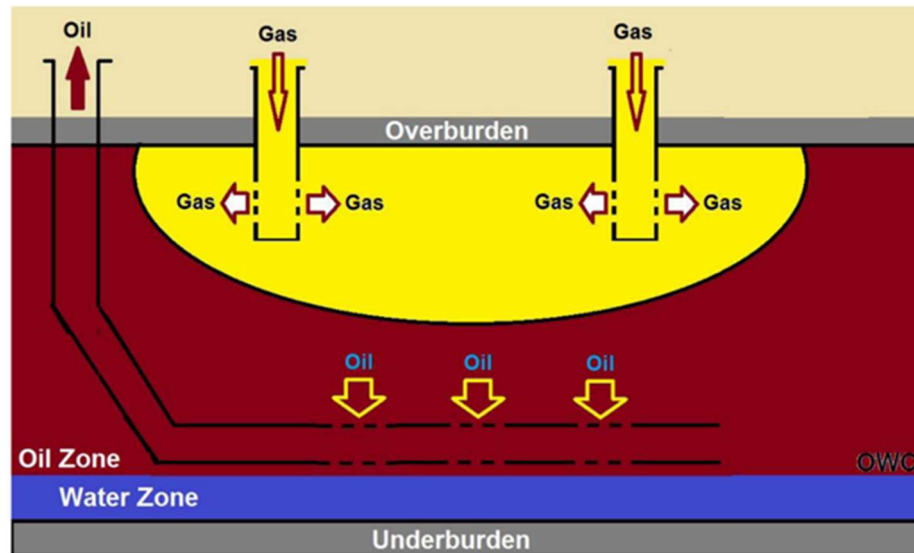


Figure 1.1. Schematic drawing of the GAGD process (Al-Mudhafar et al., 2017)

## 1.2. Problem Statement and Motivation

The key to successful recovery in secondary and tertiary processes in oil reservoirs is determined by reservoir wettability. Better understating of such a complex area of research led to successful planning for future GAGD projects and bring a better conception of the enigma of wettability (Agbalaka et al., 2008). Wettability of the porous media and spreading properties of fluids dominate the influential factors in gravity drainage of three phases while injecting gas (Vizika and Lombard, 1996).

The fraction of the total surface area of the rock that prefers oil or water is different in each reservoir and is one of the main causes of different wettability conditions. The focus of Brown and Fatt (1956) was only to introduce a novel way to measure and quantify the fraction of oil wet and

water wet areas using nuclear magnetic relaxation. Previous research work focused only on studying uniformly water-wet media neglecting the investigation of oil-wet systems (Baker, 1988).

Recently, further studies examined the effect of water-wet, oil-wet, mixed-wet, and fractional-wet in sandpacks (Oak et al., 1990; Vizika and Lombard, 1996; Jerauld, 1997; Sahni et al., 1998; D. Zhou and M. Blunt, 1998; Dicarolo et al., 2000) but most of these studies used a sand composed of 50% initially water-wet sand and 50% modified oil-wet only. The latest experimental work conducted by Dzulkarnain (2018) at the Louisiana State University to study the effect of spreading coefficient and wettability in water-wet, oil-wet, and fractional wet (50% oil-wet and 50% water-wet) pores in the GAGD process. The proposed work plan is to use different combinations of oil-wet/water-wet sand beyond the typical (50/50) fraction to inspect the changes in wettability tendencies and its effects on GAGD performance in sandpacks and ultimately on production performance.

Even with the knowledge of the critical role of the wettability phenomena in petroleum engineering, no sufficient attention had been given to it in early research (the 1950s), one reason for this lack of knowledge would be due to its complexity (Donaldson and Alam, 2008). Fatt and Klikoff (1959) studied the fractional wettability and its effects on multiphase flow in porous media. The authors found that both capillary pressure and relative permeability of unconsolidated sand are functions of fractional wettability. In this paper, two questions were elucidated; first, what is the reservoir's original wettability of a given rock? Second, how does the wettability play a role in the determination of multiphase fluid flow properties of the same given rock?

The paper gave no emphases on in-situ wettability. Motivated by this past work, the current interest is focused on finding some answers to the second question; results show that fractional wettability has a significant impact on the multiphase flow in sandpacks.

In this current work, it is also planned to answer the second question for Fatt and Klikoff (1959) with emphasis on the GAGD process. Also, the desire is to be one step closer towards a better understanding of the rock and three phase fluids interactions.

The objective of this work is to evaluate the success of the GAGD process in a wide range of oil reservoirs. The ultimate motivation is to obtain the ultimate recovery with a minimum economic cost and extend the range of the possibility of applying a successful GAGD project.

### **1.3. Research Objectives and Anticipated Results**

The objectives of this work are:

1. To experimentally determine the effect of fractional wettability and spreading conditions on the performance of the GAGD process.
2. To study the consequence of oil-wet and water-wet states in different fractional combinations in a porous medium on three-phase fluid flow, and the gravity-drainage process during gas injection.
3. Gaining a better understanding of wettability and spreading phenomena in the application of enhanced oil recovery with gas injection.
4. Trying to distinguish or identify the specific percentage of fractional wettability in which the behavior of the sandpack will change from water-wet to oil-wet behavior or vice versa.

The expected results of this research, in summary, will give a better understanding of potential oil recoveries from the GAGD process as a function of fractional wettability and spreading conditions.



#### **1.4. Study Plan**

Through the utilization of different sandpacks as a porous medium, this study will model different cases of various reservoir wettability conditions. Sand is easy to categorize, handle and treat chemically. Immiscible gas injection experiments will be conducted using two different spreading oils (Positive/Negative) to study two different spreading systems. Performance of each case will be plotted and compared with other cases, and the consolidated results will be examined against other literature review experimental findings.

Work planned will further the Dzulkarnain (2018) experiments on fractional-wet sandpack to beyond the 50/50 (water-wet/oil-wet). The target was experimenting with different combinations of sandpack depending on the results of the previous one. As an example, the first sandpack (SP-1) to be prepared was 25% oil-wet/ 75% water-wet. Furthermore, depending on SP-1 performance the decision of increasing/decreasing the oil-wet percent will be made.

## CHAPTER 2. LITERATURE REVIEW

The significance of three-phase flow behavior in porous media falls in different fields of science and engineering. Industrial significant examples evolve in radionuclide migration from nuclear waste deposits, the flow of groundwater related to organic liquids surface spills and infiltration from subsurface storage tanks effects on groundwater condition, and finally on current work subject of enhanced oil recovery procedures in which gases injected into oil reservoirs where water also co-exists with oil.

### 2.1. Fundamentals of Pore-scale Physics

At pore-scale, wettability role come to the picture. However, what it is wettability? Generally, it is “the tendency of one fluid to spread on or adhere to a solid surface in the presence of other immiscible fluids” (Craig, 1971). More specifically, in petroleum engineering, it is “the tendency of reservoir rock surface to prefer contacting a particular fluid in multi-phase or two-phase fluid system” (Agbalaka et al., 2008).

When more than one immiscible phase co-exists in a porous medium, one phase at least will be more wetting to the surfaces of pores (wetting phase) than the other phase(s). At equilibrium, the wetting phase tend to occupy the smaller pores while the non-wetting phase tends to occupy open channels and larger pores and will have higher relative permeability comparing to the wetting phase (Ahmed, 2006; Zahoor et al., 2009).

Spreading coefficient is responsible for the way the three phases arrange. A resultant of fluids and rock surfaces interactions is the stable configuration of gas, oil, and water in the pore space.

F.-M. Kalaydjian (1992) and F.-M. Kalaydjian et al. (1993) derived the formula of the contact angle of the gas/ oil interface on a water surface (measured through the oil), with the assumption of the existence of a thin covering layer of the wetting phase.

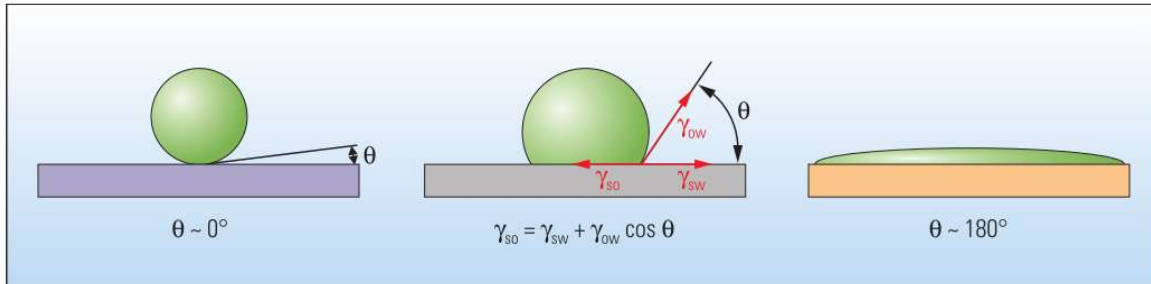


Figure 2.1. Contact Angle. An oil drop (green) surrounded by water (blue) on a water-wet surface (left) forms a bead. The contact angle  $\theta$  is approximately zero. On an oil-wet surface (right), the drop spreads, resulting in a contact angle of about  $180^\circ$ . An intermediate-wet surface (center) also forms a bead, after (Abdallah et al.,2007).

Øren and Pinczewski (1995) illustrated the static and dynamic distribution of three phase fluids comprehensively in pore-scale and the displacement structures of three-phase movement in strongly-wet systems with non-wetting phase as the displacing fluid (gas) in this case. Demonstration of the fluids in pore-scale revealed that there are three distinct patterns the fluids may take. Each type of pattern is governed by the values of three fluids interfacial tensions and the solid wetting condition. Two fundamental techniques for displacing the fluid proceed by: a direct drainage method (two-phase displacement) and a double drainage method (three-phase displacement). A network micromodel has been utilized for recoveries calculations. The experiments results have been compared with simulated findings and showed proper matching. It has been suggested to consider the model as the basis for three-phase flow modeling in the actual porous medium.

Darcy's law and measured saturation-related relationships for phase relative permeability and capillary pressure are commonly used to express the macroscopic multi-phase flow in porous media. Experimentally it is challenging to determine three-phase flow behavior using these saturation-related relationships, leading to estimating three-phase performance from two-phase saturation-related data using empirical models. Leverett (1941) first proposed a model, and then others extended his work (Stone, 1970; Parker and Lenhard, 1990) proposing new models for multi-phase flow estimation. However, F.-M. Kalaydjian (1992) raised a substantial imperfection on the empirical quality of the standing (at that time) theory of three-phase flow in porous media. Utilizing the two-phase flow mechanism into real porous media is governed by a clear understanding of the pore space complex nature.

Øren and Pinczewski (1995) implied that it might be possible to describe the pore-scale displacement for the drainage-dominated flow of three-phases solely for strong (fully-perfect) wetting systems. Therefore, three-phase displacement could express using a simple generalization of two-phase flow mechanisms where the function of the wettability effect in two-phase flow is substituted by spreading effect for three-phase flow. Again, this study investigated only the case where there is a liquid phase that wets the solid surface strongly. Systems of mixed-wet, intermediate-wet, or fractional-wet were out of the scope of this study.

A micromodel of interconnected pores pattern for the porous medium is composed of large pores (pore bodies) which connected by narrower pores (pore throats). Within the pore space, the transport characteristics of the phases are controlled by the distribution of the fluids.

The static equilibrium pore-scale distribution of three fluids in the porous system driven by a multiplex interaction involves the following physical phenomena:

1. Wettability - interactions between the fluids and the solid in the system.
2. Capillary pressure- interactions between bulk fluids across curved interfaces.
3. Spreading Coefficient- (three-phase contact lines) - interactions between the three fluid phases.

Figure 2.2 shows the fluids system as fluid-1, fluid-2, and fluid-3, with fluid-3 as the most wetting phase in the system, the phases can allocate in one of the three modes shown below.

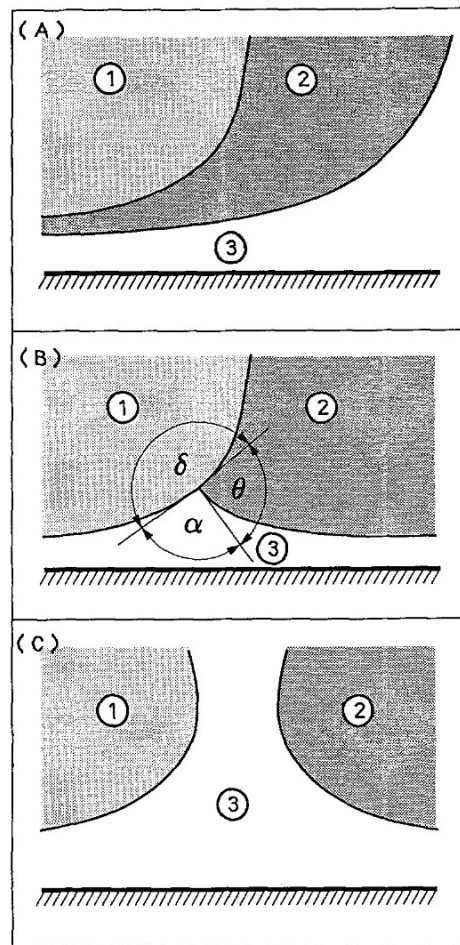


Figure 2.2. Three-phase fluid system with strong wetting conditions (A, B, and C: are the possible allocations fluids might take) after Øren and Pinczewski (1995)

Wettability is defined here under the spreading coefficient (denoted by capital "S") effect, as the solid wetting preference for the supreme wetting phase (fluid-3 in this case) proportional to fluid-1 (utmost non-wetting phase "conditionally") in this case where two fluids (fluid-1/fluid-3) are in interaction with a solid (represented by a small "s"). The spreading is found from the interfacial tensions using equation 2.1:

$$S = \sigma_{s1} - \sigma_{s3} - \sigma_{13} \quad (2.1)$$

The interfacial tension for solid~fluid-1, solid~fluid-3, and fluid-1~fluid-3 are symbolized by  $\sigma_{s1}$  ,  $\sigma_{s3}$  , and  $\sigma_{13}$  , Respectively. Fluid-3 wets the solid surface completely, and the contact angle is zero; only in this case, S is a positive value. In a different situation, the liquid partly wets the solid; in this case, S is a negative value. The contact angle is given by Young's formula:

$$\cos \theta = 1 + \frac{S}{\sigma_{13}} \quad (2.2)$$

It has been assumed in this work that fluid-3 wets the solid completely, and the solid surface is covered by a thin wetting layer everywhere (has been illustrated in Figure 2.2). For capillary pressure effect, it has been stated that pore throat (occupied with fluid-3) connecting a pore body (occupied with non-wetting fluid-1 or fluid-2), capillary forces block the non-wetting fluid from impulsively entering the pore throat.

The nonwetting phase can only enter the pore throat under one condition, which is once the pressure of the nonwetting fluid exceeds the pressure in the wetting fluid by a value identical to the capillary pressure threshold,  $P_c$ , known by:

$$P_c = \sigma \left[ \frac{1}{R_1} + \frac{1}{R_2} \right] = \frac{2\sigma}{r_t} \quad (2.3)$$

The term  $\sigma$  is the interfacial tension and the terms  $R1$  and  $R2$  represent the principal radii of the interface curvature. For the interface of the pore throat, the term  $r_t$ , define the effective radius of curvature. Firstly, when the interface is situated in the pore throat, the non-wetting phase enters spontaneously a neighboring pore body filled with the wetting phase. It happens due to the existence of surplus capillary pressure which equals the difference between the capillary pressure for the interface in the pore throat and the interface in the pore body. Surplus capillary pressure ( $\Delta P_c$ ) is given by:

$$\Delta P_c = 2\sigma \left[ \frac{1}{r_t} - \frac{1}{r_b} \right] \quad (2.4)$$

$r_t$  is the effective radii of the pore throat and  $r_b$  represents the effective radii of the pore body.

In a two-phase medium, capillary pressure is the principal controller of distribution of fluids, with the condition of having one fluid wetting the solid perfectly. Moreover, because of capillary pressure effect, the pore bodies will be favorably conquered by the nonwetting fluid and might be interconnected by nonwetting fluid-filled pore throats, whereas the pore throats favorably conquered by the wetting fluid and might be interconnected by wetting fluid-filled pore bodies.

While for three phases porous medium, two nonwetting phases exist (fluid-1 and fluid-2). In the zones of the pore space that inhabited by two phases (the wetting phase and only one of the nonwetting phases) the distribution of fluids is similar to that of a two-phase scheme. While, in zones that all three fluids co-exist, one of the nonwetting fluids will have a superior surplus capillary pressure given by equation(X) above. That fluid can be fluid-1 if the condition below satisfied:

$$\sigma_{13} > \sigma_{23}$$

In this case, fluid-1 entitled as the *nonwetting phase* and fluid-2 as the *intermediate phase*.

### 2.1.1. Wettability

In literature, there are different classifications of wettability. Donaldson and Alam (2008) categorized the four states of wettability into Water-wet, Oil-wet, Mixed-wet, and fractional wet. A classification of wettability types shown below in Figure 2.4. Mixed and fractional wettability were previously explained and difference between these two wetting types is shown in Figure 2.5. Water-wet is the term used to describe a porous media where more than 50% of its pore surfaces are preferably in contact with water. Water exists as a continuous film in the smaller pores and oil occupying the larger pores and as drops resting on the water film. In the oil-wet system, the description above is reversed.

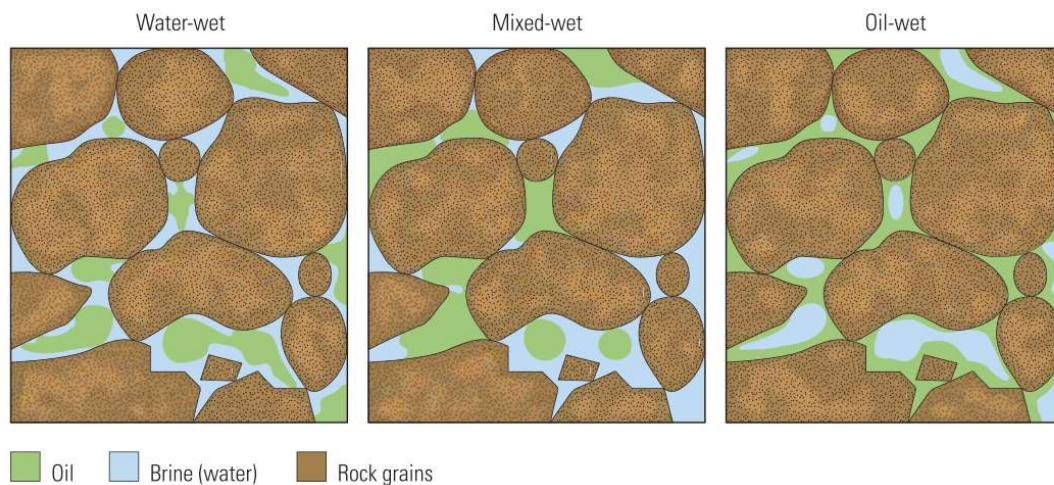


Figure 2.3. The wettability of pores. In a water-wet case (left), oil remains in the center of the pores. The reverse condition holds if all surfaces are oil-wet (right). In the mixed-wet case, oil has displaced water from some of the surfaces but is still in the centers of water-wet pores (middle). The three conditions shown have a similar saturation of water and oil, after (Abdallah et al., 2007).

In case the system is not strongly oil/water wet a contact angle ( $\theta$ ) occur between the fluids and the solid surface (Abdallah et al., 2007). Complete wetting ( $\theta = \text{zero}$ ) is considered the extremely water-wet system, while complete non-wetting system ( $\theta=180$ ) is considered extremely oil-wet (Ahmed, 2006).



Nevertheless, the majority of oil reservoirs wettability are fractional in nature which means that a broad spectrum of wettability may exist (D. Zhou and M. Blunt, 1998).

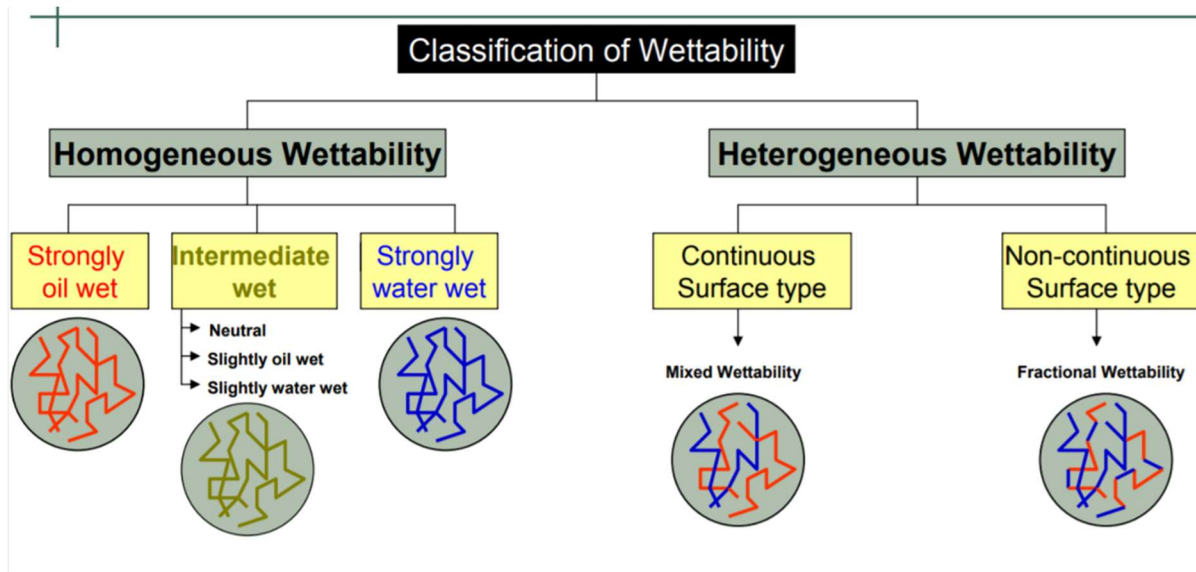


Figure 2.4. Classification of wettability illustrating the difference between mixed and fractional wettability (Dernaika et al., 2009)

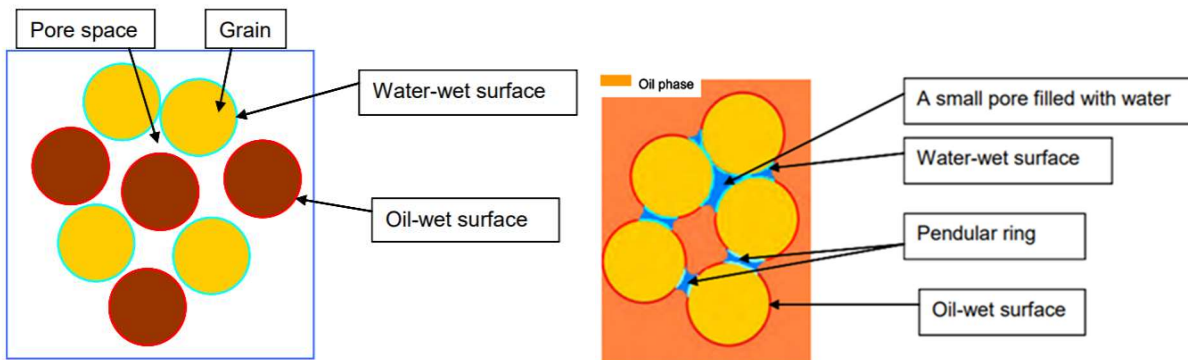


Figure 2.5. The difference between (left) fractional wetting sand particles and (right) mixed wetting sand particles (Motealleh et al., 2008)

Previous studies worked on quantifying the wettability to identify the heterogeneity of reservoir rocks.

Brown and Fatt (1956) conducted their experiments using unconsolidated sandpacks saturated with water where the sand was a mixture of water and oil wet. Sand mixtures were prepared by blend untreated Nevada white sand with the same sand processed with SF 99 Dri-film. The treatment performed by soaking the sand in a solution of 10% by volume Hexane. Then, the sand heated to 300 F and finally, both the treated and non-treated sands were mixed together using a blender. The results showed a linear relationship between the relaxation rate of water and the percent of Dri-filmed sand (oil wet fraction) in a fractional wettability rock. It was suggested to use this non-destructive method to obtain the fractional of the surface area which prefers oil wet in the natural reservoir rock.

Holbrook and Bernard (1958), used a basic dye adsorption method to acquire the fraction of wettability. Amott (1959), coming with wettability index scale employs the displacement and flooding of fluids to classify wettability as the fractional type when attaining a range of (0.25 - 0.75) fractional water wettability. Jennings (1958) justifies that changing the porous medium fractional water wettability from unity to zero will accordingly change the relative permeability of that medium. Both capillary pressure and relative permeability curves are used to illustrate the effects of known fractional wettability sandpacks on multiphase flow.

Experimental apparatus used in Fatt and Klikoff (1959) work to calculate the capillary pressure. relative permeability curves acquired using Welge calculation applied to the data of water flooding of sand mixture. Sand used in all tests was Ottawa sand consists of almost pure silica. The original untreated sand was the water-wet portion, while the oil-wet sand was same original sand treated with organosilane vapors (General Electric Dri-film No. SC 77). Then, both portions of the sand were mixed with gentle handling.

In conclusion, it found that in the same uniform grain-size geometry sandpack the capillary pressure curve is decreased with the increase of fractional oil wettability. The shape of the curves is preserved. Also, it proved that relative permeability changes continuously as the fraction of oil wettability changed.

#### 2.1.2. Capillary Pressure and Interfacial Tension

Kantzas et al. (1998) studied three immiscible phase flow through the utilizing the behavior of capillary pressure. Earlier, F.-M. Kalaydjian (1992) employed the drainage capillary pressure in predicting the difference in residual oil saturation between the positive and negative oil spreading systems. Kalaydjian observed higher quantities of residual oil saturation left in the negative spreading system compared with the positive one.

Capillary pressure of three phases system (in an equilibrium state) controls the mobility of the fluids. Hence there is a diversity of configurations in the way the three phases distributed in a single body. The fluid may be allocated as concentric rings, or two fluids may scatter as globules separated and fall within the third fluid. While changing the capillary pressure amends the initial spatial configuration of the fluids, this change can occur as a result of flowing of any phase through porous media.

To understand the concept of capillary pressure, consider a system of only two immiscible fluids at equilibrium state in porous media. The forces are influenced by two factors which are: the dimensions of every pore, and the interfacial tensions of fluids. The quantum of forces determined by the applying of the well-known Young–Laplace equation:

$$P_c = P_{nw} - P_w = 2\sigma/r_m \quad (2.5)$$

Whereas  $P_c$  represent the capillary pressure of the system,  $P_{nw}$  represent the pressure of the non-wetting phase, and  $P_w$  represent the pressure of the wetting phase.  $\sigma$  Is the interfacial tension. And  $r_m$  is the mean radius of interface curvature between the two immiscible phases.

Introducing a pressure gradient results in equilibrium disturbance which tends to make the fluids move to a newly found equilibrium position, which subsequently leads to a shift in fluid saturations. This shift can be seen through the curves of the capillary pressure of the system. When the disturbance leads to an increase in the saturation of the wetting phase, the process is considered imbibition, while if the disturbance leads to increasing the non-wetting phase saturation the process is considered drainage.

Demonstrating the capillary pressure concept in a two-phase system, can be done by taking a rectangular pore cross-section as illustrated in Figure 2.6 In the event of complete saturation of the cross-section with the wetting phase, no interfaces exist (Figure 2.6a). Once a second (non-wetting) phase enters the pore space, the capillary pressure arranges the shape of the interface (Figure 2.6b). In the situation of capillary pressure increase, the non-wetting phase expels the wetting phase-out of the pore and occupies a more significant portion of the pore space (Figure 2.6c). Inversely, when the capillary pressure decreases, the wetting phase expels the non-wetting phase-out of the pore and occupies a more significant portion of the pore space (Figure 2.6d) in a way similar to the configuration before the increase of capillary pressure occurs.

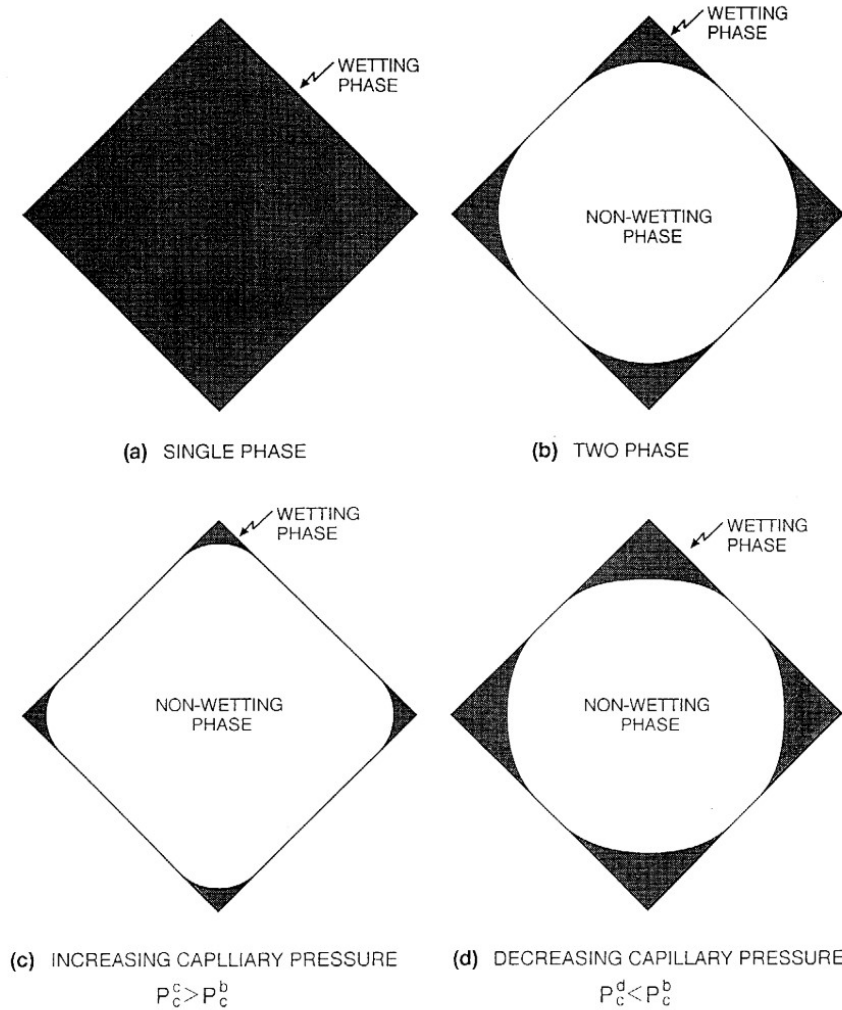


Figure 2.6. Effect of capillary pressure on the distribution of two immiscible phases (cross-sectional pore body) after Kantzas et al. (1998)

With the understanding of the concept of two-phase system capillary pressure, it is of ease to discuss the capillary pressure of a more complex system which is the three-phase system. Revisiting the pore space aforementioned in (Figure 2.6b) also in (Figure 2.6a), two immiscible phases inhabited this pore. Assuming that a new third phase enters the pore and this third phase is immiscible to both of the other phases. Two possible scenarios for the way fluids will arrange, depending on the spreading coefficient of the system.

When the spreading coefficient is a positive value, the wetting phase will adhere entirely to the walls of the pore (the illustration shows a high concentration or banks of wetting phase in the pore corners). Also, one of the non-wetting fluids will spread in-between the wetting, and the other non-wetting fluids are dispersing these two phases yielding concentric rings or semi-rings shape interfaces as shown in Figure 2.7b.

A different situation is when the spreading coefficient is of a negative value, the two non-wetting phases are split by the wetting phase and do not come into any contact as they can be seen from the cross-sectional point of view as two individual floating blobs enclosed by the wetting phase as manifested in Figure 2.7c. In three phases system where gas, water, and oil represent the phases. Consider this system to be with a positive spreading coefficient and water-wet solid surface. In such conditions, when the water is the wetting phase, oil will spread between water and gas and is considered as an intermediate non-wetting phase. In this scenario, gas is the most non-wetting phase and considered the ultimate non-wetting phase. When we consider the same system with one different variable, wettability, an oil-wet media, where the wetting phase will be oil, both gas and water will be equally non-wetting and separated by oil. For this scenario, the spreading coefficient will also be considered negative.

Observing the differences in fluid distribution for the two scenarios above. Hence a various final saturation will be attained when there is a disturbance strike the capillary equilibrium. A glance on both Figure 2.7b and Figure 2.7c give some speculation of the simultaneous fluids flow. In Figure 2.7c (negative spreading), gas and water mutually flow through a relatively regular shaped channel or duct whereas oil will have to go through asymmetrical films, wedges, and corners.

In Figure 2.7b (Positive spreading), the explanation of flow rates and velocity of fluids considered complex.

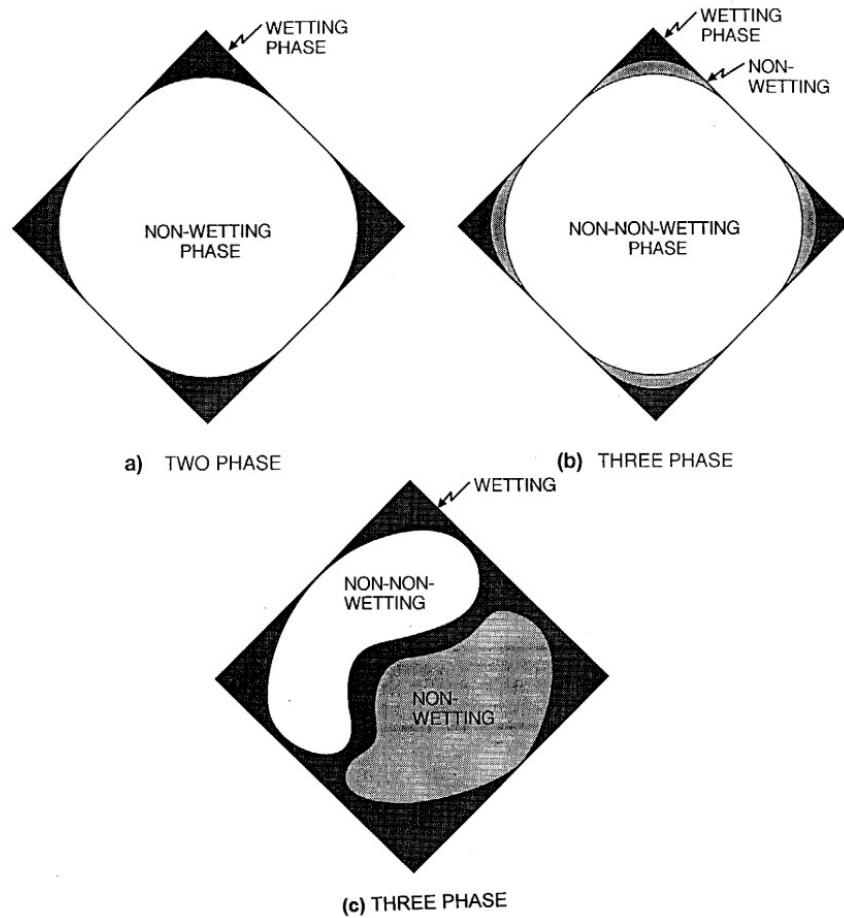


Figure 2.7. Effect of capillary pressure on fluids distribution inside the pore body of (A) two immiscible phases; (B) three immiscible phases – positive spreading coefficient; (C) three immiscible phases – negative spreading coefficient. After Kantzas et al. (1998)

A practical application of the three-phase capillary pressure phenomena is Gravity Assisted Immiscible Gas Injection (GAIGI). Immiscible gas has been already used efficiently to recover oil and water from reservoirs regardless of the oil saturation and wettability status.

Experimental work on cores indicate that as oil is flowing through a series of pathways to the producing end, these pathways are formed by the spreading (effect) of oil between water and gas. Improved oil recoveries have been detected, under the condition of low draw-down and

keeping the gas from break-through. GAIGI has also been used in the miscible mode in extreme cases where the disconnected residual oil exists.

Kantzas et al. (1998) mentioned that the three-phase capillary pressures may not influence much when dealing with conventional secondary recovery processes like water flooding. However, the importance of this phenomena increases when it comes to deal with slow displacement schemes with gas used as the displacing phase. It also concluded that saturation history, pore geometry, and spreading coefficients are vital factors that affect the distribution of fluids equilibrium. There is a need for further research and experiments needed to reach more definitive findings. However, for this work, it has been found that in case of water-wet medium, with a positive spreading system and irreducible water saturation conditions, the three-phase capillary pressure curve can be simplified into two-phase capillary pressure equivalents. With the use of immiscible gas injection, two-phase algorithms can be used to provide an acceptable approximation of a three-phase system. The capillary pressure curves for a three-phase media can be characterized using a ternary diagram or through using a group of two-phase capillary pressure curve that illustrates relative saturation changes as a function of pressure change of one phase.

### 2.1.3. Spreading

A pioneer work done by J. M. Dumore and Schols (1974) showed that gravity drainage in water wet medium resulted a high oil recovery, and few percent residual oil saturation in the three-phase system (existence of gas and water besides oil), which is way lower residual oil than the case of the existence of water alone. Later experimental studies conducted using sandstone cores and bead or sandpacks (I. Chatzis et al., 1988; A. Kantzas et al., 1988; Vizika, 1993) strengthened J. M. Dumore and Schols (1974) outcomes.



It was proposed that a high oil recovery is related to drainage through thin oil films that exist amidst the water and the gas in pore space. These oil films have been spotted precisely using 2D glass micromodel networks in the work of numerous scholars (A. Kantzas et al., 1988; F.-M. Kalaydjian, 1992; Oren et al., 1992; Soll et al., 1993; Oren and Pinczewski, 1994). Still, the circumstances in which drainage by oil layers would take place has not been clearly identified. A theory postulated that systems with positive spreading, in which the oil phase spreads naturally over a flat water/gas interface, could undergo film drainage resulting in high recovery. While non-spreading systems in which the oil phase do not spreads on the other fluids, these systems exhibited lower recovery.

The contradiction between Dumore and Schols (1974) conclusions as an equivalent residual oil saturation (3% approximately) for both of the systems (spreading and non-spreading) was attained. Moreover, Oren et al. (1992); Oren and Pinczewski (1994); Vizika (1993) experiments in which been found a more significant recovery for positive spreading coefficient systems compared with negative spreading coefficient systems. A. Kantzas et al. (1988) raised an interesting point that is recovery is directed by the stability of the film, this stability is dominated by capillary and intermolecular forces and as opposed to the spreading coefficient alone. In non-spreading systems, no oil films identified using experiments in micromodel and capillary tubes scale. While, in core flooding experiments, stabilized by capillary forces oil layers formed as an oil cluster moves across the system, and thick oil layers can subsist in both spreading and non-spreading systems.

Blunt et al. (1994) studied the three-phase flow theoretically and experimentally in the water-wet system in pore and core scale. In the literature, it has been identified that most oil types will spread over water, but ultimately form a film (0.1-5) nm thickness. Spreading of oil between

gas and water is shown below in Figure 2.8. Capillary pressure and the way the film formed (thinning a thick layer or invading a clean interface) determine the thickness of these films. Thin films developed in spreading and non-spreading oils. However, experimental results shown no effect of films on recoveries since drainage through these films considered significantly slow. In low surface tension experiments thick oil layer (many microns thick) has been located amidst water and gas which stabilized by capillary pressure. While, in high surface tension tests, oil film exists as merely a molecular thick. Blunt et al. (1994) work investigated the following: (1) the thickness and stability of oil thin films which governed by intermolecular forces; (2) the thickness of oil layer meanwhile the process of drainage occurs (3) the flow rate of these films; (4) the ultimate oil recovery.

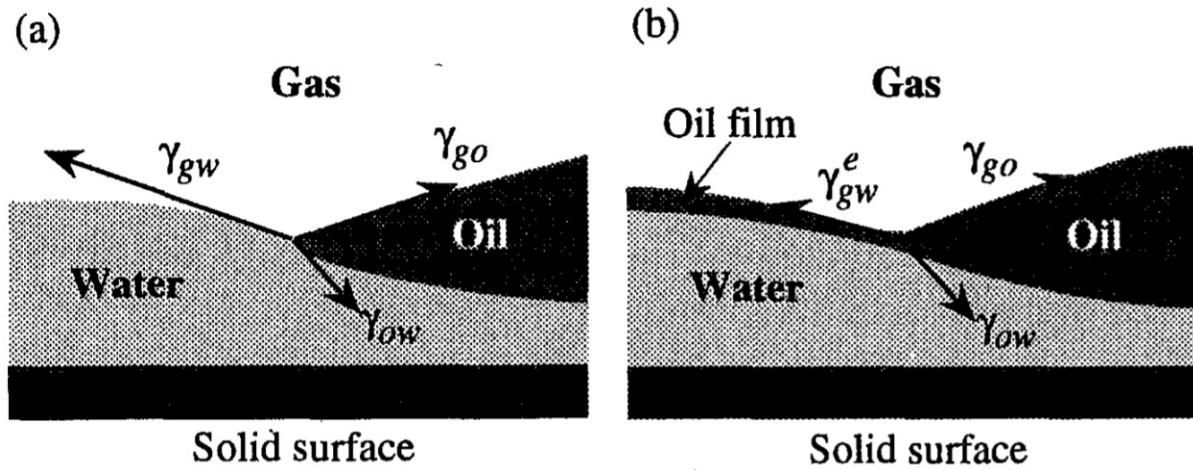


Figure 2.8. the spreading phenomnon (Blunt et al., 1994)

In a three-fluid system in which the fluids are in contact, when a drop of oil with a size greater than the range of intermolecular forces range (approximately  $0.1 \mu\text{m}$ ), is placed on a water surface, preliminary spreading of the drop is subject to the spreading coefficient ( $C_s$ ),

$C_s$  is defined by:

$$C_s = \gamma_{gw} - \gamma_{go} - \gamma_{ow} \quad (2.6)$$

The gas/water, gas/oil, and oil/water surface tensions denoted respectively by  $\gamma_{gw}$ ,  $\gamma_{go}$ , and  $\gamma_{ow}$ .

If the flowing conditions met:

$$\gamma_{gw} > \gamma_{go} + \gamma_{ow}, \text{ leading to:}$$

$$C_s > 0$$

A spreading coefficient ( $C_s$ ) more prominent than zero (positive value), signaling an oil can spreads (in a spontaneous way between the gas and water). Additionally, the contact line in-between the three phases is unstable leading to oil spread. When the oil forms a thin film between the gas and the water, the same system where oil spread initially may reach a state of equilibrium or balance with a macroscopic blob of oil, if condition below has met:

$$C_s^e < 0$$

The previous equation will be modified into:

$$C_s^e = \gamma_{gw}^e - \gamma_{go} - \gamma_{ow} \quad (2.7)$$

Where  $\gamma_{gw}^e$  Is referring to the effective surface tension, indicating the free energy per oil film unit area. Structural forces come vital, once the thickness of the film is almost a molecular size. However, Van der Waals forces are unable alone to form a thick film (5 nm or larger) in a porous medium.

Majority of oil types do spread on water establishing a film, which stabilized by structural forces. The thickness of these mentioned films is governed by the way the layer was created and is a capillary pressure dependent. Initially positive spreading systems develop oil films all the time.

Non-spreading systems, on the other hand, can solely start oil films when the film is a resultant of thinning of a thicker oil layer.

Aforementioned is the reason for not spotting any films of oil in the micromodels and capillary tube experiments when  $C_s < 0$ . while for sandpacks and coreflooding experiments a stable oil films for non-spreading oils recognized also at the trailing edge of oil bank. Nevertheless, as these films are molecularly thin, flow across them is insignificant and improbable that they alone can contribute for a high recovery in gravity drainage experiments. Additionally, the existence of oil film providing a pressure continuity for the oil phase; during gas injection, the originally isolated oil ganglia before gas injection become connected. Drainage can improve through the swelling oil layers, flow through these swollen layers is more significant than flow via a molecular film and can significantly reflect an improved recovery and drainage rates exposed experimentally.

Capillary tubes experiments conducted was a useful aid for mathematical modeling. However, since natural porous media encompass crevices and grooves, oil layer may form. Circular tubes experiments (artificially made) conceal some physics of natural flow found in rough and cornered paths of real porous media. For that reason, sand columns used to evaluate the residual oil saturation in the section above oil bank (which called transition zone) showed in Figure 2.9.

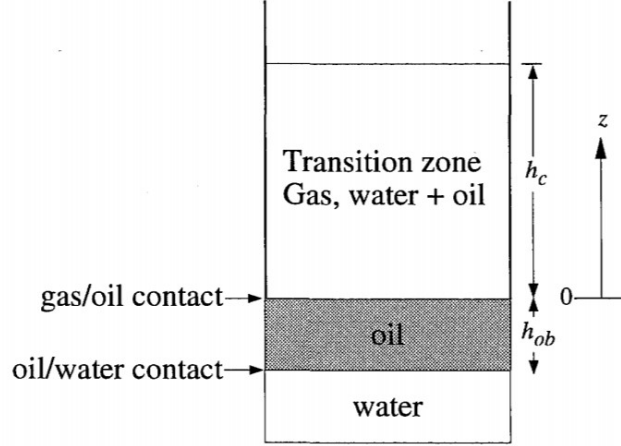


Figure 2.9. Vertical equilibrium of oil, water, and gas (Blunt et al., 1994)

Where  $h_{ob}$  is the height of the oil bank,  $h_c$  is the height of the transition zone (three fluids co-exists).  $h_c$  is calculated using the parameter ( $\alpha$ ), where  $\alpha$  represents the fluid properties defined below:

$$\alpha = \frac{\gamma_{ow}(\rho_o - \rho_g)}{\gamma_{go}(\rho_w - \rho_o)} \quad (2.8)$$

Moreover,  $h_c$  will be:

$$h_c = \frac{h_{ob}}{\alpha - 1} \quad (2.9)$$

So, the larger the value of  $\alpha$ , the lesser value of  $h_c$ , which indicates that there is less oil left behind in the stable layer of the transition zone, which leads to higher ultimate oil recovery. When  $\alpha < 1$ , means that there is a stable oil layer above oil bank at all heights, it believed that this layer could maintain a considerable amount of connected oil. The final configuration of fluids in ( $\alpha < 1$ ) system indicates that more oil will remain in thick, stock layers of pore space above oil bank. While in case  $\alpha > 1$  the oil phase becomes disconnected (disregarding the molecular film), in the finite height ( $h_c$ ). Reaching a capillary equilibrium occurs by the drains of oil ganglia and swelling of oil layer despite the value of  $\alpha$ .

To sum up, most oils do spread on water forming a nanometer film. This film is stabilized by structural forces. Moreover, the thickness of these films depends on capillary pressure and history of fluids displacement. Regardless of the initial spreading coefficient (positive or negative), a stable film will exist in the system if the oil film formed from an initial thicker layer of retreats oil (like the lagging edge of oil accumulation).

Oren and Pinczewski (1994) investigated the influence of oil films on oil recovery - specifically, the tertiary recovery of oil after a secondary recovery using waterflooding. In this paper, the oil-wet model was introduced as this work is a subsequent of the work of Oren and Pinczewski (1991), Oren et al. (1992), and continuous work from Oren (1992). A 2D glass micromodel was utilized to study the role of oil films presence on the oil recovery by immiscible gas injection. Oil films term represents two substantial phenomena that impact the recovery of oil. These two natural interactions are the fluid/fluid interactions and the fluid/solid interactions termed spreading coefficient and wettability respectively. The work indicated that similar to strong water-wet model the oil-wet model also drained by the double-drainage mechanism. In addition to double-drainage mechanism oil also displaced by gas directly.

Two combinations of fluids were used: air used as the gaseous phase, distilled water as an intermediate phase, and Soltrol-130 (oil) as the wetting phase. This system of fluids gave a positive spreading coefficient ( $S_{o/w}=+17.7$ ).

For studying the effect of negative spreading, a small amount of isobutanol was added to the water to alter the system into a negative spreading coefficient ( $S_{o/w}=-8.1$ ). For analyzing the oil-wet behavior, the model has been treated with 2% solution of dimethyl 1-dichlorosilane in 1,1,1-trichloroethane (silanization solution).

Experiments took place under room temperature and pressure with no gravity forces affecting the flow due to the micromodel oriented horizontally. A brief experimental procedure is as follows: the model was first fully saturated with water, a high-rate oil-flooding rate was maintained until irreducible water saturation was achieved, a low-rate waterflooding rate until residual oil saturation was achieved, and finally, a tertiary gas-flooding was performed to recover the residual oil left from the secondary waterflooding.

Microscopic Figures show the fluids displacement behavior in distinct, detailed approach. In these Figures, it was clear that oil is the wetting phase and it been suggested that all over the walls of the model channels oil forms continuous wetting films.

Oil trapping in (Figure 2.10a) appeared as water loops blocked the flow of oil significantly. Approximately 2 PV of water contributed in the low-rate flooding step. However, this amount is inadequate for oil films to contribute considerably in the oil recovery. A significant amount of residual oil saturation was left after waterflooding. This has been shown in (Figure 2.10b) with the black region as the oil phase in a soltrol/water arrangement. The residual oil was predominantly trapped in pore throats. This is directly linked to oil-wetting setting, leading oil to inhabit the small pores and throats favorably. The aforementioned is similarly applicable to soltrol/water/isobutanol (non-spreading) system. Waterflooding recovery was similar for both positive spreading oil (Soltrol/water) and negative spreading oil (Soltrol/water/isobutanol) they were respectively 58%(OOIP) and 59%(OOIP) waterflooding oil recovery. Oil estimation before and after waterflooding revealed that the majority of residual oil remains in the throats of the network (75% of total residual oil), unlike water-wet model performance which reveals a roughly even distribution of residual oil between pore throats and pore bodies 50%/50%.

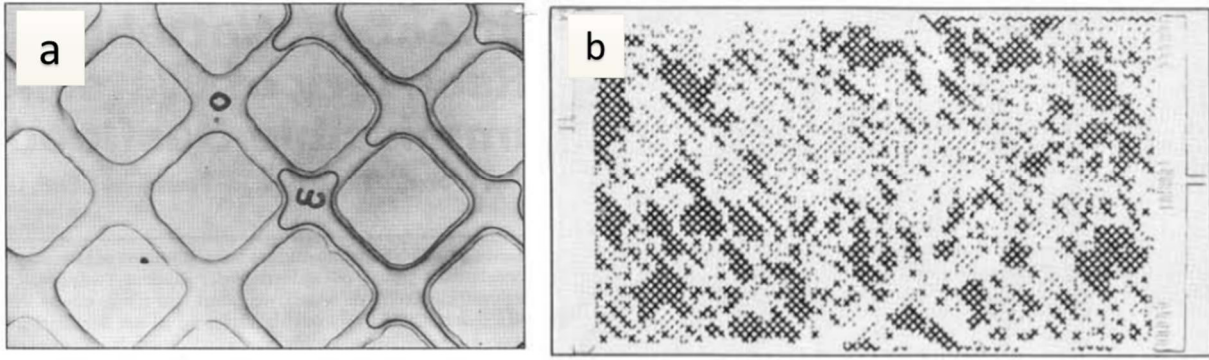


Figure 2.10. (a) fluid distribution in waterflood; (b) residual oil saturation of waterflood (Oren and Pinczewski, 1994)

The allocation and displacement structures of the three-phase fluids in the strongly oil-wet model demonstrated a similar form (Figure 2.11). Specifically, the pore-scale displacement which was proved by the displacement findings. An important difference between positive and negative spreading systems in the oil-wet system was the meetings points of gas and water phases in the network of the model. In the positive spreading system, a thin and stable oil film split the gas and water phases apart (Figure 2.12), this oil film is in equilibrium with the thick oil-wet film throughout the model network. London and van der Waals dispersion forces stabilize the thin oil film; these forces are known to be weak and temporary in the intermolecular level. Still, the film is harmonious with the positive spreading coefficient of oil/water. On the other hand, In the event of negative spreading system, the oil thin film is unstable and rapidly bursts to yield a small three-phase interaction line. Furthermore, the intermediate phase (water) doesn't construct any continuous spreading films.



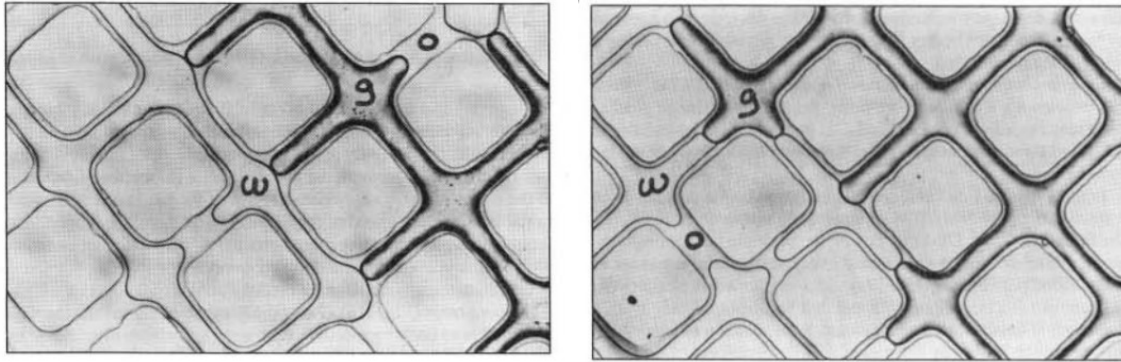


Figure 2.11. Distribution of oil, water, and gas in the oil-wet system  
(left) Positive spreading (right) negative spreading (Oren and Pinczewski, 1994)

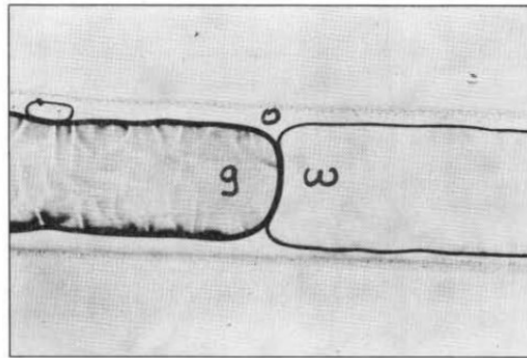


Figure 2.12. The gas interface at the start of the tertiary gas flood (Oren and Pinczewski, 1994)

Gasflooding progress depends on the following factors: (1) capillary pressure threshold associating with oil/water and gas/oil interfaces ( $\sigma_{ow}$  and  $\sigma_{go}$ ); (2) relative throat sizes; and, (3) topographic factors that may influence the behavior. The gas progress is occur either by the encroachment of oil-filled throat (oil direct displacement), or by the double drainage method similar to water-wet model shown in previous study by Oren (Oren et al., 1992), oil produced from the model outlet by water drive that been initiated and displaced by gas (indirect oil displacement).

When gas proceeds in the model network and starts displacing oil, oil displaces directly until the gas faced a pore body saturated with water (Figure 2.13a). In this situation, the gas

interface has two options:(1) to conquer the pore body saturated with water via a double-drainage method or, (2) to occupy oil saturated throat and continue displacing oil through the direct-drainage method. The gas favorably continues displacing oil through the direct-drainage method, and that occur due to important reason, which is the pressure threshold of the throat for the direct-drainage method is subordinate to that for the double-drainage method. The gas keeps displacing oil thru direct-drainage method until additional proceeds are blocked by pore body saturated with water. Eventually, the gas must enter a pore body saturated with water.

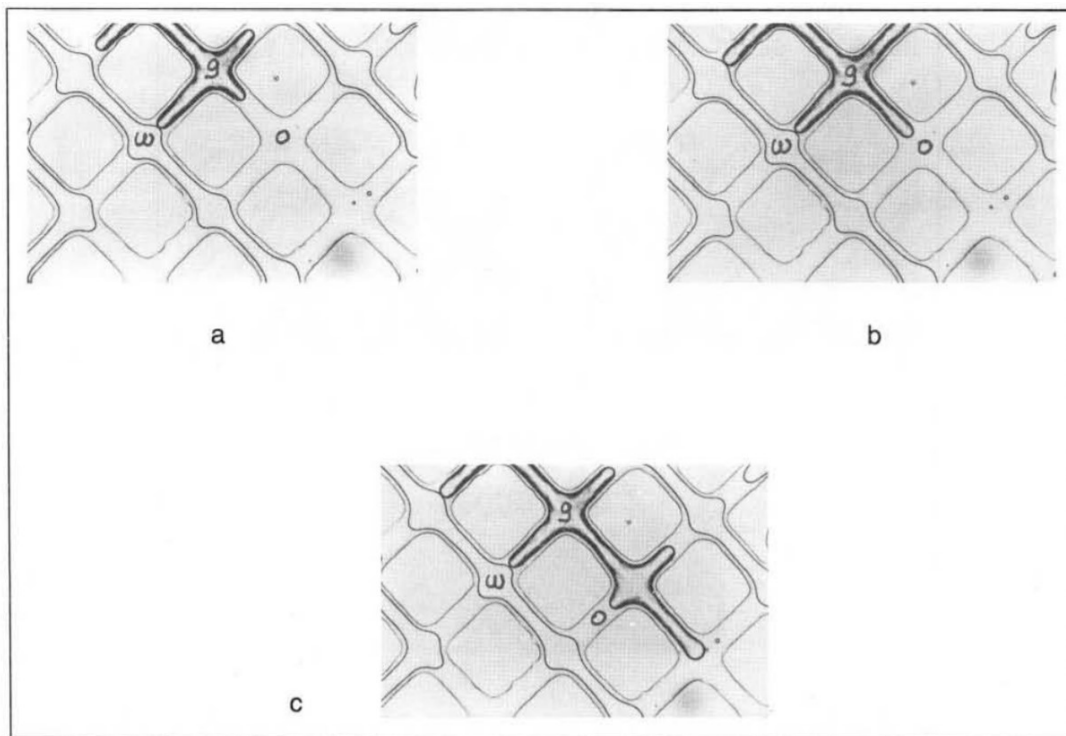


Figure 2.13. (a) Gas meeting a water-filled pore body; (b and c) invading oil-filled ore throats (Oren and Pinczewski, 1994)

The micromodel gas tracing for oil recovery in the tertiary mode indicated no significant difference between the positive and negative spreading systems. In the Figure 2.14 below for oil-wet positive spreading system gas (in black) clearly has swept the model exceedingly excluding the north-east angle of the model (noticeable white chunk) contiguous to the capillary barrier wall.

The reduced pore dimensions in this portion of the model due to inconsistencies in model manufacture stage led to this consequence. The role of the intermediate phase (Water) in the displacement development combined with the pore-scale displacement sequences led to good gas sweep performance. The absent of poor sweep gas performance is associated with the widespread blockage of water-filled pore bodies that the invading gas fingers faced in their way.

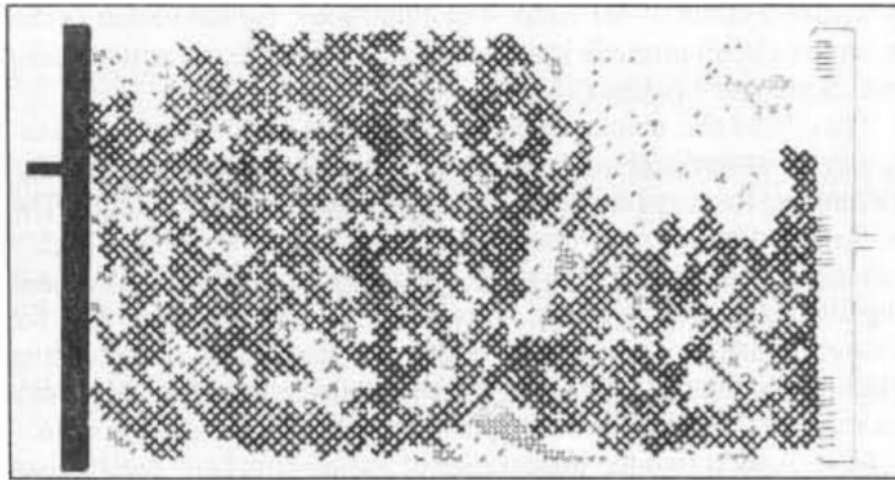


Figure 2.14. Gas (in black) breakthrough in micromodel (oil-wet, positive spreading system) after Oren and Pinczewski (1994)

Lack of distinguishable oil accumulation in oil-wet experiments is the result of the double flow means first by low resistance paths (oil-filled interconnected pore throats and bodies) and second by high resistance paths (oil-wet films). This is a crucial difference from water-wet experiments where oil consistency was a vital requirement for the recovery of oil.

A simultaneous flow in the same pore space is feasible under the existence of continuous wetting and spreading films. In contrast with that, the lack of spreading films led to the possibility of only two phases to flow concurrently. Furthermore, direct nonwetting-/wetting-phase boundaries exist. The three-phases mobility and initial distribution establish the growth of displacement for the three phases.

Oren and Pinczewski (1994) work explained the conventional displacement stages as the following: (1) Gas flowing (non-wetting phase) as injected fluid from the model inlet to displacement location; (2a) Oil or Water displacement as the intermediate phase, or (2b) oil or water displacement as a wetting phase. By the non-wetting phase (first drainage event of the double drainage method). (3a) displaced wetting phase flowing to the model outlet, or (3b) displaced intermediate phase flowing to the second drainage event location. (4) wetting phase is displacing by the intermediate phase (second drainage event). (5) wetting phase (displaced earlier) flowing to the model outlet.

Film flow significance has been evident in the results of the residual oil of waterflood recovery. For the oil-wet condition, the oil recovery was high for both negative and positive spreading situations as the oil-wetting films exist for both positive and negative spreading conditions and play a role in the in the steady high oil recovery. These films suggested being thicker and more conductive when comparing it to oil-spreading films (that exists in positive spreading strongly water-wet system). These films do not exist in the negative spreading strongly water-wet system. Oil recovery showed lower values for a strongly water-wet system this addressed to the nonexistence of the films in the negative spreading case and the unfavorable features (thickness and conductance) comparing it to the oil-wet system.

It has been concluded that gas-flooding project for the oil-wet scheme is of less difficulty and more successful. This is because of: (1) oil-wetting films favorable features aforementioned; (2) enhanced local sweep efficacy were water phase blocks the gas fingers progress; and (3) independence of oil-wet system oil recovery on the sign of the spreading coefficient, whereas water-wet system sign plays a role in the existence of oil-spreading films and ultimately on oil

recovery. In all wettability cases (Strongly- oil/water), the intermediate phase displaced by double drainage method.

However, the wetting phase displacement method is either double drainage or direct in two-phase drainage. Regardless of the method, the result is wetting phase has been produced, and the recovery is always high (compared to intermediate-wet phase). The maximum recovery of waterflood residual oil using gas-flooding is when oil is the strong wetting phase (strongly oil-wet system) with a relatively small difference (10%) for the sign of spreading coefficient. On the contrary, the least oil recovery examined under a strong water-wet system with negative spreading coefficient with no oil films spotted. While, a strong water-wet system with positive spreading coefficient recorded oil recovery value nearly amidst the utmost, and the least values were oil-spreading films occurs.

Spreading effect form the three-phase contact lines, where the three-phases co-exist in one zone of the pore space the equilibrium scheme can choose one of the three arrangements shown in Figure 2.2. The scheme is different in the allocation of Fluid-2 (the intermediate phase) position regarding the other two fluids. Figure 2.2 (A), fluid-2, spreads impromptu between fluid-1 and fluid-3 and wets the wetting phase (fluid-3) completely. Figure 2.2 (B), fluid-2, construct a three-phase contact line (due to fractional wetting between fluid-2 and fluid-3) identified by the three contact angles  $\alpha$ ,  $\theta$ , and  $\delta$  and. Figure 2.2 (C), fluid-2, do not spread or develop a contact line and both the intermediate and nonwetting phases are entirely confined within the wetting phase.

The realistic arrangement of fluids taken by a specific three-phase system is ruled by the wetting preference of fluid-3 and the likelihood of stable contact angles existence.

$S_{23}$  represents the spreading coefficient of the wetting preference of fluid-3, it is given by: -

$$S_{23} = \sigma_{31} - \sigma_{32} - \sigma_{12} \quad (2.10)$$

Where  $\sigma_{31}$ ,  $\sigma_{32}$ , and  $\sigma_{12}$  are the interfacial tensions interfaces for the fluid-3/fluid-1, fluid -3/fluid-2, and fluid-1/fluid-2, respectively.

In the case of  $S_{23}$  having a positive value, fluid -2 spreads in between fluid-1 and fluid-3 and fully surround fluid-1, and phases take the arrangement of Figure 2.2(A). However, when the spreading coefficient has a negative value, spreading of fluid-2 does not occur leading the phases arrangement into adopting either one of Figure 2.2 (B or C). When a three-phase contact line subsists, three forces execute at this line because of the interfacial tensions. While in the event of line tension absence, a balancing force between the three phases at equilibrium demands the fulfillment of the vectorial equation below:

$$\sigma_{13} + \sigma_{23} + \sigma_{12} = 0 \quad (2.11)$$

This equation known as the law of Neumann's triangle (Dullien, 1979), may be used to calculate the contact angles  $\alpha$ ,  $\theta$ , and  $\delta$ , as below:

$$\cos \alpha = \frac{\sigma_{12}^2 - \sigma_{23}^2 - \sigma_{13}^2}{2 \sigma_{13} \sigma_{23}} \quad (2.12)$$

$$\cos \theta = \frac{\sigma_{13}^2 - \sigma_{23}^2 - \sigma_{12}^2}{2 \sigma_{12} \sigma_{23}} \quad (2.13)$$

$$\cos \delta = \frac{\sigma_{23}^2 - \sigma_{12}^2 - \sigma_{13}^2}{2 \sigma_{12} \sigma_{13}} \quad (2.14)$$

While the hypothesis of the existence of the contact line tension was discussed before (del Cerro and Jameson, 1978), the previous literature (Pujado and Scriven, 1972; del Cerro and Jameson, 1978) predicted a prospective small overall effect on the contact angles estimated by the equations above. The presence of a stable three-phase contact line is subjunctive to the following expressions: -

$$S_{23} < 0$$

$$\frac{\sigma_{13}}{|\sigma_{12} - \sigma_{23}|} > 1$$

If the above conditions are satisfied, then the fluids form a stable three-phase contact line, and the phases distribution is following the one in Figure 2.2(B). Provided that the inequalities not be satisfied with the spreading coefficient having a negative value, there will be no contact line and no spreading of fluid-2 and that fluids allocation will be taking the one in Figure 2.2(C). With the information of the three interfacial tensions and the wetting tendency of the solid, equations (2.10 - 2.14) can be used to evaluate approximately the pore-scale fluid distribution for the three-phase systems in a porous medium.

In conclusion, in porous media when one of the three phases wet a solid strongly, pore-scale distribution of the fluids is distinctively governed by wettability, capillary pressure, and the spreading coefficient of the fluids in the medium. In a pore-scale measure, three-phase displacements follow either a double drainage method if the nonwetting phase is the displacing phase in the system, or an imbibition-drainage method if the intermediate phase is the displacing phase. Spreading influence in three-phase flow is substituting the role of wettability in two-phase flow considering a simple generalization of two-phase flow to describe three-phase flow mechanisms. That is shown in the sharing of the principle of the pore invasions progression which is controlled by pore capillary pressures threshold.

Vizika and Lombard (1996) proposed that both the wettability of the porous media and spreading properties of fluids dominate gravity drainage of three-phase during injection of gas. Experiments have been conducted on water-wet, oil-wet, and fractional-wet sandpacks using different spreading fluids systems, followed by, a numerical simulation and history matching

performed to calculate the relative permeability of fluids. The goal was to measure the effect of wettability and spreading on the recovery of oil and the distribution of fluids in the porous medium.

The authors established the presence of "wetting and spreading oil films" because of both wettability and spreading phenomenon. These films impact three-phase flow and ultimately the recovery of oil.  $K$  defined as the equilibrium between the interfacial tensions in the system, which refer to the spreading coefficient of oil on water with gas existence.

The formula below shows the value of  $K$  (when water spread on oil the coefficient of spreading will be indicated by  $K'$ ):

$$K = \sigma_{wg} - (\sigma_{wo} + \sigma_{og}) \quad (2.15)$$

Six experiments conducted, two for each type of wettability (water, oil, and fractional). The fractional wettability sandpack contains (50% water-wet and 50% oil-wet) sand.

CT and gamma-ray have been used to generate porosity profiles. Three combinations of fluids used interchangeably, two of these were with negative  $K$  (non-spreading condition), and one was positive  $K$  (spreading condition). An approximate of 2% isobutanol to the brine will alter the polarity of the spreading coefficient from positive to negative. The findings of Vizika and Lombard are summarized in the following points: first, the spreading coefficient of oil on water ( $K$ ) is the main factor affecting recovery in both water-wet and fractional-wet systems. In oil-wet case ( $K'$ ) does not influence the recovery but involved in the distribution of the three phases in the medium. Second, the highest recovery of oil for positive  $K$  and water-wet or fractional-wet, this because of the flow of oil via spreading films maintained by hydraulic continuity.



## 2.2. Studies of Core-scale

In the literature reviewed, it is shown that significant work has been done previously on uniform water-wet systems and, multiple authors achieved low oil saturation. Oak et al. (1990) used an intermediate-wet Berea sandstone to study relative permeabilities of the three-phase system. Jerauld (1997) structured a model to analyze the three-phase relative permeability of Prudhoe Bay reservoir which has been reported as a mixed-wet reservoir. Sahni et al. (1998) utilized computerized tomography (CT) scanning to quantify oil and water relative permeability in water-wet systems with consideration and analysis of the spreading coefficient (Dicarlo et al., 2000).

Zhou and Blunt (1998) studied the role that fractional wettability plays in gravity drainage of the three-phase system. They noticed a definite bond between the final oil saturation and the fraction of oil-wet sand. They performed the experiments on sandpacks with different fractions of oil/water sand to enhance and better understand the gas gravity drainage which is used in EOR projects. As a motivation for their work, they reasoned that gravity drainage had been proven in literature to be an effective method in the recovery of oil in strongly water-wet environments. Controlling and specifying the fraction of water/oil-wet surfaces in sandpacks eliminates the effect of wettability from the other factors, whereas reservoir cores need sophisticated care and handling to preserve the reservoir in-situ properties and measure and quantify these properties precisely. In their paper, the influence of wettability of fluids distribution has been analyzed. It has been considered that in the oil-wet system, water is the extreme nonwetting phase, not the gas.

Experiments executed using Isooctane, distilled water and air. Seven drainage experiments have been accomplished with sandpacks of an oil-wet sand fraction of (0,25,40,50,60,75) and 100%. This oil-wet sand prepared by soaking the sand in heavy crude oil for a minimum of 24 hrs. Before being washed with isooctane and oven dried.

Furthermore, Zhou and Blunt (1998) addressed in their study the stable configuration of fluids (gas, oil, and water) in pore space. Since there are interactions between these fluids and the solid surfaces, there are different types of setting the fluid take, depending on the strength of wettability of the solid. In their work they suggested in case the surface was strongly water-wet, a water film can form covering the surface, and this water film prevents oil and gas from contacting the solid. However, in case the solid was weakly water-wetted this water film will not form. Characterizing this situation is more complicated. Strong oil-wet solid system, oil forms films covering the solid surface. In case the oil-wetting the surface weakly these films do not exist (Figure 2.15 shows these four cases).

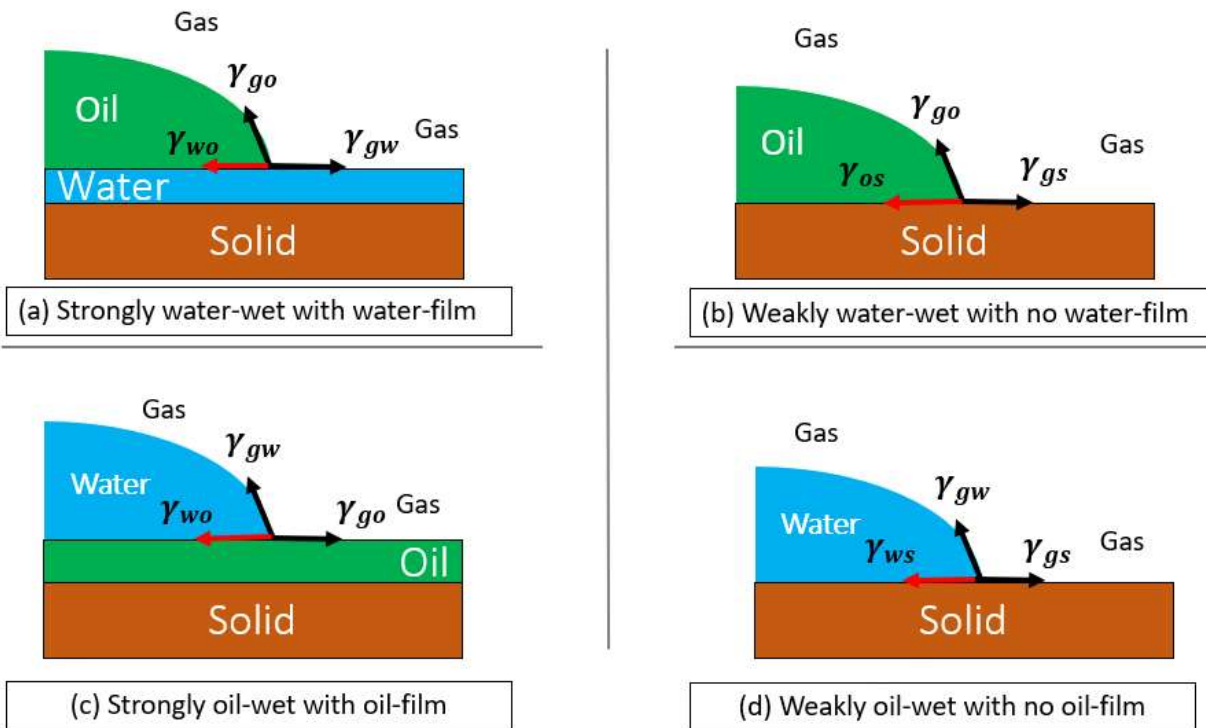


Figure 2.15. Different configurations of oil, water, and gas on a flat solid surface. (A) a strongly water-wet surface coated by a water film; (b) a weakly water-wet surface with no film; (c) a strongly oil-wet surface coated by oil, and (d) a weakly oil-wet surface with no oil film. After Zhou and Blunt (1998)

Ultimately, it is found from the experimental and theoretical results that in oil-wet sandpacks, the extreme non-wet phase is water and gas is the moderate wetting phase. The minimum saturation of water been noticed in two sandpacks one with 25% oil-wet sand the other with 75% oil-wet sand with a maximum saturation in case of 50% oil fraction.

The residual oil saturation at the end of gravity drainage rises as the percentage of oil-wet sand increased. The performance of residual water saturation was in three different zones: one is ruled by snap-off, the isolation of perfect water-wet pores controls the second, and the last zone is influenced by the seizure of water found in water wet corners (Zhou and Blunt, 1998).

Dicarlo et al. (2000) thoroughly analyzed the relative permeability behavior with different sets of wettability in sandpacks. Capillary pressure for two-phase(water/oil) curves was plotted versus water saturation  $S_w$  to depict the wettability of each sandpack. By measuring the saturation in situ along the pack length using computerized tomography (CT) scanning, the oil, and water relative permeability been acquired midst three-phase gravity drainage. Gas relative permeability has also been attained by measuring the pressure gradients in the gas phase. Several findings have been achieved, these findings explained regarding two parameters which are wetting and spreading. The authors referenced the fundamental importance of three-phase flow understanding in oil reservoir enhance oil recovery projects. Three-phase flow occurs during some regular processes like thermal flooding, gas cap expansion, and gas injection.

The presence of three-phase flow led to having a moderate-wetting phase neither wetting nor nonwetting which will position exceptionally in the porous media, and eventually affect macroscopic characteristics like relative permeability and residual saturation.

Gravity drainage can merely defined as the gravity-driven displacement of reservoir fluids (oil and water) by gas (can be injected gas or can be air through free fall experiments). The

phenomenon considers a substantial three-phase process which takes place within gas cap expansion in reservoirs. Hysteresis consequence is not considered when it comes to gravity drainage analysis, which is one of the reasons that ease the experimental study of gravity drainage even with the significant importance of hysteresis in the flow of three-phase in porous media.

Sandpacks have been used due to that it can be easily characterized. Sand used is industrial (No. 60, Corona Industrial Sand Co., Corona, CA) which naturally water-wet. The sand was sieved to remove and fine particles. Oil-wet sand prepared by soaking the original sand in a mixture of 20% crude oil (Thums Inc., Long Beach, CA) and 80% isooctane for 24 hours. After, the soaked sand was washed with fresh iso-octane and left to dry by air (Dicarlo et al, 2000).

Fractional-wet sandpack recovery curve was in between the recovery curves of oil-wet and water-wet sandpacks. Even it appears as obvious conclusion yet; it encloses valuable concepts. Oil in the spreading system is always hydraulically connected despite the fraction of oil-wet sand in a fractional-wet sandpack since oil can reside in the corners of the pores in case of oil was the most wetting fluid, or in layers in case, oil was an intermediate-wetting fluid. Adhere to that Kro will not reach the value of a zero but approaches this value at residual oil saturation and this for all wettability types. Also, the saturation of trapped water is a bit higher for fractional-wet media when comparing with oil-wet media (Dicarlo et al, 2000).

The reason is due to the poor connection between the oil-wet zones in the sand-pack which leads to a considerable amount of trapped water, this phenomena been explained in more profound extent by Zhou and Blunt. In sandpack experiments, all the pores are formed by several grain surfaces. A noticeable feature is the corners of pores which influence the fluids configurations.

Zhou and Blunt (1998) used an equilateral triangle (as a simplistic approach) to substitute for a cross-section of pores. Every two surfaces formed a corner. In perfect water-wet pore water

inhibits the smaller crevices (triangle corners) while oil exists as films on water, and gas (most non-wetting phase) occupy the center of the pores (shown in Figure 2.16 triangle a). In a perfect oil-wet pore system oil occupy the corners, gas will be in contact with oil, and water (as the most non-wetting phase) occupies the center of the triangle. Donaldson and Crocker (1977) revised the model with a buffer of more wetting gas since the interfacial tension of gas-oil is low (shown in Figure 2.16 triangle b). Finally, intermediate (fractional) wetting pores are the most complex one. It is assumed that gas occupies the center of the pores and water and oil arbitrarily occupy the crevices (shown in Figure 2.16 triangle c).

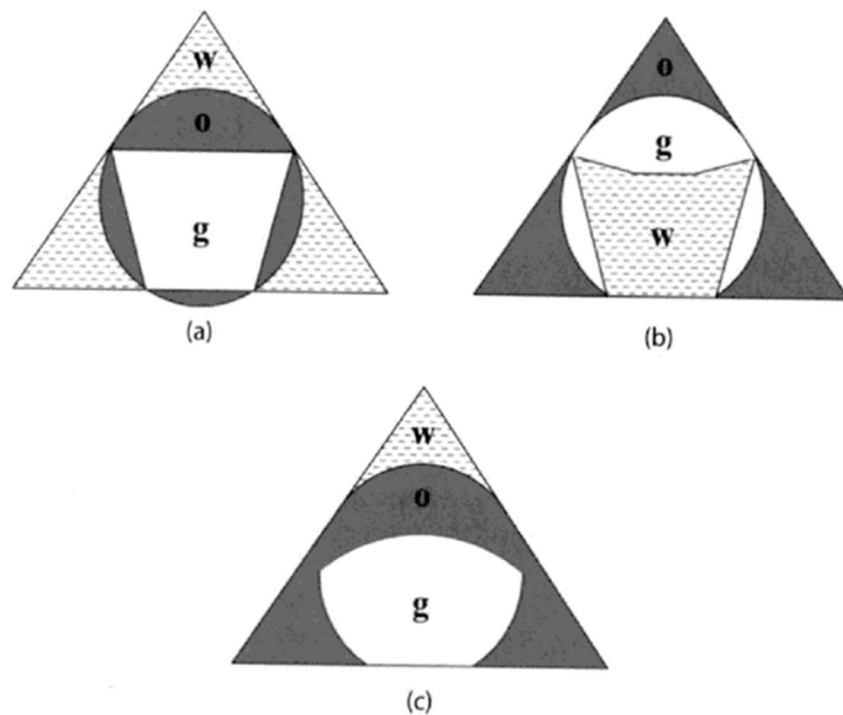


Figure 2.16. Possible static positions of gas, water, and oil in three overall conditions of wettability. (a) water-wet pores with water in the corners and oil spread over the water, (b) oil-wet with oil occupying the corners and gas (more wetting to oil than to water) in contact with the oil, (c) intermediate-wet where corners contain either water or oil depending on the preferential wetting conditions of exposed faces of individual grains (Zhou and Blunt, 1998).

Further clarification for pore-scale physics role in was made the experiments been performed by Dicarolo et al. (2000). Similar behavior of the relative permeability of the strong wetting phase in both oil and water wettability systems was observed. The utmost wetting phase fills the smaller pores, and corners, grooves, and cracks in the bigger pores. Nevertheless, there is no precise universal function for relative permeability since it depends on the porous medium. However, there is ordinary merit for  $K_r$  which that it will approach the value of zero but will never be equal to zero at adequate high capillary pressure, demonstrating that the most wetting phase is still connected, even though poorly, through wetting films in slits of the medium shallow to minimal saturation.

Also, it has been noticed at low saturation entirely different curves for  $K_{ro}$  in the water-wet system and  $K_{rw}$  in the oil-wet system. Whereas the saturation of fluids is low, the wetting films (layers) of fluids maybe still connected in the microscopic angles of the pore system. This exact connectivity controls  $K_r$  in the state of low saturation. Pore-scale arrangement and connectivity are distinctly different between the water-wet and oil-wet mediums. The surface of pores coated by the most-wetting phase and the consequence of the imbalance of interfacial tensions is the presence of contact angle between the three phases (oil, water, and gas) which rule the position of the phase in the pore space, assuming the existence of thick wetting layer coating the solid surface.

Fractional-wet systems were used previously (Vizika and Lombard, 1996; Zhou and Blunt, 1998; and Dicarolo et al., 2000). However, Dicarolo et al. (2000) debated the limitation of the fractional-wet system and the need to include a mixed-wet one, because it is more realistic when it comes to the imitation of physical sequence of wettability alteration in an experimental laboratory work, which eventually promotes a system contain a pore-scale model of wettability demonstrates a natural reservoir rock. The mixed-wet system prepared by injecting crude oil to

water-wet water filled sandpack with aging the oil for several days. The process results in a wettability alteration for the sand surfaces that came in contact with the crude oil. Moreover, ultimately the result is a mixed-wet system with water filling the small pores and pore angles as their wettability did not change and stayed water-wet, while the larger pores are filled with the injected oil since the wettability is changed there. Fluids used in the experiments are n-hexane, n-octane, or n-decane as an oil phase, distilled water as a water phase, and air as a gas phase.

Results of the fractional-wet system recorded a high value for both the connate water saturation  $S_{wc}$  and the residual oil saturation  $S_{or}$  (compared to water-wet, oil-wet, and mixed-wet). This result is explained by the presence of pockets of oil-wet and water-wet zones since oil-wet, and water-wet surfaces are interconnected randomly. Due to the random distribution of the sand grains network, each sand is either water or oil wet, and that led to a pore side wetting with either water or oil. This setting led to no pore size preference for oil or water (no specific wettability segregation dependence on pore size).

### **2.3. Applications on Field-scale**

Considering a reservoir scale problem, when primary recovery ends, and a significant amount of oil is left behind, the oil in place that “trapped” in the pore space of the reservoir sometimes may be as high as 80-90 percent (Melzer, 2012).

Secondary production is used to increase the percent of the recovered oil, where water or gas injection (flooding) may be used. The injected fluid is used to sweep the trapped oil through pressure maintenance and displaced it towards the producing wells. A successful project will eventually leave 50-70 percent of the reservoir original oil in place (OOIP). A partial sweep event

is a result of fluid bypassing the oil in the formation since no interaction or mixing is taking place (Melzer, 2012).

Enhanced oil recovery (EOR) was introduced to the industry as conventional waterfloods recovery rarely exceed 40 percent of (OOIP). EOR can be divided mainly into three categories: Thermal, chemical, and miscible. Thermal method principally deals with heavy oil by lowering the viscosity to enhance oil recovery. Whereas, chemical and miscible target the light and medium gravity oils by adjusting the interfacial tension, viscosity, and other factors by oil/gas interaction (in gas injection case) (Rao, 2001). Recently, because of the environmental benefits and the continuous developments of the CO<sub>2</sub> gas injection method, it is beginning to grow compared to other methods and compared to first years of usage (Koottungal, 2008).

CO<sub>2</sub> is selected for the advantage of improving the oil recovery by reducing the interfacial tension, lowering oil viscosity, and swelling the oil which all ultimately helps to mobilize the components of oil (Verma, 2015).

The Gas Assisted Gravity Drainage (GAGD) process utilize the natural segregation phenomena of fluids in the reservoir, oil displacement occurs with gravity support and improves oil recovery take place. The GAGD process consists of utilizing a group of vertical injectors to inject CO<sub>2</sub> to develop a gas cap working as a piston-like to drain the oil and water down to horizontal producer(s). Figure 2.17 shows the count of different EOR methods.



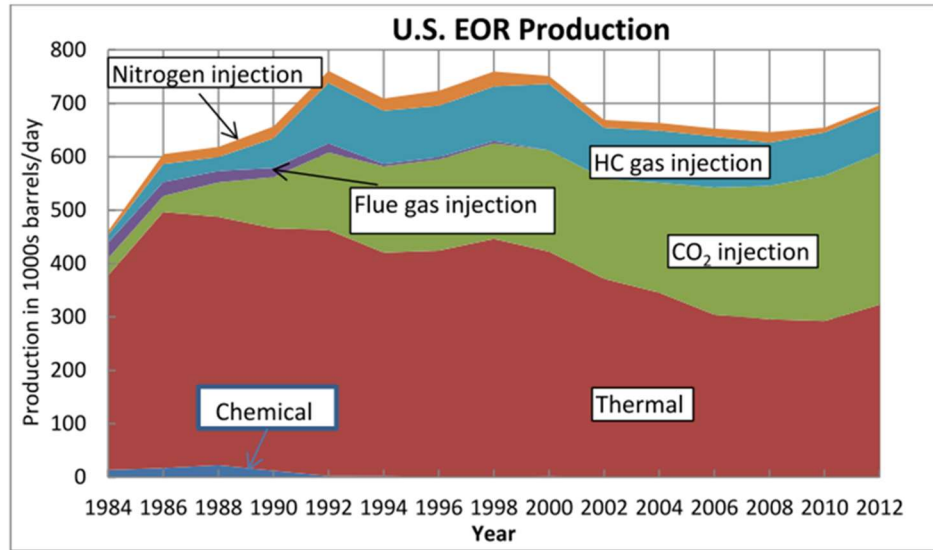


Figure 2.17. Plot is showing U.S. oil production in barrels per day associated with various enhanced oil recovery (EOR) methods (Koottungal, 2012, and Kuuskraa, 2012). HC, hydrocarbon; CO<sub>2</sub>, carbon dioxide.

Through field-scale simulations of cyclic CO<sub>2</sub> and Continuous injection methods of the GAGD process in a heterogeneous sandstone oil reservoir in South Rumaila oil field, it observed that the process is efficient in improving oil recovery. It is also identified that using the cyclic injection GAGD method was superior to the continuous gas injection (CGI) for higher oil production, and reduced gas injection/injection pressure. In conclusion, both experimental and field scale application reveals that the GAGD process is improving the oil recovery in different reservoirs, such as sandstone and carbonates. Furthermore, the GAGD process accomplished higher recovery factors in field scale application than the continuous gas injection (CGI) and Water Alternative Gas (WAG)(Al-Mudhafar et al., 2017).

## **CHAPTER 3. EXPERIMENTAL MATERIALS, APPARATUS, AND PROCEDURES**

### **3.1. Materials Used in the Experiments**

To construct a porous medium which represents a model for a realistic oil reservoir and to study the three-phase flow in gravity drainage mode, a selection of solids and fluids (three-phases) were chosen. Sand from US Silica (AFS 50/70) was used as the reservoir rock (solid) in the experiments. The three phases were: deionized water serves as the water phase, Decane or Soltrol (170) as the oil phase and Nitrogen (N<sub>2</sub>) as the gaseous phase. More details on materials are specified below.

#### **3.1.1. Sand Description**

"The Original Ottawa Silica" sand was used throughout all the experiments. With the AFS 50/70 filling the pack fully except a small two layer (each layer was  $0.5 \pm 0.2$  in) of Filter Sand "QUIKRETE® Pool Filter Sand (No. 1153)". The Filter Sand packed in the bottom and the top (both ends of sandpack). Filter Sand is coarser compared to AFS 50/70, and it has been added to reduce the entry capillary pressure the fluids facing at the start or end of the saturating process of a sand column packed completely with AFS 50/70 fine size sand and to avoid flooded sandpack events. Filter Sand is a high quality, narrowly graded, and clean dry silica sand with a particle size of (0.85-0.425 mm). The AFS 50/70 is composed predominantly of Silicon dioxide (99.8%), with a median particle size of 0.26 mm and bulk density of 1.5 g/mL.

### 3.1.2. Fluids Description

All the experiments have been conducted with the following fluids:

- 1- Deionized water: a pure pretreated water source used for all experiment as the aquatic phase and all (solid/water), (oil/water), and (gas/water) interactions was used. DI water was used to saturate the sandpack in order to calculate the porosity and Absolute permeability ( $k_{abs}$ ).
- 2- Nitrogen(N<sub>2</sub>): Nitrogen gas was injected from a compressed gas cylinder and used as the displacing gas phase, regulated using a flowmeter and a pressure regulator to flow with constant rate and constant pressure (immiscible mode).
- 3- Decane or Soltrol: the oil phase used in the experiments was either Decane or Soltrol depending on the desired spreading coefficient of the system. Using Decane revealed a non-spreading system ( $S_{ow} = -ve$ ), where oil (Decane) does not spread over water. Using Soltrol-170 revealed a spreading system ( $S_{ow} = +ve$ ), where oil (Soltrol) does spread between water and gas. Both oils are originally transparent, but was colored red using Sudan IV dye so that the oil phase can be recognized visually in the sandpack through the experiment.

A summary of the fluids physical properties listed in Table 3.1. Also, interfacial tensions and spreading conditions for the systems used are listed in Table 3.2 below. These measurements collected on Decane, water, and Nitrogen were from Zhou and Blunt (1997); Sharma and Rao (2008). Similarly, Soltrol-170 from Chatzis and Ayatollahi (1993).

Table 3.1. Physical properties of experiments fluids (at room temperature)

Fluid	$\mu$ (cP)	$\rho$ (g/mL)
Water	1.00	0.9982
Nitrogen	0.01755	0.001165
Decane	0.84	0.734
Soltrol-170	2.72	0.781

Table 3.2. Experiments systems: interfacial tensions and spreading conditions values

System (Spreading condition)	$\sigma_{wg}$ (dyne cm <sup>-1</sup> )	$\sigma_{ow}$ (dyne cm <sup>-1</sup> )	$\sigma_{og}$ (dyne cm <sup>-1</sup> )	$S_{ow}$ (dyne cm <sup>-1</sup> )
Decane + H <sub>2</sub> O + N <sub>2</sub> (-ve)	72.1	52.0	23.5	-3.4
Soltrol + H <sub>2</sub> O + N <sub>2</sub> (+ve)	71.0	35.0	24.0	+12.0

### 3.2. Experimental Apparatus

The experimental apparatus was constructed with a group of units that were connected through a network of plastic capillary pipes that can be screwed together using metallic connections. Each unit composed of the sand container (Porous media), fluid containers (graduated cylinder/gas cylinder), and measurement devices (gauge/burette). Some peripheral equipment such as tongs (utility clamps) and ring stand were also used. Main component details are listed later in this section.

#### 3.2.1. Apparatus Configurations

There are three main configurations for the apparatus, these include: -

A- Water saturation configuration: -

Used at the beginning of each experiment (when the sandpack is new and the sand has not yet been in contact with any fluids) to inject water into the porous media in order to obtain the porosity of the sandpack, the absolute permeability, and establish the saturation history. This configuration includes: the sandpack, burette, gauge, HPLC pump, and graduated cylinder. The configuration shown in Figure 3.1.

B- Oil saturation configuration: -

After water saturation, the apparatus is reconfigured to be prepared for oil saturation. Oil was stored and injected with the help of fluid transfer vessel. Oil saturated the sandpack completely to further establish a complete saturation history at the connate water ( $S_{wc}$ ).

The oil saturation configuration includes all the parts used in water saturation configuration except for adding the fluid transfer vessel. The configuration shown in Figure 3.2

C- Gas Injection configuration: -

This configuration was used to inject the gas into the oil-saturated sandpack in order to obtain the recovered oil (production). This configuration is identical to the oil saturation configuration to the right of the pressure gauge. While to the left of pressure gauge the system connected with a gas cylinder through a flowmeter with a valve. The configuration shown in Figure 3.3

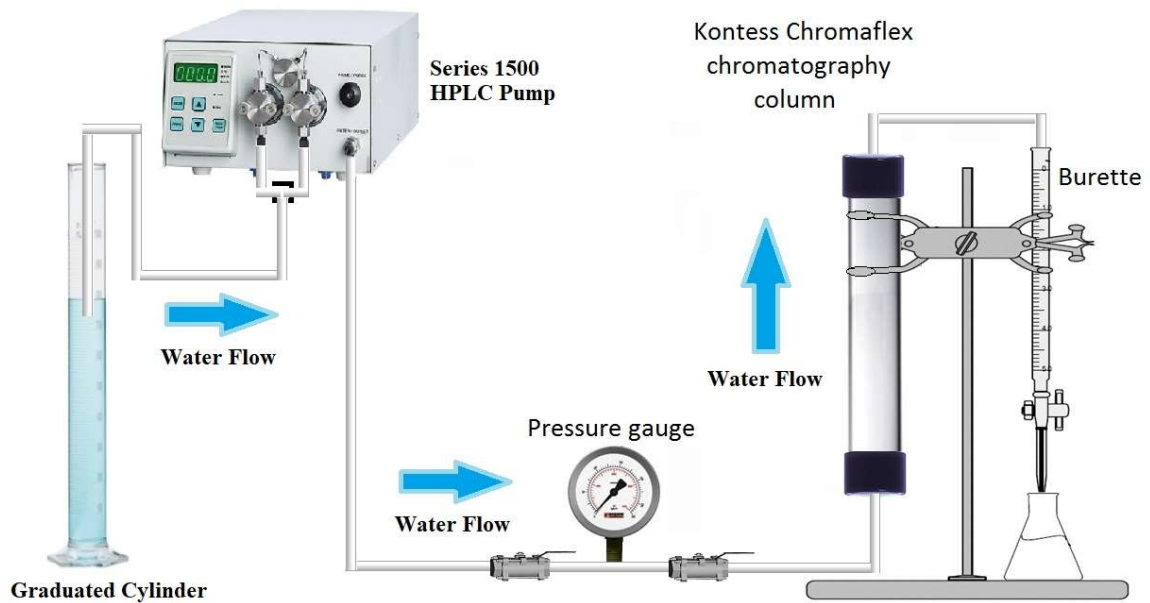


Figure 3.1. Experiment configuration for water saturation.

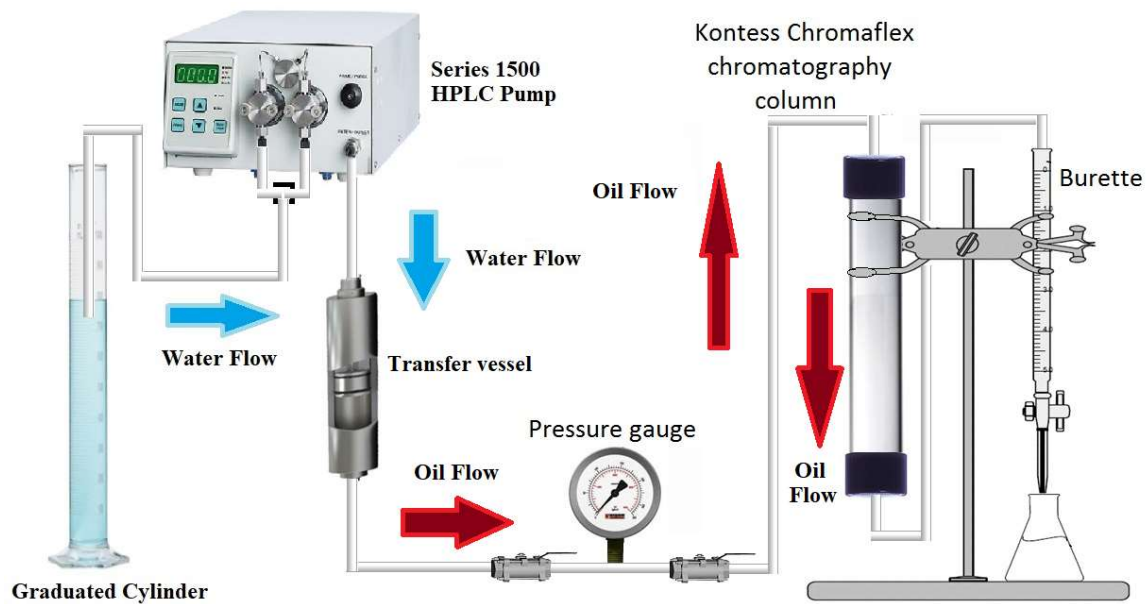


Figure 3.2. Experiment configuration for oil saturation

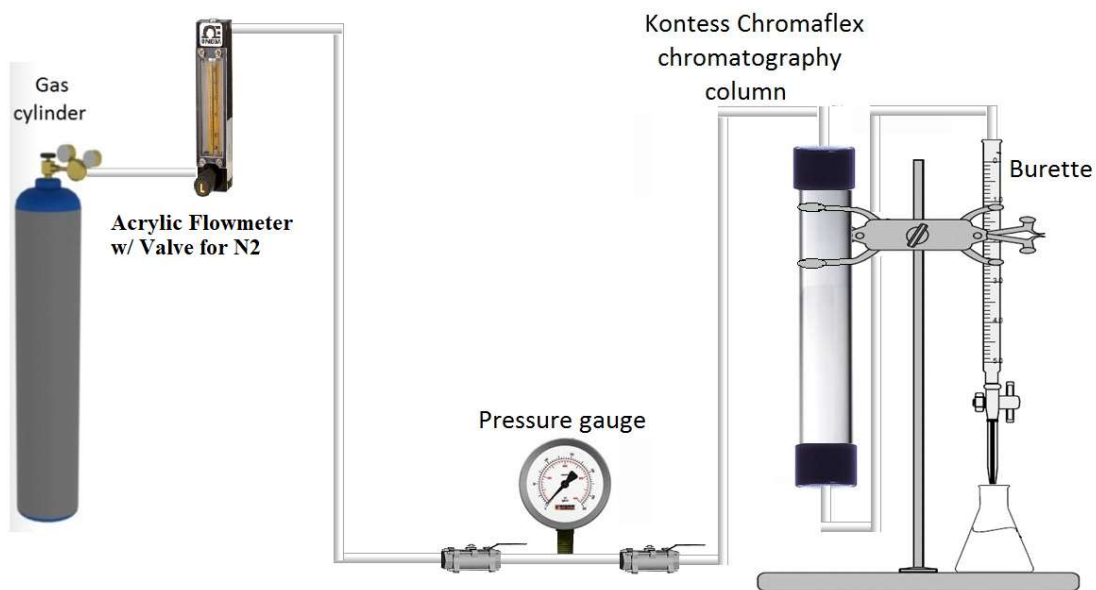


Figure 3.3. Experiment configuration for gas injection

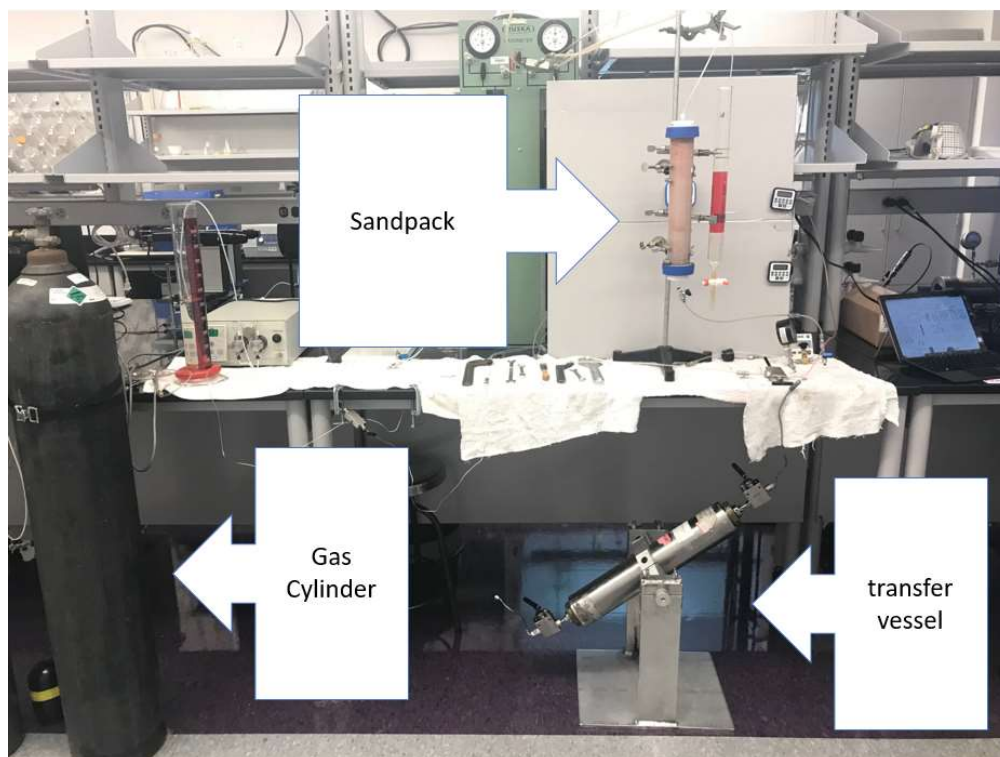


Figure 3.4. Picture of the laboratory apparatus used in the experiments

### 3.2.2. Apparatus Components Description

In this section, each component will be described in more details: -

**The Sandpack (Sand container):** the container used is a Kontes® CHROMAFLEX® Chromatography Column. This sand column comes in different standard specifications and types; the one used in the experiments is the 420830 Series. It is made of Class A Borosilicate Glass and has a cylindrical shape with a length of 30 cm and internal diameter (ID) of 4.8 cm. This gives a bulk volume of 543 mL. With this ID, the column withstands 50 psi of maximum pressure at 50°C. The endcaps are equipped with High-Density Polyethylene (HDPE) filter which has a micro-porosity (20-micron nominal) that prevent sand from flowing out of the column and allow only fluids to flow when needed.

This chromatography column was chosen because it was designed to prevent leakage and promote ease of handling, also the ease of cleaning after changing the sand patches after every experiment. Likewise, for being ideal for the aqueous and organic mobile phases.

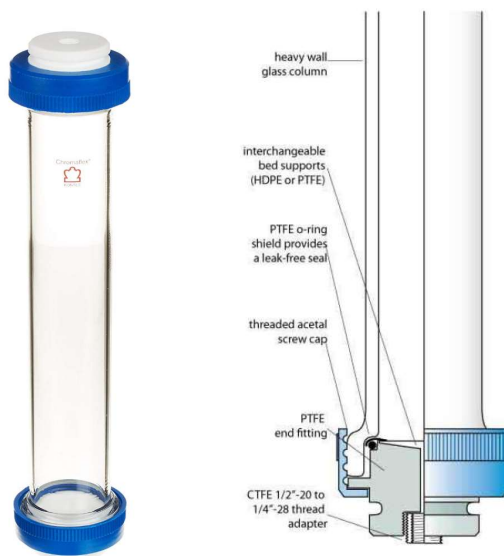


Figure 3.5. (left): Picture of an empty sand column, (right): a cross-section through an end cap of the column showing the bed support parts.

**HPLC pump:** A High-performance liquid chromatography (HPLC) model 1500 Dual Piston Pump was used to pump water from a graduated cylinder. Pump flow rate capacity is 0.001 mL with increments from 0.000 to 12.000 mL/min. The pump was used in both the water and oil saturation configuration. However, due to the existence of wetted materials parts (such as stainless steel) inside the pump (pump heads, check valve bodies, and tubing), the pump was used only to inject water (no direct contact with oil) since the wetted materials can be damaged when injecting oil directly. For that reason, a transfer vessel was added for the oil saturation configuration.



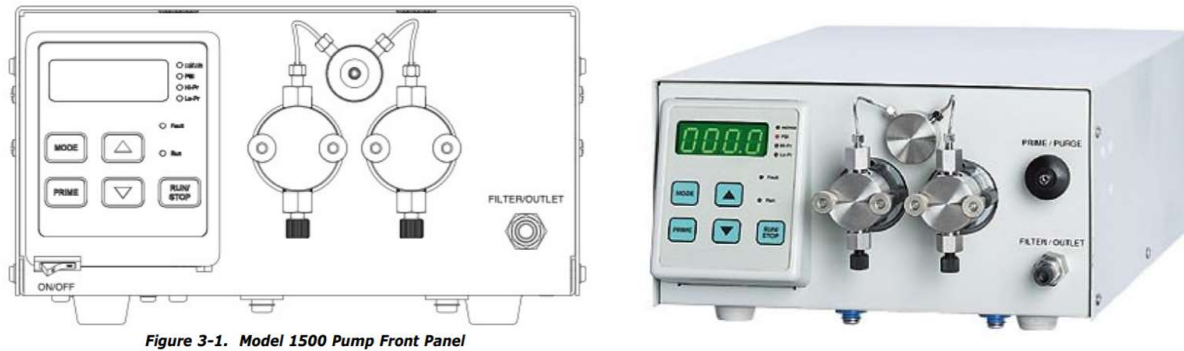


Figure 3-1. Model 1500 Pump Front Panel

Figure 3.6. HPLC pump (left) schematic frontal view (right) actual view

**Graduated cylinder:** Used as a water source for the pump. Is graduated at 5 ml interval and can contain up to 1000 mL of liquid. The water was used to either: pump directly into the sandpack or to push the piston inside the transfer vessel.

**Transfer vessel:** Used as an oil source for the sandpack. It can contain up to 500 mL of oil. This vessel has a piston that divides it into two separate compartments. One contains the water that is injected by the pump which pushes the piston, the other contains the oil that is injected by piston movement (refer to Figure 3.2). The transfer vessel was used only with the oil saturation configuration due to the possible damage that can occur when injecting oil directly.

**Pressure gauge:** A low-pressure mechanical dial type “US Gauge series 734” was used for these experiments with a range of 0 – 5 psi. Since the sandpack used in the experiments is unconsolidated sand, a low-pressure gauge is ideal for accurate measurements of pressure fluctuations. Experimentally, it is used in the calculation of permeability using Darcy’s law.

**Burette:** Used as a container and separator for the produced fluids (water/oil). It is graduated at 1 mL interval and it can contain up to 250 mL of fluids. With plastic stopcock at the lower end, and it is graduated from (250-0) mL bottom-top. Water was filled to the 250 mL line to mark the base for volume measurements. The burette was held using a ring stand.

**Gas cylinder:** The gas source was pressurized nitrogen ( $N_2$ ) stored and used to inject the gas phase. As a safety measure, the cylinder is secured firmly in upright position to the laboratory worktable using a clamp with strap and chain both wrapped around its body. The cylinder was fitted with a pressure regulator to control the pressure of the flowing gas into a constant value of approximately 5 psi. The low pressure achieved with the flowmeter was used to maintain a stable rate of gas injection that guarantees a stable gravity-drainage process needed in the experiment.

**Flowmeter:** Used to sustain a constant gas flow rate of 2.5 mL/min (the minimum scale rate available). This acrylic flowmeter is designed for fluids such as air, oxygen, nitrogen, carbon dioxide. It equipped with a low hysteresis needle valve to control the rate with stable, easy-to-read float. All the experiments were used with these conditions (Gas flow rate = 2.5 mL/min, Pressure= 5 psi) unless different conditions noted.

**Peripheral components:** A computer used to record and plot the data and measurements and analyze them. Various timing equipment was used, and a video recorder system (Sony HDR CX440) to monitor the gas advancement using video capture with Long Play (LP) mode since each experiment takes many hours. A tripod stand used to fix the system in a proper position. Another small mobile phone camera was used to take close-up shots.

### 3.3. Experimental Procedures

In this section, the experimental procedure will be explained in detail. This section has two parts: the first procedure, performed as a continuous from Dzulkarnain (2018) work where the experiments are conducted using 2 cc/min flow rate for water and oil saturation. After a series of trial experiments, an optimum procedure was developed and has been proposed.

In addition to the 2 cc/min flow rate, a slower flow rate of 0.25 cc/min for water and oil saturation was also used. Using the slower second flow rate helped produce better saturation profiles and more accurate results. Regardless of how the saturation procedure was performed, the preparation of the sandpack was the same.

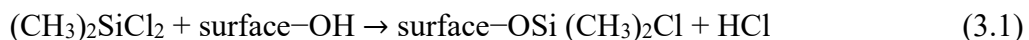
### 3.3.1. Wettability Alteration of the Sand

The sand is originally water-wet. In order to study the sand's behavior under oil-wet conditions, the porous media requires an alteration of sand wettability. The sand was first found to be water-wet through the visual testing of pipetting water droplets on sand particles that are placed on a cellophane strip and observing these drops spreads entirely. This resulted in a contact angle of about  $180^\circ$  revealing a perfect water-wet scenario. Also, as per of Seed (2001) since the sand grain surface contains a silanol group, it is considered as water-wet.

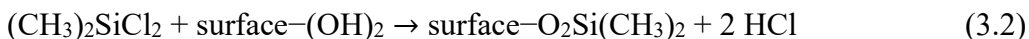
The wettability alteration process is called silanization. This process starts with treating the sand with a silylating agent (dichlorodimethylsilane ( $(\text{CH}_3)_2\text{SiCl}_2$  or DCDMS) is used in this case), the agent used to change the sand grain to be water repellant. DCDMS reaction forms a light oil coating the sand grain surface this coating is bonded chemically to the grain surface. This oily coating is responsible for shifting the wettability of sand into oil-wet (Dzulkarnain, 2018).

The mechanism for this process is through DCDMS reacting with the silanol groups, forming siloxane (Si–O–Si) linkage and liberating HCl as chemical interaction result.

Herzberg and Erwin (1970) expressed the reaction as chemisorption process on the surface and state it with the following equations:



The second reaction occurs as the second chlorine in  $(\text{CH}_3)_2\text{SiCl}_2$  additionally reacts with the hydroxyl group located on the surface of the sand, as the formula describes:



This second reaction forms more siloxane polymers and releases HCl. The presence of water as an adsorbed phase on the sand surface is essential for the reaction, as water hydrolyzes the silanes and acts as a catalyst. The sand grain surface becomes hydrophobic as the resultant of the mentioned reactions (polymeric siloxane) coats it (the grain) with silicone oil (Dzulkarnain, 2018).

Experimentally, the laboratory procedure to alter the wettability is divided into two operations. The first one is where the wettability alteration occurs while the second one is a follow-up process that is guaranteeing that the solvent in the first step is in full contact with all the sand grains. Details of both operations (these operations need to be conducted inside the fume hood and ensuring the lab operator is wearing all the required PPE (personal protective equipment), especially eye goggles and standard respirator) in the following steps:

Step 1: A solvent of 5% by volume of DCDMS in toluene prepared, this solvent reaction releases a hazardous HCl (cautious required consider warnings mentioned above).

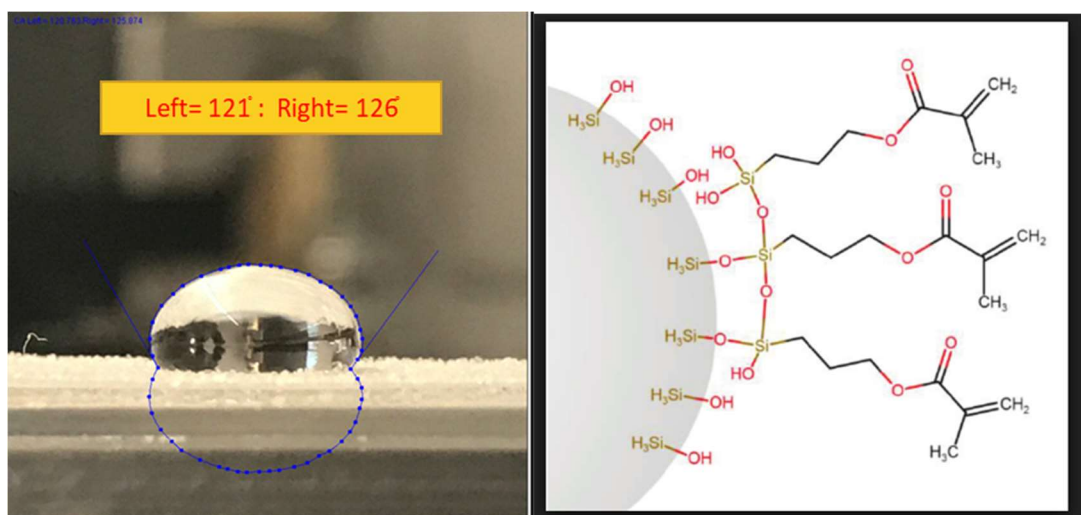
Step 2: Soaking the sand in the prepared solution for 15 minutes keeping it in the fume hood.

Step 3: The soaked sand was rinsed with Methanol (used as an organic solvent).

Step 4: The sand patch was left overnight in the fume hood to dry and evaporate the methanol.

Step 5: The sand was dried by baking it in a special oven at approximately 90°C for four hours.

Despite silanization process effects on sand grain surface chemically, the microscopic observation of Vizika and Lombard (1996) confirms no changes in either grain size distribution or grain surface morphology.



### 3.3.2. Preparing and Packing the Sand in the Sand Holder

When dealing with a clean sandpack (further actions needed when dealing with a used sandpack), the first step is to obtain the right combination of fractional wettability sand. When packing a (25% oil-wet/ 75% water-wet) sandpack as an example. Since the bulk density of the sand is equal to 1.5 g/mL, and the bulk volume of the sand container is equal to 543 mL an approximate of 815 g of sand is needed to fill the container completely. Therefore, a 204 g of oil-wet sand (that was already prepared earlier as per the last section) is mixed with a 611 g of water-wet sand in Erlenmeyer flask with the cap. The flask needs to be shaken thoroughly to ensure that all grains mixed arbitrarily.

The mixed sand was spread in glass plate to be packed. Scooping from the glass plate into the sandpack was done haphazardly from different points to increase the uncertainty of the packed sand structure. The empty sand container was gripped with a ring stand, then filled gradually and slowly with sand using a small 25 g scoop. To spread the sand evenly, rotating and shaking the sandpack was used because a mechanical means of helping to evenly distribute the sample was not available. As per of Oliviera et al. (1996) procedure, a solid object used for sandpacking after every sand accumulation of 1 cm, this method guarantees a regular and consistent packing. After filling the sandpack completely, the end bed cap used to plug the hole and press the sand column before screw the threaded cap a last visual check is useful to ensure the column is fully stuffed with sand.

### 3.3.3. Conducting the Experiments

As outlined before, the experiments can be divided into two main categories depending on the operation procedure conditions. The first group, performed with fluid (water/oil) flow rate for saturation of 2 mL/min. for the second one, a slower flow rate proposed for optimum saturation

rates the flow rate was of 0.25 mL/min. Before conducting every experiment, a functionality test was performed on the HPLC pump to certify its accuracy.

#### 3.3.3.1. Procedure (A): Saturation Flow Rate of 2 mL/min

This procedure contains the following steps:

##### **Step 1: Injecting water bottom-to-top to determine the pore volume (PV), porosity ( $\phi$ ), and absolute permeability ( $k_{abs}$ )**

All experiments start with establishing the saturation history by saturating the sandpack with water bottom top. The water injection rate was equal to 2 mL/min and was controlled by the pump (water source is the graduated cylinder filled with 1000 mL of DI water), this step also used to calculate the porosity of the sandpack since the bulk volume of the sand container is known and equal to 543 mL. Moreover, the pore volume was identical to the amount of water used to saturate the sand in the column (a quick reading from the water reservoir (graduated cylinder connected to the pump) give the volume). The porosity was determined by dividing the pore volume (PV) by the bulk volume (BV):

$$\text{Porosity } (\phi) = \frac{PV}{BV} \quad (3.3)$$

The absolute permeability calculated with the help of the pressure gauge. After measuring pore volume, the sandpack will be fully saturated, and the water will start producing at the other end (at the top end of the sandpack keeping the flow rate constant at 2 mL/min all the times).

The pressure reading will be fluctuating at that moment when water starts producing from the top end. After the pressure reaches a stable state (3 to 4 mins) a pressure reading was recorded versus flow rate. Increasing the flow rate by (+1 mL/min) at a time and recording the pressure reading against each flow rate reveal a linear behavior when applying Darcy's law:

$$k_{abs} = \frac{q\mu L}{A \Delta P} \quad (3.4)$$

Where:

$k_{abs}$ : is absolute permeability measured in *Darcy*,  
 $q$ : is the average flow rate measured in mL/min,  
 $A$ : is the cross-section area of the cylindrical sandpack,  
 $\mu$ : is the viscosity of the displaced fluid in cp,  
 $L$ : is the sandpack length in cm, and  
 $\Delta P$ : is the pressure drop in atm.

Using Darcy's equation with the data acquired and the known constants then plotting  $q/A$  on the Y-Axis and  $\Delta P/L\mu$  on the x-axis the slope of the line fitted to the data gives the desired unknown  $k_{abs}$ .

## **Step 2: Injecting Oil top-to-bottom to complete establishing the saturation history and calculate original oil in place**

After the sandpack is fully saturated with water from Step-1, the lines and connections will be adjusted from the water saturation configuration shown Figure 3.1 to oil saturation configuration shown Figure 3.2. As explained before in the apparatus configurations a fluid transfer vessel was used as the oil reservoir to inject into the sandpack, and the saturation direction was from top to bottom of the sandpack. A constant oil flow injection rate was used (2 mL/min) with the control of the HPLC pump. The oil saturation stopped when the oil break-through and no more water produced noticed anymore (Around 2-3 PV).

After this step the original oil in place (OOIP) and the irreducible water saturation ( $S_{wc}$ ) were calculated using the following equation:

$$S_{wc} = \frac{PV-OO}{PV} \quad (3.5)$$

While the initial oil saturation calculated using:  $S_{oi} = 1 - S_{wc}$



OOIP is equal to the volume of water displaced (produced) by the oil till the end of oil saturation.

### **Step 3: Free-Fall Gravity Drainage (FFGD)**

The oil saturation configuration from the last step was the same except for one change, where the top cap of the sandpack unscrewed, and the cap bed removed allowing the atmosphere pressure to apply as the gravity drainage taken place without gas injection (Free-Fall). The experiment continued for 12 hours, and both the oil recovery and pressure were recorded against time (minutes).

### **Step 4: Re-saturating (2<sup>nd</sup> time) sandpack with oil top-to-bottom**

After the FFGD, the sandpack is re-injected with oil to arrive at the state before the FFGD. An assumption of  $S_{wc}$ ,  $S_{oi}$  being identical to the one calculated before the FFGD process taken place.

### **Step 5: Secondary Gas-assisted gravity drainage (Sec. GAGD)**

After the sandpack has been pre-saturated with oil, the apparatus was converted into the gas injection configuration. With the top cap being closed Nitrogen( $N_2$ ) and injected at a rate of 2.5 mL/min (controlled using the wheel on flowmeter) from the top at constant pressure. The experiment lasted for 12 hours, both oil recovery (at the bottom end) and pressure reading been recorded against time.

### **Step 6: Re-saturating (3<sup>rd</sup> time) sandpack with oil top-to-bottom**

This step is similar to the procedure conducted after the FFGD, where the sandpack has been re-injected with oil. The assumption in step-4 is still effective here.

**Step 7: Secondary water-flooding**

To prepare for a tertiary mode recovery, a water-flooding secondary recovery is needed. Therefore, a water-flooding process was performed before the tertiary GAGD. In this step, a water-flood oil residual saturation was instituted. A 0.35 PV of water injected bottom to top at a constant rate of 2 mL/min, an adequate amount of oil remains in the sandpack for tertiary mode recovery. As before, oil recovery and pressure reading was recorded during this step.

**Step 8: Tertiary Gas-assisted gravity drainage (Tert. GAGD)**

Tert GAGD was performed directly after the water-flooding (no re-saturation occurs before Tert. GAGD). Nitrogen gas (N<sub>2</sub>) injected from the top at a constant pressure similar to secondary GAGD process for 12 hours. Corresponding to another drainage process the oil recovery and pressure drop reading were recorded. However, an extra data output was water recovery readings.

A summary of the procedure steps demonstrated in Figure 3.8 below:

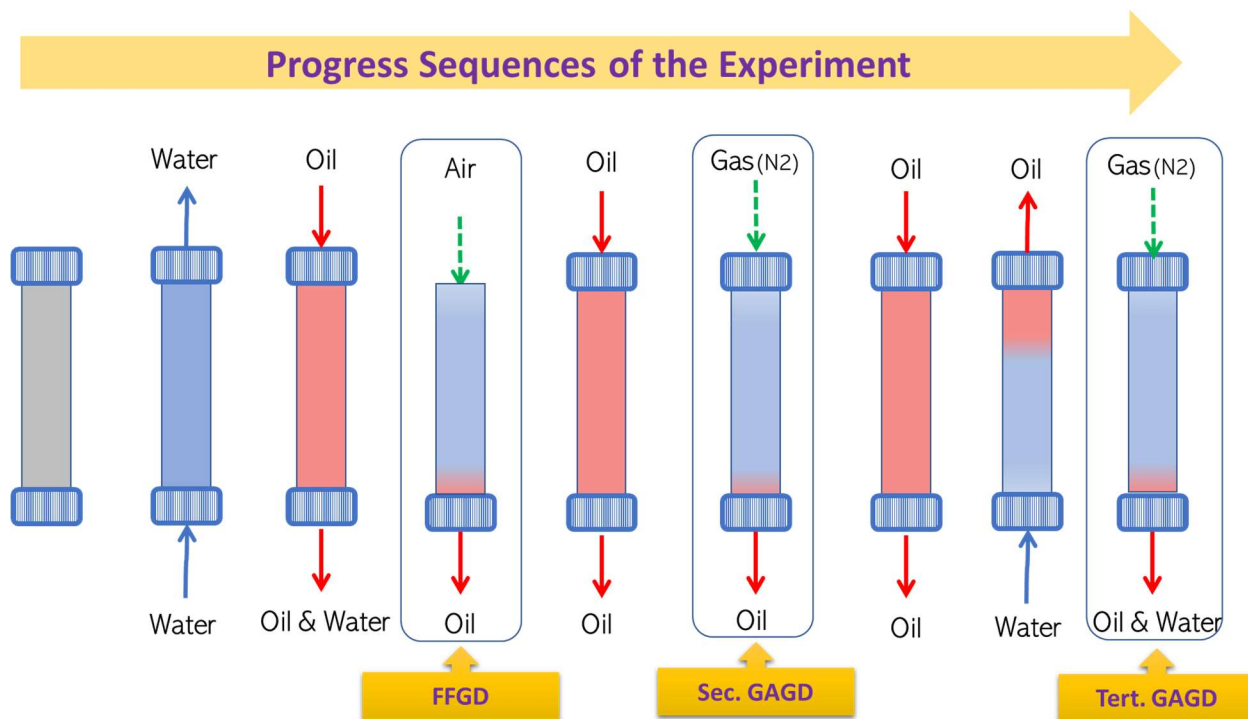


Figure 3.8. Procedure (A) sequences of the experiment

After the experiment ended (after 12 hours of Tert. GAGD), the sandpack is disconnected from the rest of the apparatus equipment. Then the end caps of the sand container were unscrewed, and the beds removed. The used sand patch is discarded in a waste container (segregation of waste and following the safety guidelines and procedures is mandatory). Finally, the sand container is cleaned with toluene in order to remove any oily residuals and after the container is cleaned using test tube brush and detergent then rinsed with water. The sand container is dried using an air stream and kept ready for a new patch of sand. Sand pack changed for every combination of wettability + system spreading.

### 3.3.3.2. Procedure (B): Saturation Flow Rate of 0.25 mL/min

This procedure is similar to the procedure (A) except for a few minor differences. After trying the new saturation rate of 0.25 mL/min for step-1 and step-2 above, it was confirmed to provide more accurate and consistent results. However, since a lower flow rate means a longer the time to complete the saturation of the sandpack (time change from few hours to a minimum of 11 hours), a decision has been taken to focus and perform the Secondary Gas-assisted gravity drainage mode only. The decision was made specifically with the need to explore more different types of wettability and system spreading. A summary of the new procedure steps demonstrated in Figure 3.9 below:

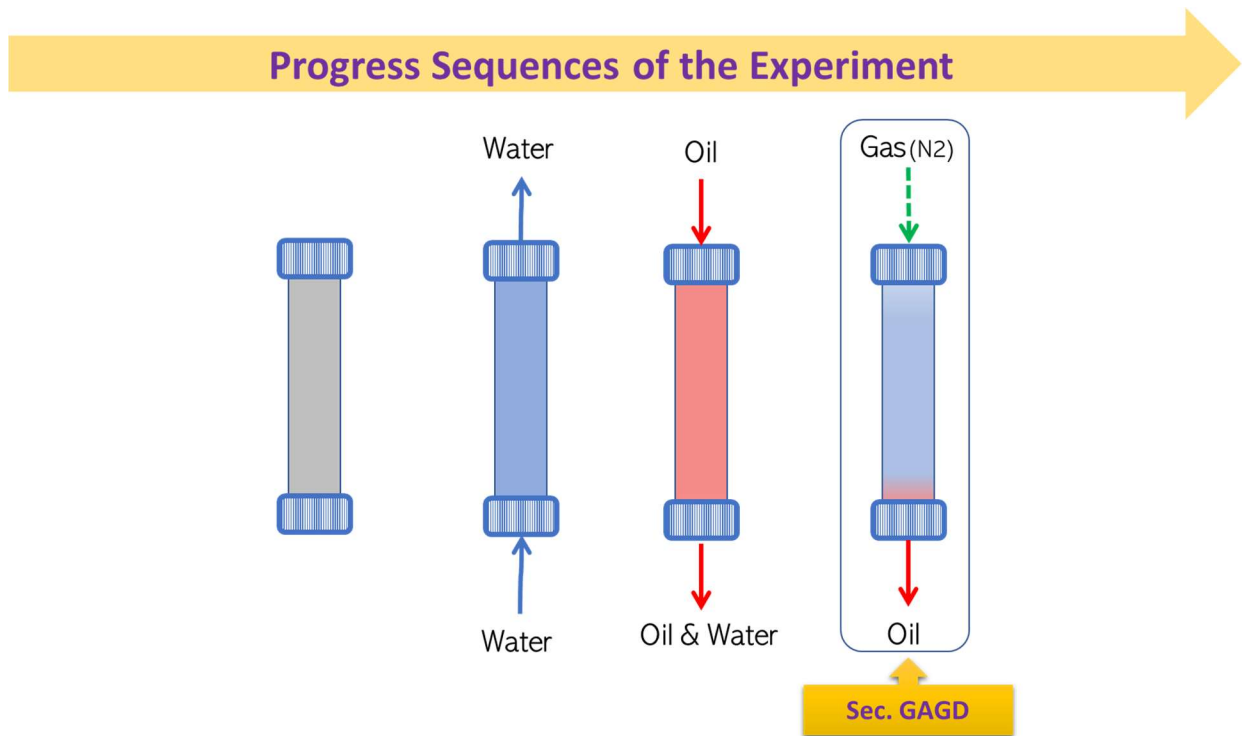


Figure 3.9. Procedure (B) sequences of the experiment

Reasons to modify the experimental from procedure (A) to procedure (B):

**First: - To obtain more stable and consistence saturation profiles:**

Before considering if the recovery of fluids is accurate and represents a practical capacity of a specific wetting sandpack and spreading conditions, it is very important to make sure that the sandpack is saturated properly and no premature fingering of saturating fluids occurs. Observations of inconsistency in saturation between the different recovery modes were one of the main reasons to further adjust the procedure. Examples of these inconsistencies shown in Figure 3.10.

**Second: - Using a stable rate that guarantees the consistency of saturation profiles**

Time is an essential factor in conducting experimental work, but the accuracy of results is more imperative. Since the results of some experiments conducted with procedure(A) deemed to be inconsistent, or not precise enough to indicate the effect of a change in oil sand percent (such as increasing oil-wet sand with 25%), a need for a specific rate was mandatory to carry on with the experiments. Dumore (1964) suggested that in order to obtain a gravity-stabilize flow where no fingering occur, a critical velocity ( $u_c$ ) which is the maximum velocity at which the interface will remain more stable is needed. Moreover, the injection of fluids needs to be maintained below this critical velocity to sustain stable flood displacement using Dumore equation below:

$$u_c = \frac{\rho_o - \rho_s}{\mu_o - \mu_s} k g \quad (3.6)$$

However, using customary units, the equation is presented by Green and Willhite (1998) in the following the form:

$$u_c = \frac{0.0439 k (\rho_d - \rho_D) \sin \theta}{\mu_D (M-1)} \quad (3.7)$$

Where: -

$u_c$ : the critical velocity in ft/day,

$D$ : symbolize a property of displacing fluid; while  $(d)$ : symbolize a property of the displaced fluid

$k$ : the permeability in *Darcy*

$\rho$ : density of the fluid

$\theta$ : the dipping angle (in this case it equal to  $90^\circ$  since we are using vertical setup)

$\mu$ : is the fluid viscosity

$M$  : is the viscosity ratio and it equal to  $= \mu_d / \mu_D$

Using the above equation 3.7, and the fluid properties in section 3.1.2. The critical velocity has been calculated, and it was 0.0076 cm/sec, or when considering the laboratory setup, it will be in a rate of 1 mL/min considering water as the displacing fluid and air as the displaced fluid (for water saturation process). The equation applied again for calculating the minimum rate of oil saturation which was 0.01235 cm/sec, in a laboratory setup, it will be equal to 1.6 mL/min. These numbers expose the reason why procedure(A) was inefficient since it performed using a flow rate of 2 mL/min, which is higher than the critical velocity computed above which in return results in an earlier breakthrough of fluid without the sandpack being fully saturated. Eventually, incompetent saturation leads to incompetent recoveries. For that, a low flow rate of 0.25 mL/min has been used for saturation of water and oil in the procedure (B) since it is way below the critical values of velocity (1 and 1.6) mL/min. The results of procedure (B) were accurate and consistent, with quite appealing saturation profiles as pictures indicate in Figure 3.10f compared to old procedure.

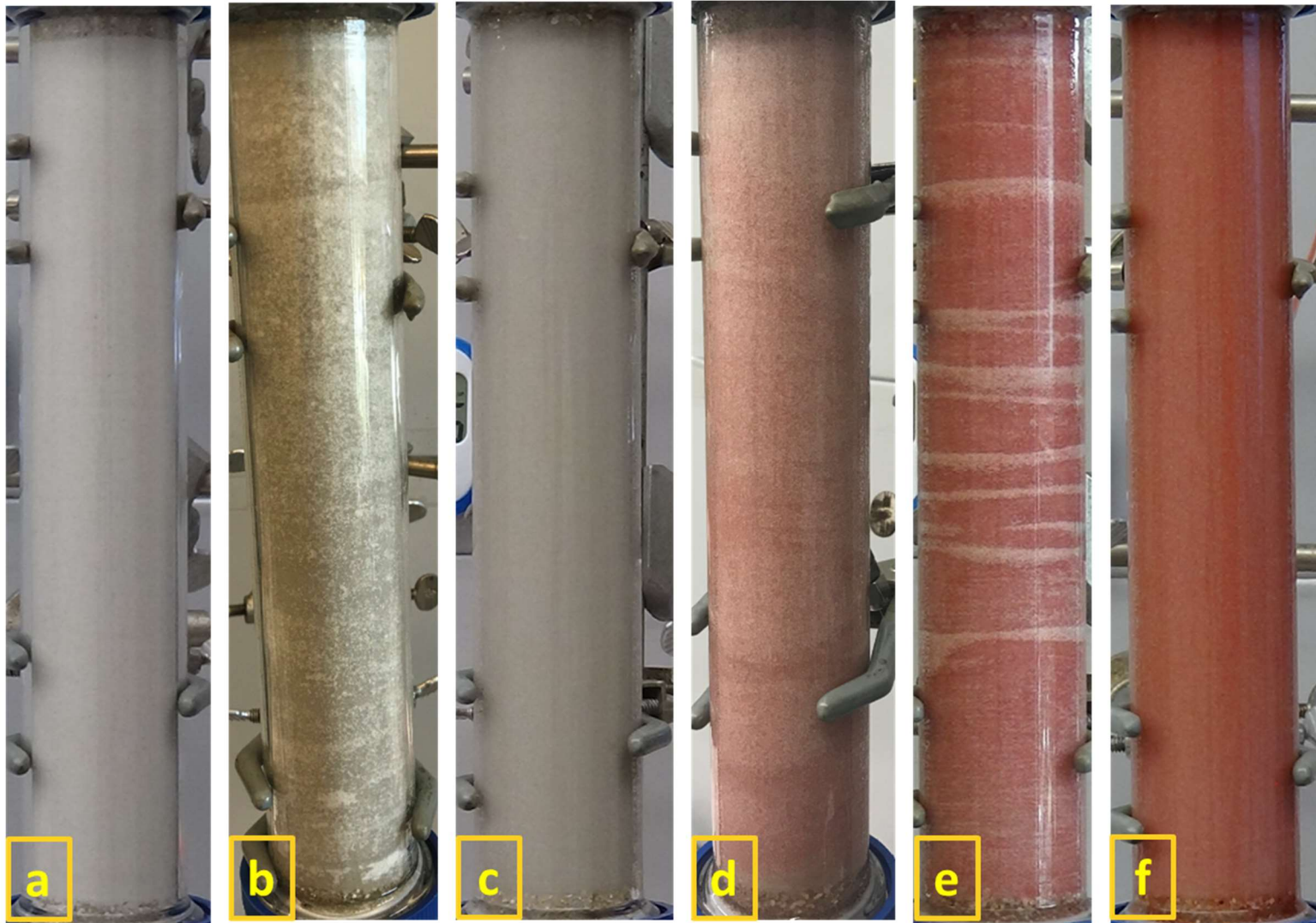


Figure 3.10. Water-wet sandpacks at different conditions: (a) new unsaturated sand; (b) improper water-saturated sand; (c) proper water-saturated sand; (d) improper oil-saturated sand; (e) improper oil-saturated sand; (f) proper oil-saturated sand

## CHAPTER 4. RESULTS AND DISCUSSION

In this chapter, the results of the conducted experiments will be presented. For the first series of experiments (procedure -A), the results were in the form of oil recoveries for three modes: Free-Fall Gravity Drainage (FFGD); Secondary Gas-assisted gravity drainage (Sec. GAGD); and, Tertiary Gas-assisted gravity drainage (Tert. GAGD). These modes performed in both spreading (Soltrol) and non-spreading (Decane) systems. Since the first group of experiments (with fluid saturation flow rate of 2 cc/min) conducted using a sand combination of (25% oil wet + 75% water-wet) revealed inconsistent results, the results were disregarded. For apparatus calibration purposes only, two (100% water-wet) experiments have been performed (one with Decane the other with Soltrol). The second series of experiments (procedure -B), has been conducted with only the Secondary Gas-assisted gravity drainage (Sec. GAGD) mode. Ten experiments were conducted in total, using both spreading (Soltrol) and non-spreading (Decane) fluid systems, and different combinations of sandpack wettability: [(0, 12.5, 25, 62.5, 100) % oil-wet sand + the rest being water-wet sand].

### 4.1. Experimental Results

The experimental results summary is displayed below. Later, the results are grouped by the wettability of the sandpack. In the end, discussion is included on the type of spreading system. All recovery percentages listed below (unless mentioned otherwise) were representing the recovery of oil as a percent of original oil in place (OOIP)%. Spreading conditions of the system will be represented using the spreading coefficient ( $So$ ), where a system with decane oil will be a negative spreading system (-ve)  $So$ , and a system with Soltrol oil will be a positive spreading system (+ve)  $So$ .



#### 4.1.1. Procedure (B) Results

A summary of the results for experiments conducted is listed in table 4.1 Below. These results show the outcome of Secondary Gas-assisted gravity drainage mode, each sandpack with the associated spreading conditions (+ve/-ve) and sand wettability percentage combinations [X% WW +(100 – X) % OW]. An average of porosity was approximately 31%, and a minimum of 30.76% the porous medium was suitable for representing a sand environment. Having consistent porosity values is an indicator of steadiness and success of the packing method.

Table 4.1. Summary of experimental results for procedure (B)

Wettability	WW	OW	Spreading conditions			$\phi$	$S_{wc}$	$S_{oi}$	Recovery
WW	100	0	Soltrol	Spreading	+ve	30.76	0.1198	0.8802	77.55
WW	100	0	Decane	non-Spreading	-ve	31.31	0.2412	0.7588	65.89
FW	87.5	12.5	Soltrol	Spreading	+ve	31.77	0.1826	0.8174	73.75
FW	87.5	12.5	Decane	non-Spreading	-ve	31.31	0.2176	0.7824	65.41
FW	75	25	Soltrol	Spreading	+ve	33.15	0.1389	0.8611	72.90
FW	75	25	Decane	non-Spreading	-ve	31.49	0.2573	0.7427	66.92
FW	37.5	62.5	Soltrol	Spreading	+ve	31.31	0.1471	0.8529	72.41
FW	37.5	62.5	Decane	non-Spreading	-ve	33.15	0.1611	0.8389	72.84
OW	0	100	Soltrol	Spreading	+ve	30.76	0.1557	0.8443	61.70
OW	0	100	Decane	non-Spreading	-ve	32.41	0.2386	0.7614	78.35

WW: Water-wet sandpack experiment

FW: Fractional-wet sandpack experiment

OW: Oil-wet sandpack experiment

$\phi$ : Porosity (dimensionless)

$S_{wc}$ : Connate water saturation (dimensionless)

$S_{oi}$ : initial oil saturation (dimensionless)

Recovery: Recovery for Secondary Gas-assisted gravity drainage mode (% OOIP)

The values of connate water saturation were particularly higher in the non-spreading fluid system compared with spreading fluid system except for sandpack containing 62.5% OW sand in which both spreading and non-spreading fluids systems have similar  $S_{wi}$ . The reason might be due to the difference in mobility ratio between the spreading and non-spreading fluid systems. In the spreading system, Soltrol has a viscosity of 2.72 cP leading to very favorable mobility ratio for Soltrol (less than 1.0) during oil injection to reach  $S_{wi}$ , which reduces the possibility of fingering and leads to a piston-like displacement (hence yields better sweep) and lower water saturation in the sandpack. In the non-spreading system, Decane has a viscosity of 0.84 cP leading to unfavorable mobility ratio for Decane (higher than 1.0) during oil injection to reach  $S_{wi}$ , which develop fingers or tongues resulting in oil by-passing water zones and higher water saturation in the sandpack (Dake, 1978).

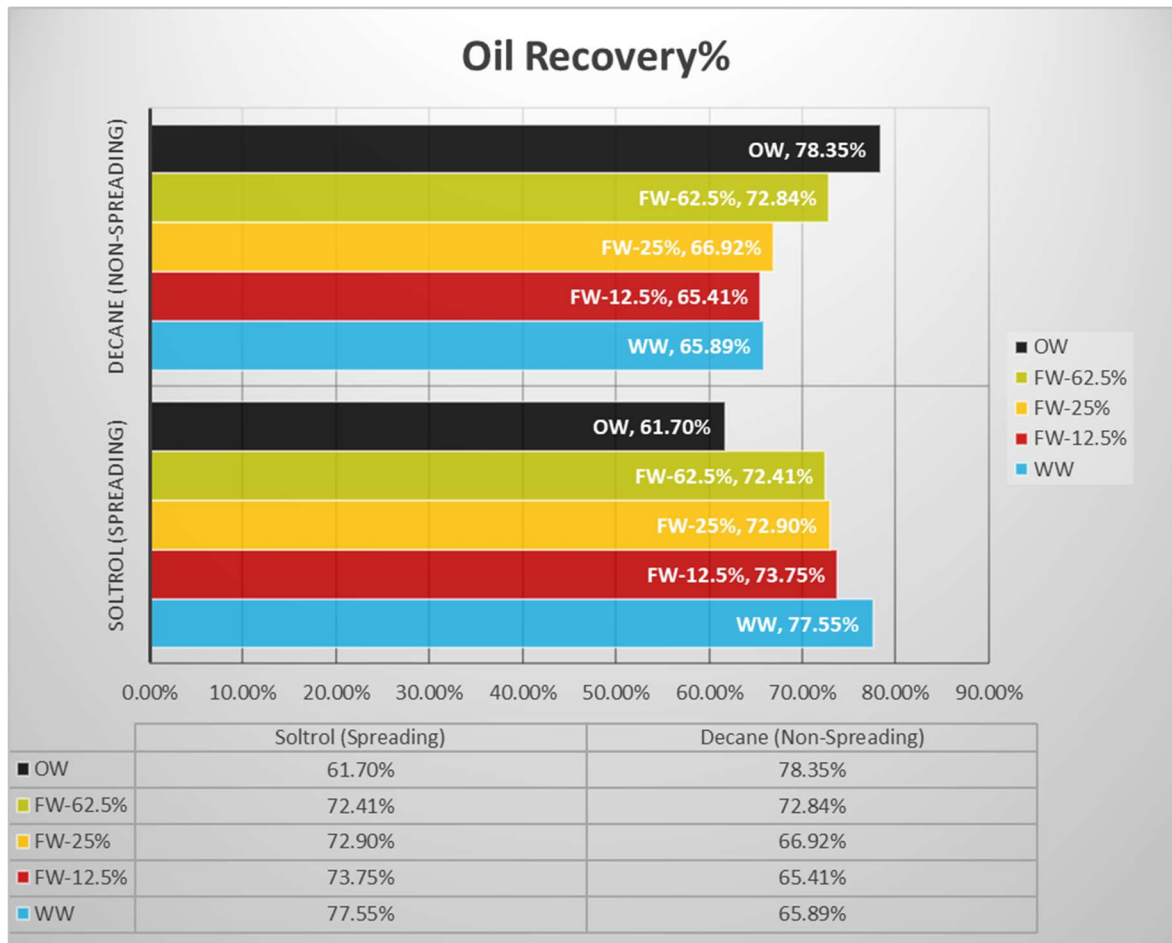


Figure 4.1. Summary of ultimate recoveries for procedure (B)

A recovery average of all experiments was 70.77(%OOIP). The highest recovery obtained were in 100% oil-wet sand with the non-spreading system (Decane) was 78.35(%OOIP), the second highest recovery attained was in 100% water-wet sand with the spreading system (Soltrol) was 77.55(%OOIP). While the lowest recovery recorded was in 100% oil-wet sand with spreading system (Soltrol) with 61.70(%OOIP), the second lowest recovery, was roughly 65(%OOIP) with non-spreading system (Decane) and shared with two sandpacks (100% WW and 12.5% OW) by neglecting the slight variation which is within the acceptable experimental error.

#### 4.1.1.1. Gas-assisted Gravity Drainage (GAGD) in Water-wet Sand

In 100% water-wet sand column with the spreading system (with Soltrol), GAGD process yielded a higher recovery of 77.55% compared to the non-spreading system (Decane) with 65.89% an increase of almost 17.7%. The oil recovery in the non-spreading system was better than the spreading system initially (between 15 minutes– 90 minutes). However the rate starts going slower until 7 hrs where recovery acted almost linearly, still spreading fluid system persistent increasing oil production until the end of the experiment helped to gain high ultimate recovery. This agrees with the visual in the time-lapsed photographs where while using Decane no major difference has noticed between 1 hour and 12 hours, but the photographs display an obvious difference in the same interval when using Soltrol. Water cut was noticeable in the spreading system it reached nearly 10% of total produced fluids, whereas very limited in a spreading system with less than 2%. The  $S_{wi}$  values for spreading and non-spreading systems were 12% vs 24%, respectively.

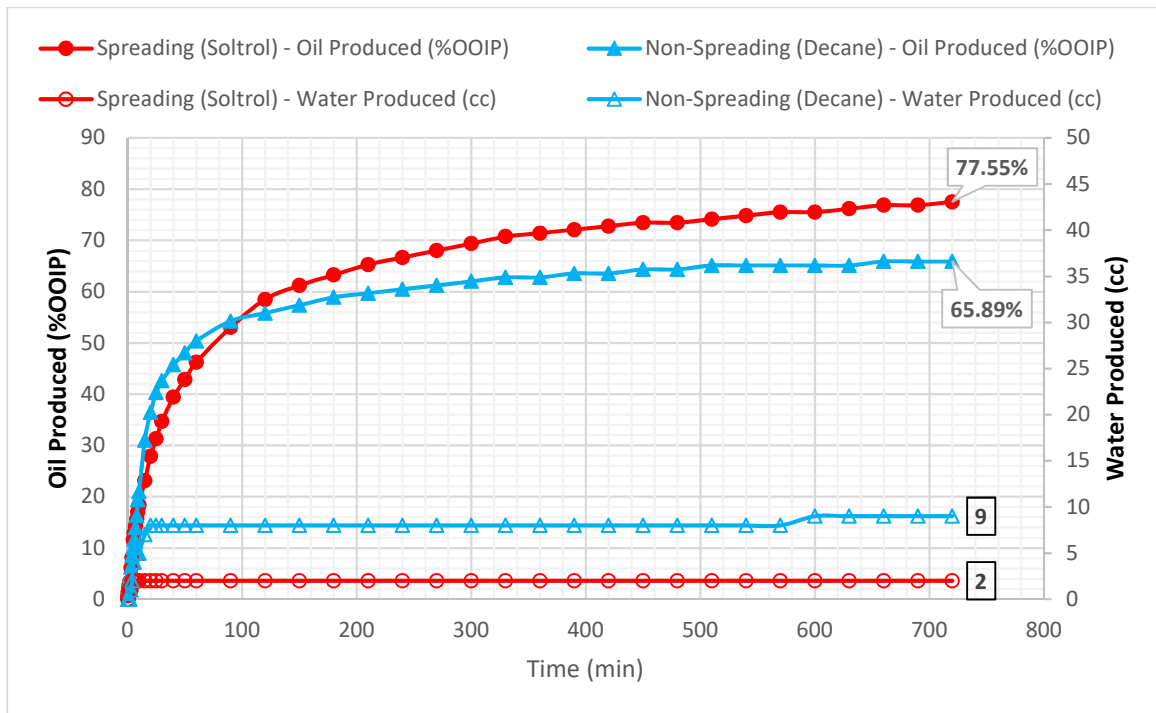


Figure 4.2. Oil and water production during GAGD floods in 100%WW sandpack

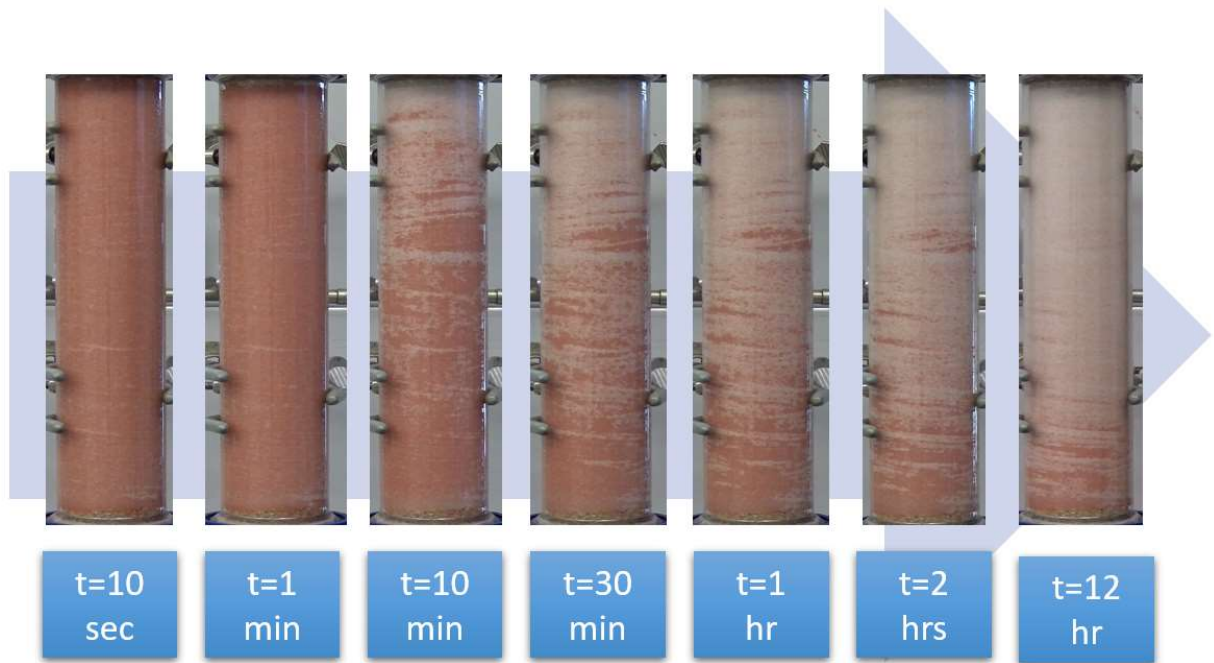


Figure 4.3. Photographs progression of GAGD floods in 100% WW sandpack with Soltrol (positive  $S_o$ )

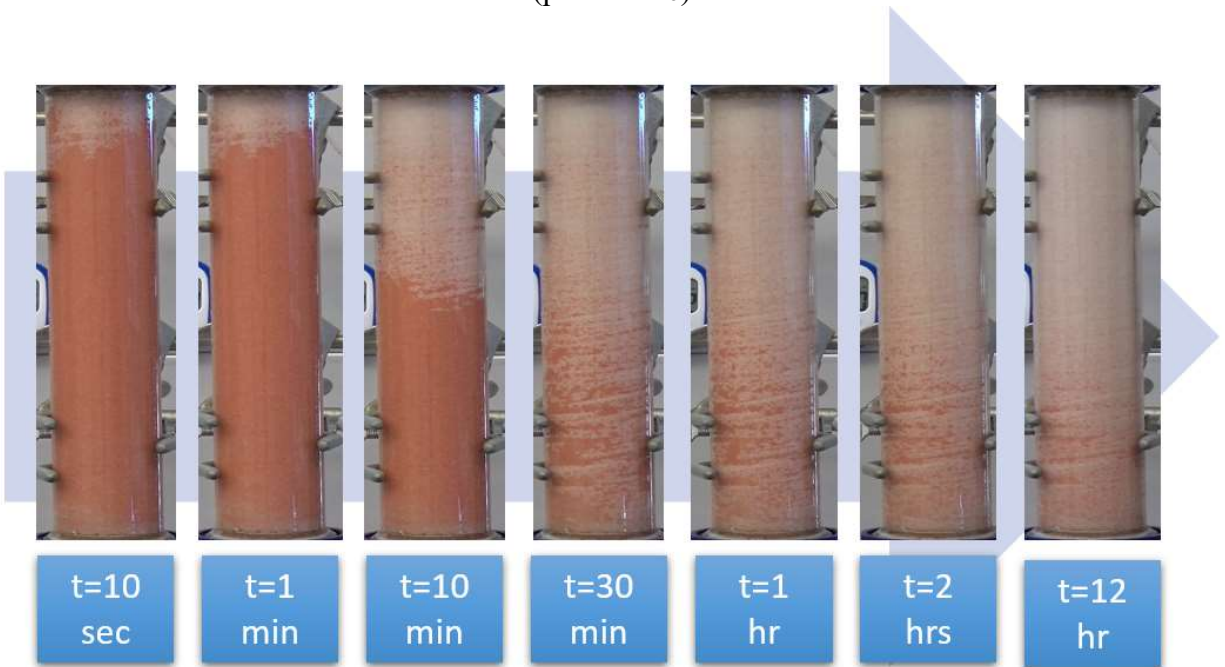


Figure 4.4. Photographs progression of GAGD floods in 100% WW sandpack with Decane (negative  $S_o$ )

#### 4.1.1.2. Gas-assisted Gravity Drainage (GAGD) in Oil-wet Sand

In 100% oil-wet sand, the scenario is inverted compared to complete water-wet sand. The non-spreading system (Decane) records a higher oil recovery compared to the spreading system (Soltrol) and they were 78.35% and 61.70% respectively, a decrease of nearly 27%. It is good to notice that the rates do not show initial overlapping (as seen in complete water-wet case), and both systems start with similar rates (gravity dominance) then approximately at 10 minutes it begins to diverge visibly and strongly. Nearly at 7 hours, both systems start to maintain behavior signaling the extreme decline of oil production. The time-lapsed picture uncovers an interesting phenomenon, with Soltrol at 10 minutes a premature breakthrough of gas occurs, and oil residuals took an extended time to be swept. Nevertheless, with Decane it is more of piston-like displacement. Water production was identical with 6 ccs for both systems.

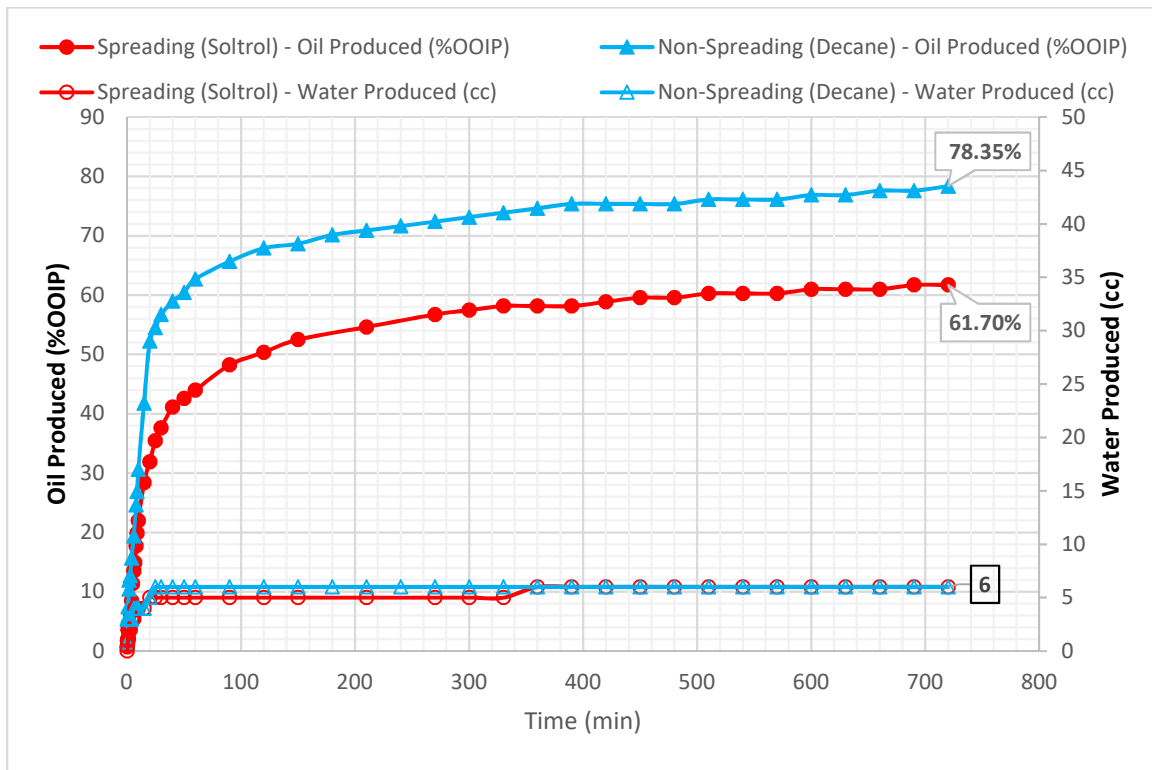


Figure 4.5. Oil and water production during GAGD floods in 100% OW sandpack



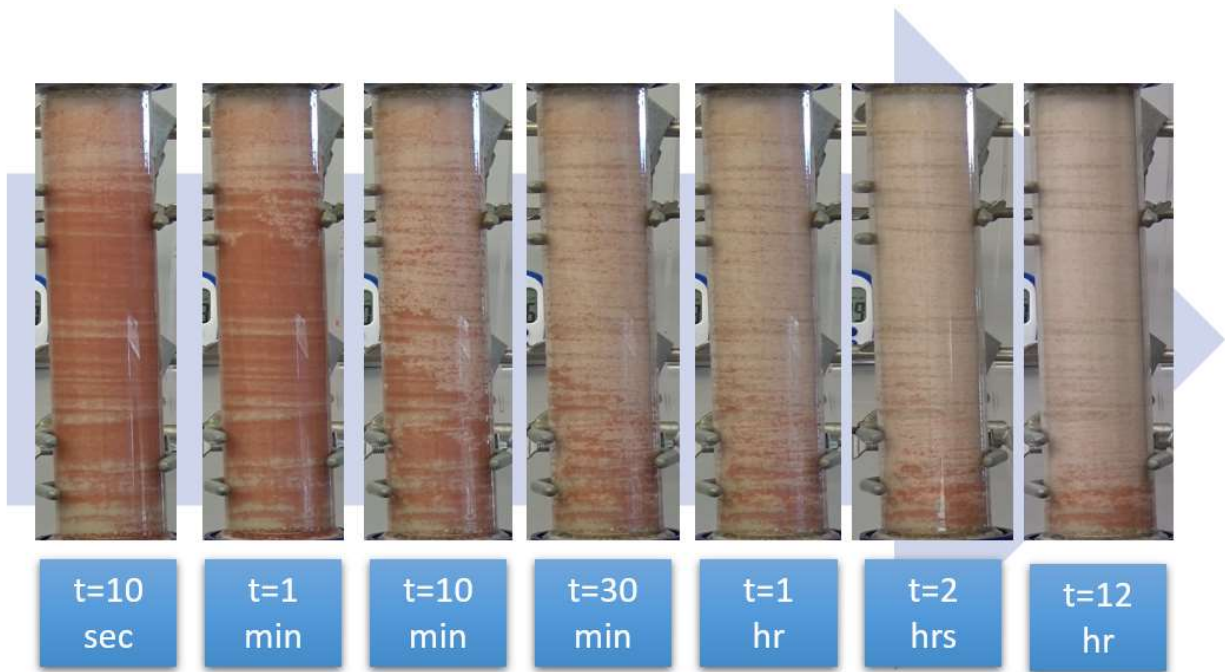


Figure 4.6. Photographs progression of GAGD floods in 100% OW sandpack with Soltrol (positive  $S_o$ )

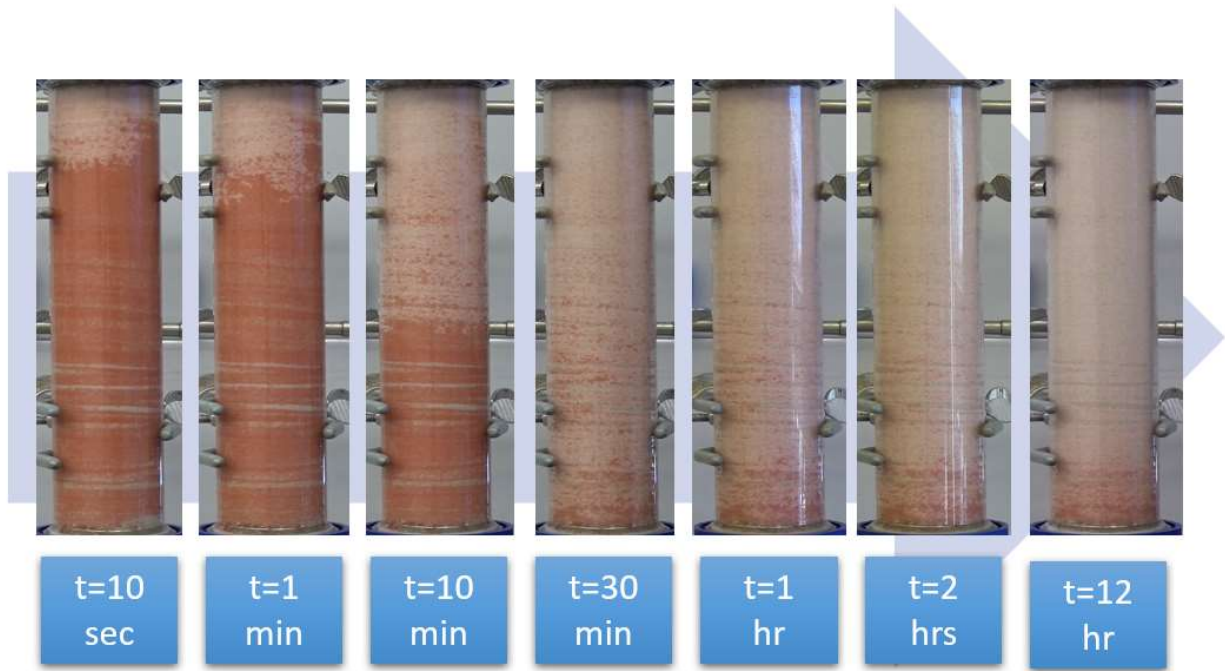


Figure 4.7. Photographs progression of GAGD floods in 100%OW sandpack with Decane (negative  $S_o$ )

#### 4.1.1.3. Gas-assisted Gravity Drainage (GAGD) in 12.5% Oil-wet Sand

The first combination of fractional wettability proceeded with (12.5% OW +87.5% WW). So, with a small variance of 12.5%, a similarity to complete water-wet behavior will not be a surprise. Indeed, generally, the profiles were quite analogous but not entirely identical. As fully water-wet experiment, GAGD process in the spreading system was more efficient with higher recovery (but with 5% reduction in ultimate recovery between 100% WW and 87.5%WW), compared to the non-spreading system where recovery was alike (both about 65%). It is quite captivating to notice both 100% WW and 87.5%WW sandpacks have the spreading/non-spreading oil recovery curves intersection at the same time (90 min, roughly 55% recovery). A hump was noticed in oil recovery of the non-spreading system causing attainment of 50% of oil at an earlier time of 30 minutes compared with 60 minutes the same system with 100% WW sand. Photographs at 30 minutes confirmed the difference. Water production was similar to 100% WW.

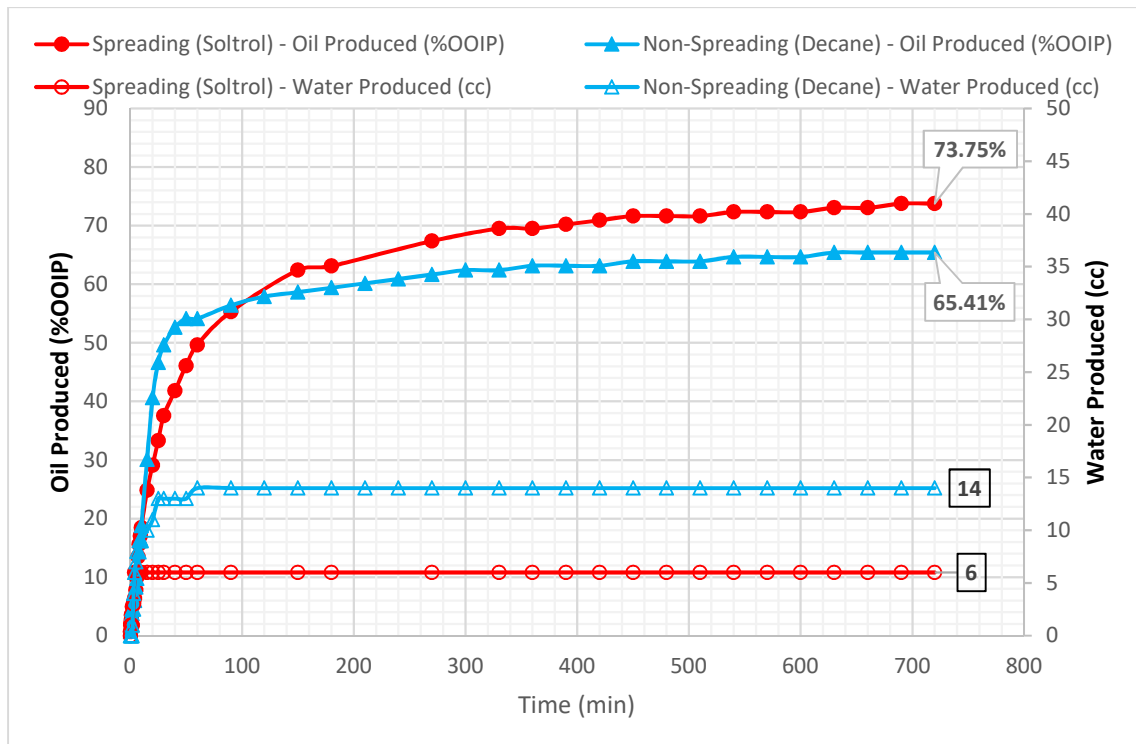


Figure 4.8. Oil and water production during GAGD floods in 12.5% OW sandpack



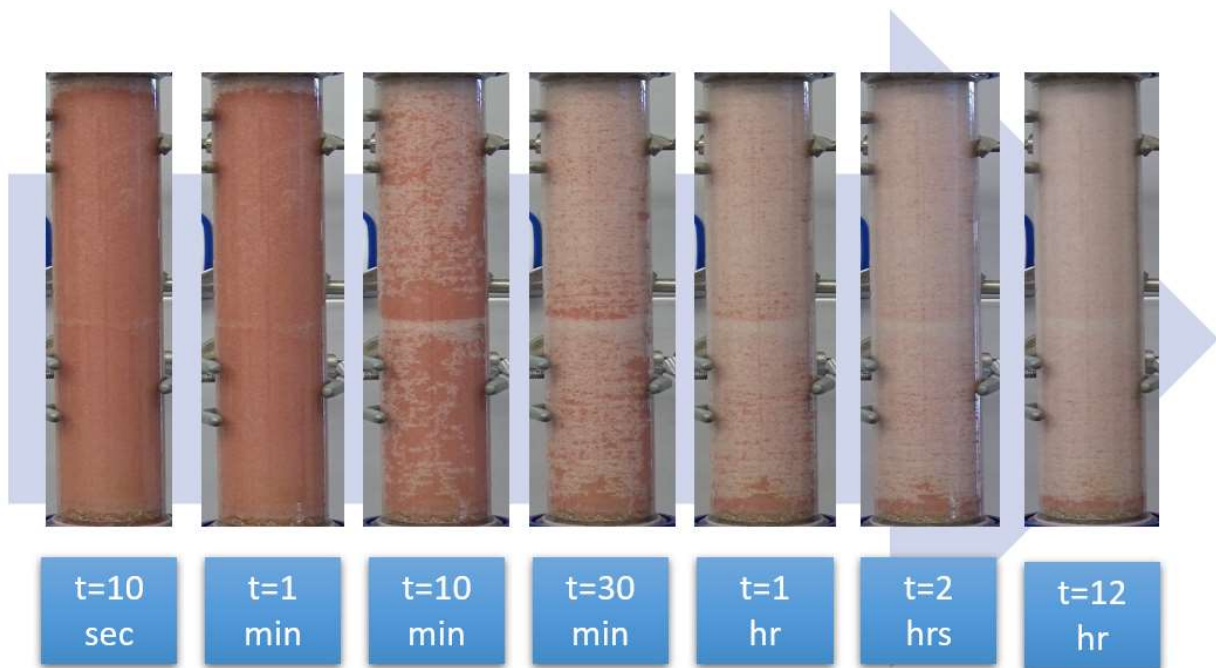


Figure 4.9. Photographs progression of GAGD floods in 12.5%OW sandpack with Soltrol (positive  $S_o$ )

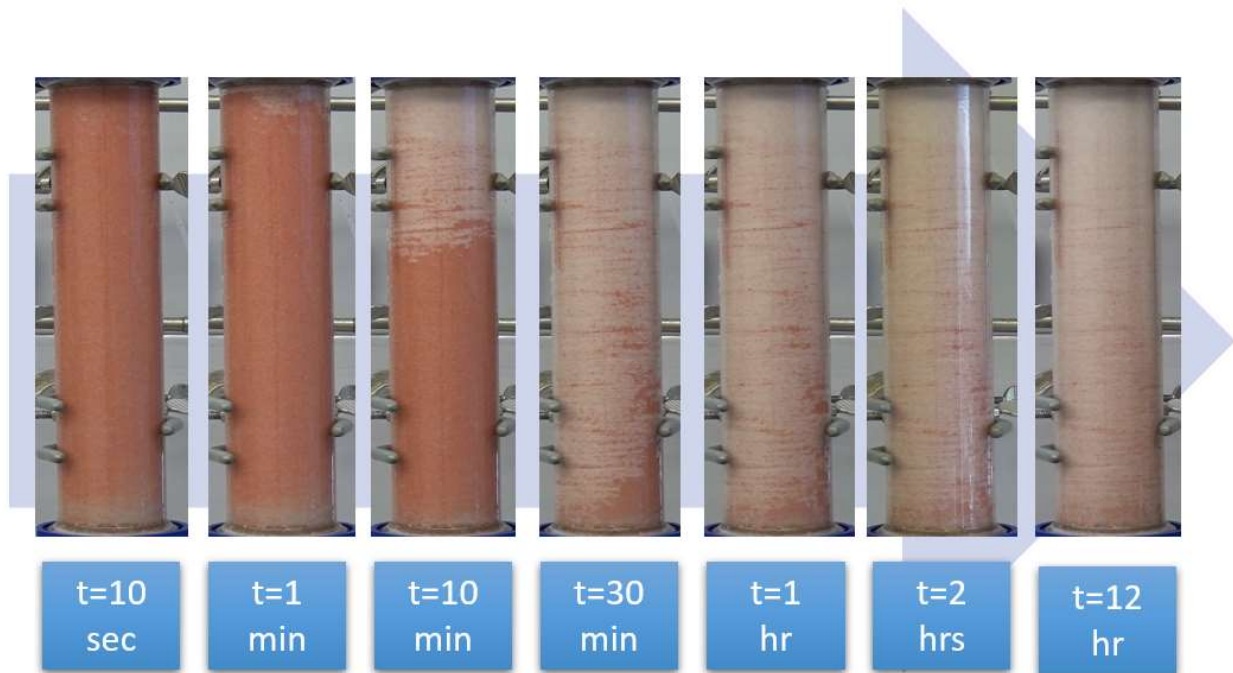


Figure 4.10. Photographs progression of GAGD floods in 12.5%OW sandpack with Decane (negative  $S_o$ )

#### 4.1.1.4. Gas-assisted Gravity Drainage (GAGD) in 25% Oil-wet Sand

With 25% oil-wet combination, a step higher has been taken to explore the effect of mixing OW percent sand on the overall performance of porous medium. Compared to 100% WW environment a numerous of similarities are observed: spreading system is still with higher recovery compared to the non-spreading system, yet the gap in ultimate recovery is obviously converging (difference from 12% in 100% WW into 6% in 75% WW); oil recovery curves are still intersecting at 90 min; also, more water was produced again in non-spreading system compared to that in spreading system. A noteworthy point that was not exhibited earlier in both 100% WW and 87.5% WW sand columns, is the persistence of oil recovery overlapping from starting of the experiment until 90 minutes. The  $S_{wi}$  values for spreading and non-spreading systems were 14% vs 26%, respectively.

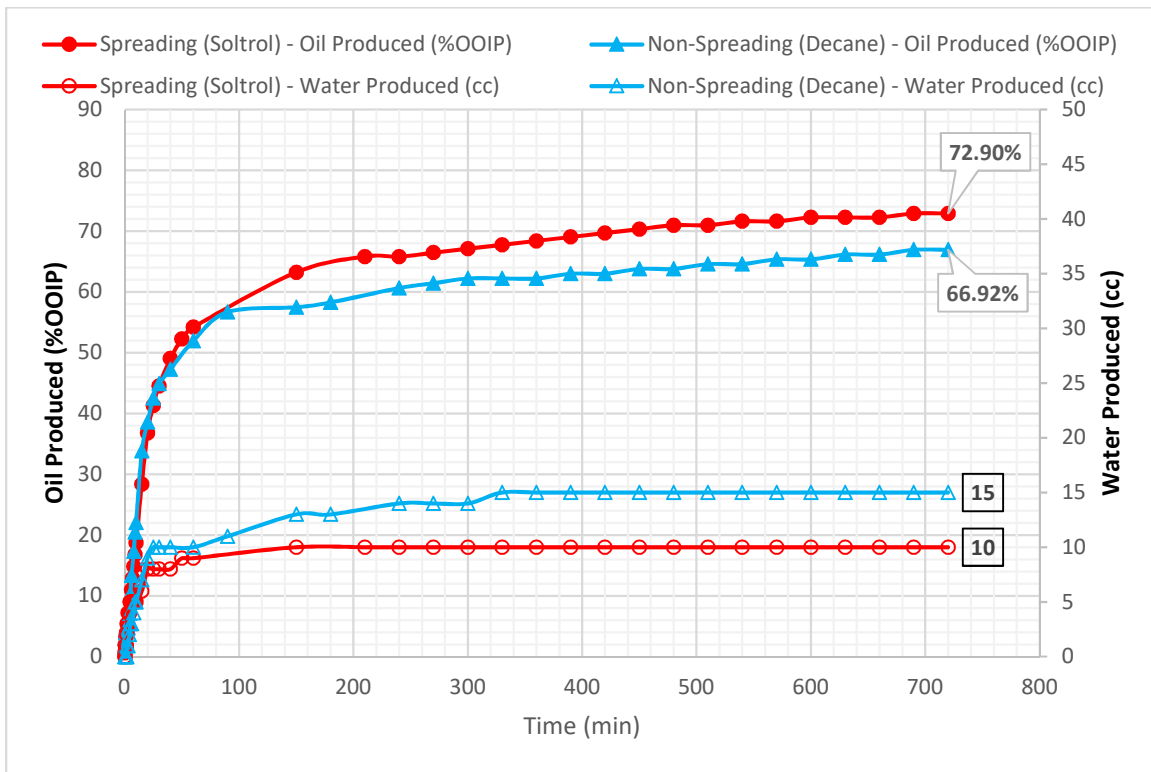


Figure 4.11. Oil and water production during GAGD floods in 25%OW sandpack

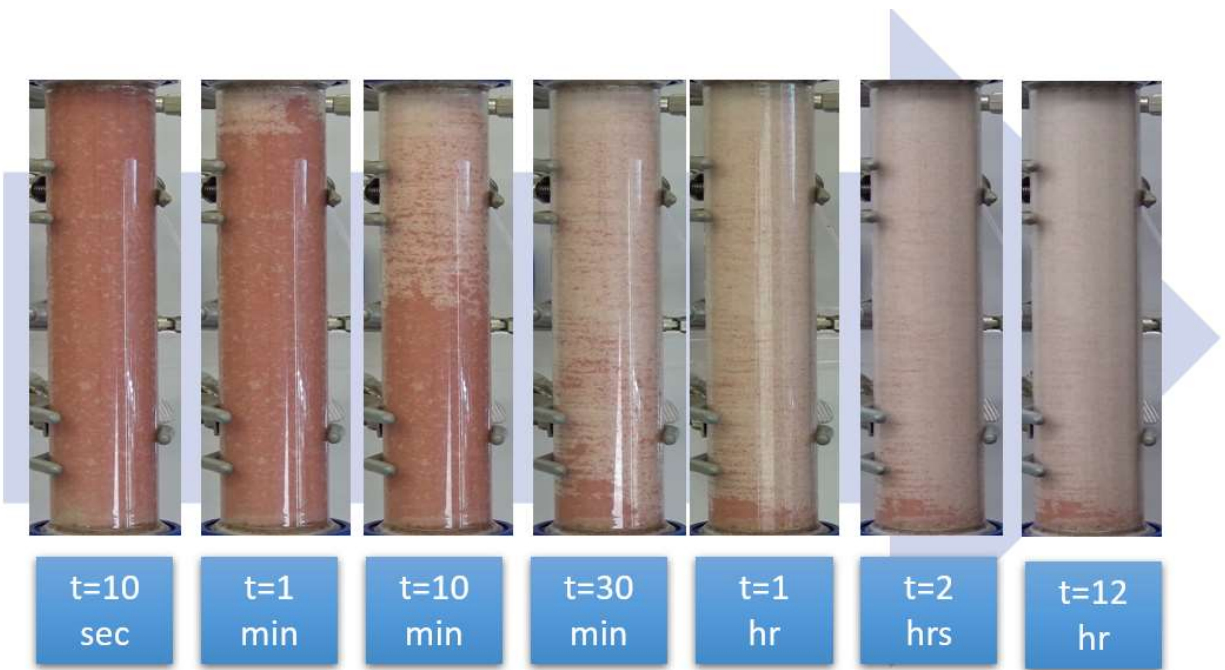


Figure 4.12. Photographs progression of GAGD floods in 25%OW sandpack with Soltrol (positive  $S_o$ )

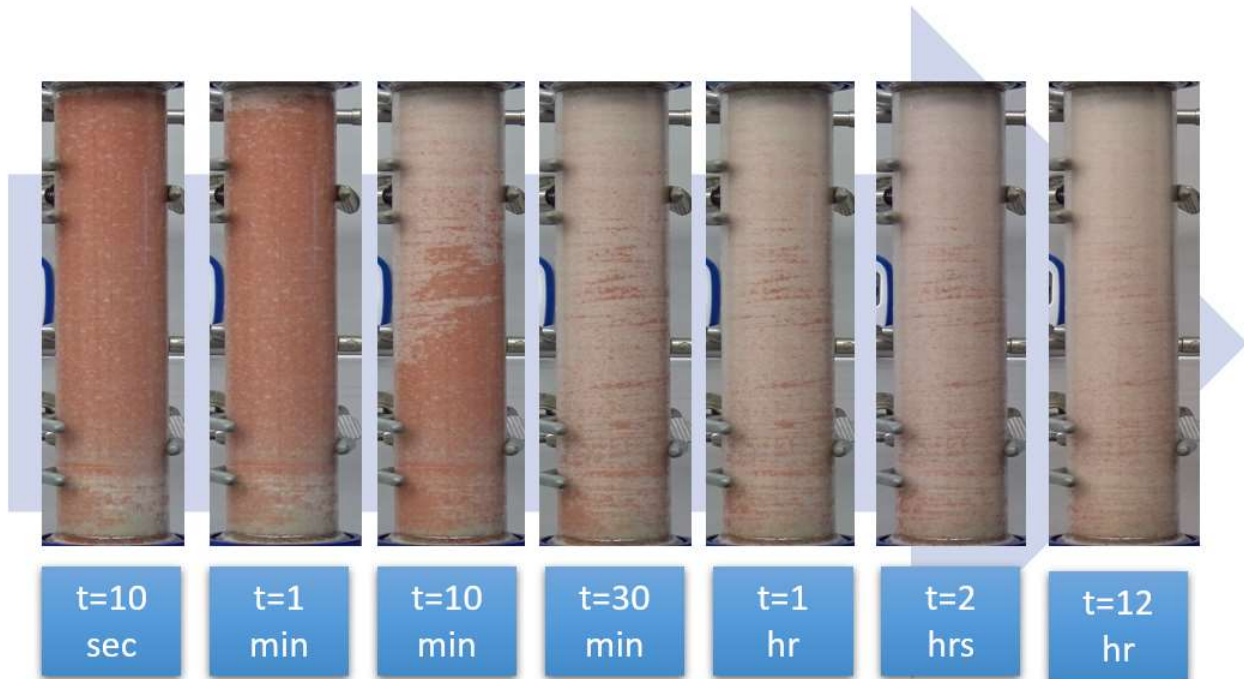


Figure 4.13. Photographs progression of GAGD floods in 25%OW / sandpack with Decane (negative  $S_o$ )

#### 4.1.1.5. Gas-assisted Gravity Drainage (GAGD) in 62.5% Oil-wet Sand

Lastly, a combination of 62.5% OW and 37.5% WW were mixed. Alluring curves were obtained in this amalgamation. Spreading and non-spreading systems mutually resulted in oil and water ultimate recovery with very similar values. Both spreading and non-spreading systems yielded oil recovery of roughly 72%, the rate of oil production curves is also overlapping each other. Time-lapsed photographs depict these outcomes specifically in the interval between the beginning of the experiment until 10 minutes where the displacement appearances are similar visually. The ultimate water recoveries are close recording 11 cc and 9 ccs for the non-spreading system and spreading system respectively. Decane system oil recovery here is the nearest to 100% OW Decane system compared to the behavior of lower percent oil-wet sandpacks 25,12.5,0 % OW sand. The  $S_{wi}$  values for spreading and non-spreading systems were 15% vs 16%, respectively.

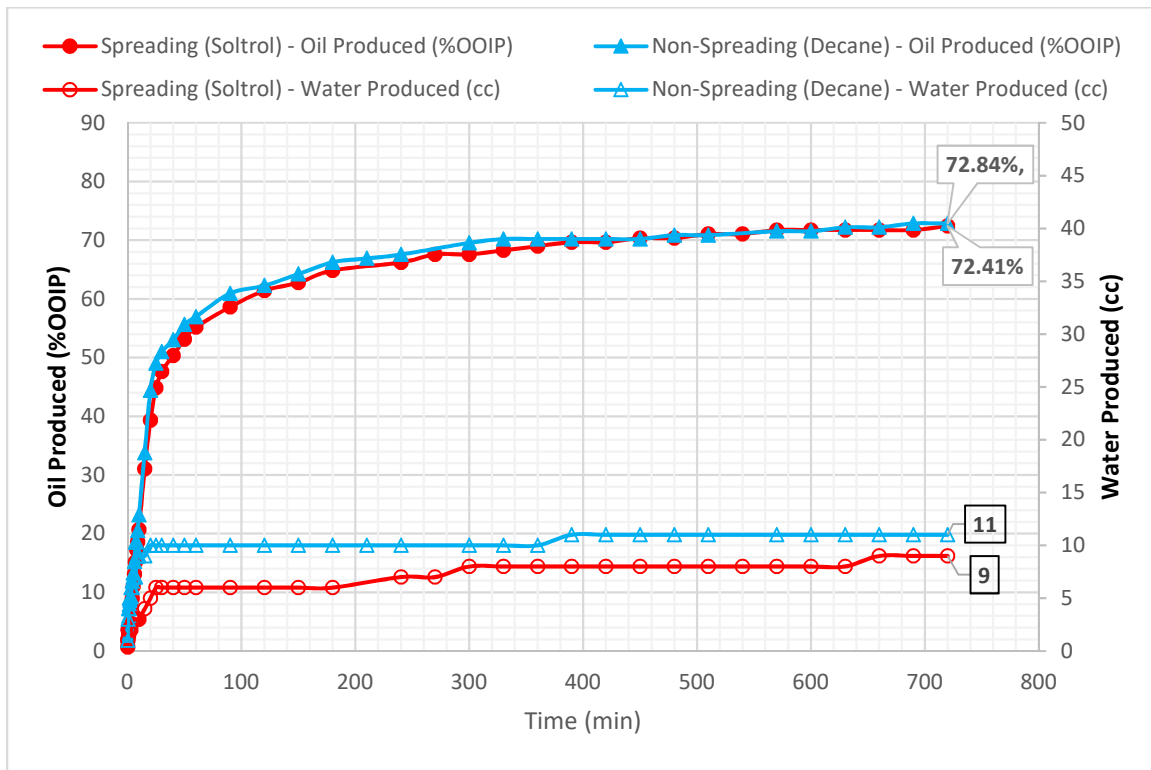


Figure 4.14. Oil and water production during GAGD floods in 62.5% OW sandpack



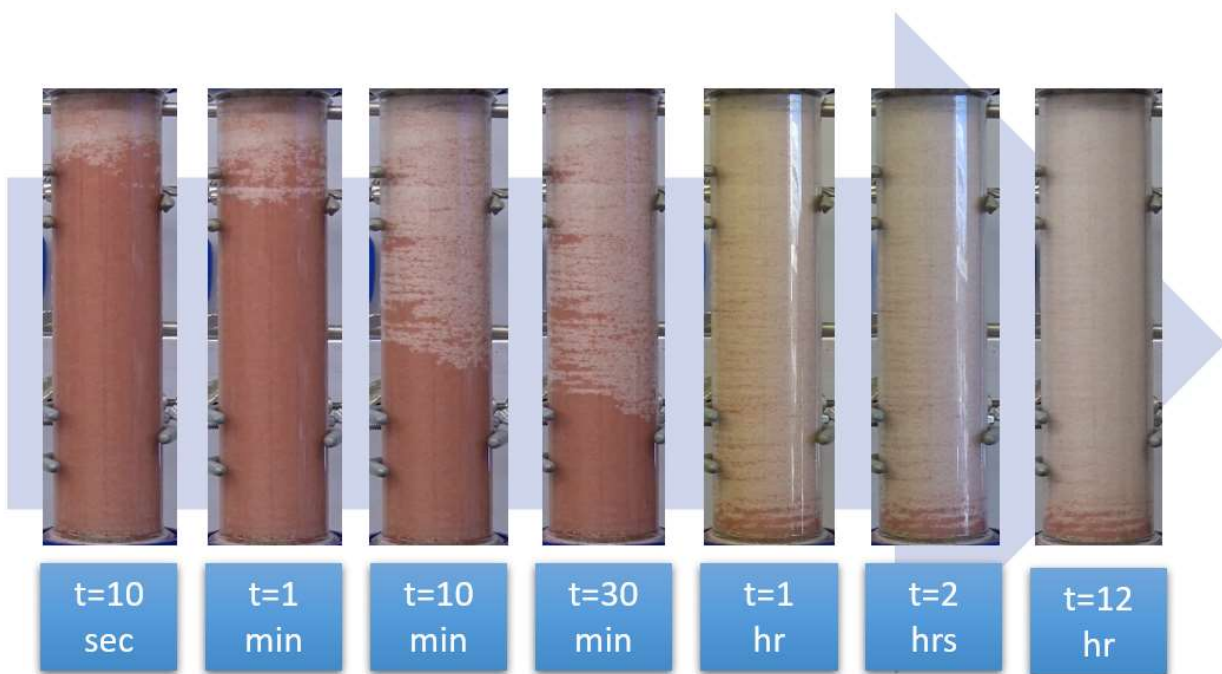


Figure 4.15. Photographs progression of GAGD floods in 62.5%OW sandpack with Soltrol (positive  $S_o$ )

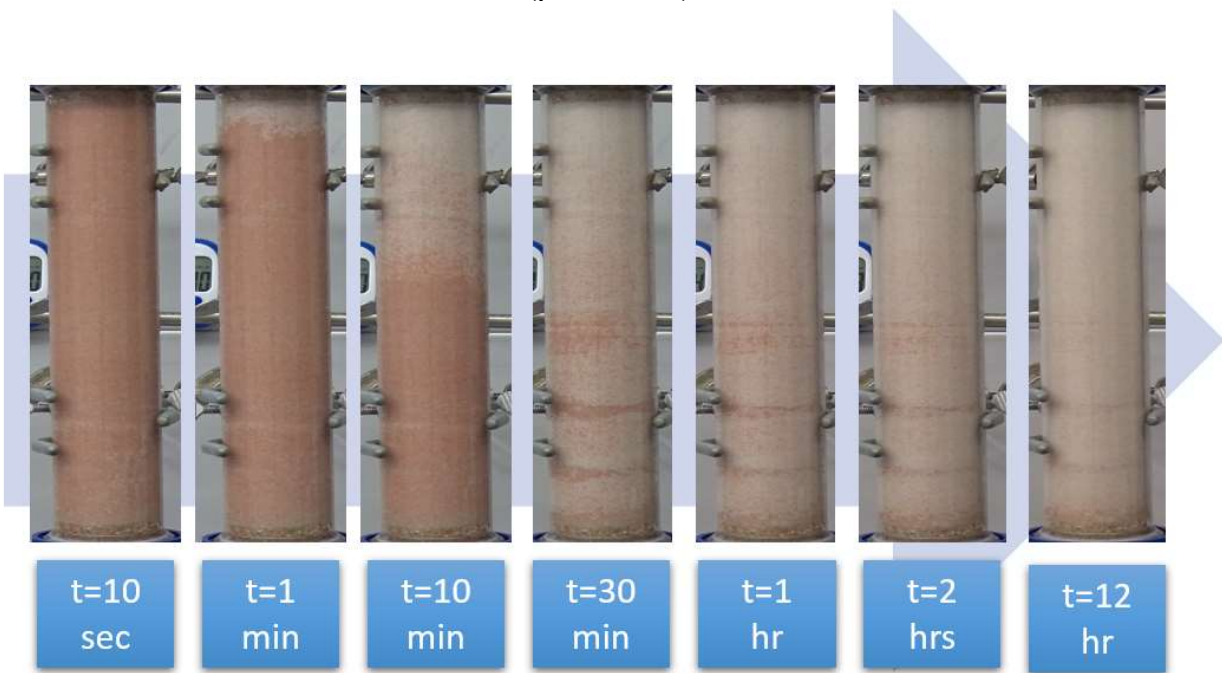


Figure 4.16. Photographs progression of GAGD floods in 62.5%OW sandpack with Decane (negative  $S_o$ )

## 4.2. Discussion of Results

It is possible to view the experiments grouped about the spreading coefficient of the system.

### 4.2.1. Non-spreading system

In Decane (negative spreading) system, oil recovery curves are clearly distinguished: 100% OW sand being the highest; 100% WW is the lowest; and, 62.5% OW sand being amidst the 100% OW and 100% WW (more close to OW performance than WW which is logical since it has 12.5% more OW sand than 50/50 fractional-wet sand), this is obviously shown in Figure 4.17.

However, the above description does not apply entirely to two fractional-wet sandpacks. Both (12.5% OW; 25% OW) sandpacks show initial high recovery rate (compared to 100% WW sand), a hump in oil production that ends around 150 minutes in which after the recovery of these two sandpacks embraced the 100% WW curves till the end of the experiment, yielding a very close ultimate recovery, this description shown in Figure 4.17.

Time-lapsed photographs correspond with the general performance of Decane production. Decane appears to be swept from the sandpack in a piston-like manner, and gas does not breakthrough early (observing 10 minutes pictures). Apart from 25% OW sandpack photos gas appears to be faced some fingering (this might explain some of the wavy behavior of 25% OW oil recovery curves comparing 100% WW curve).

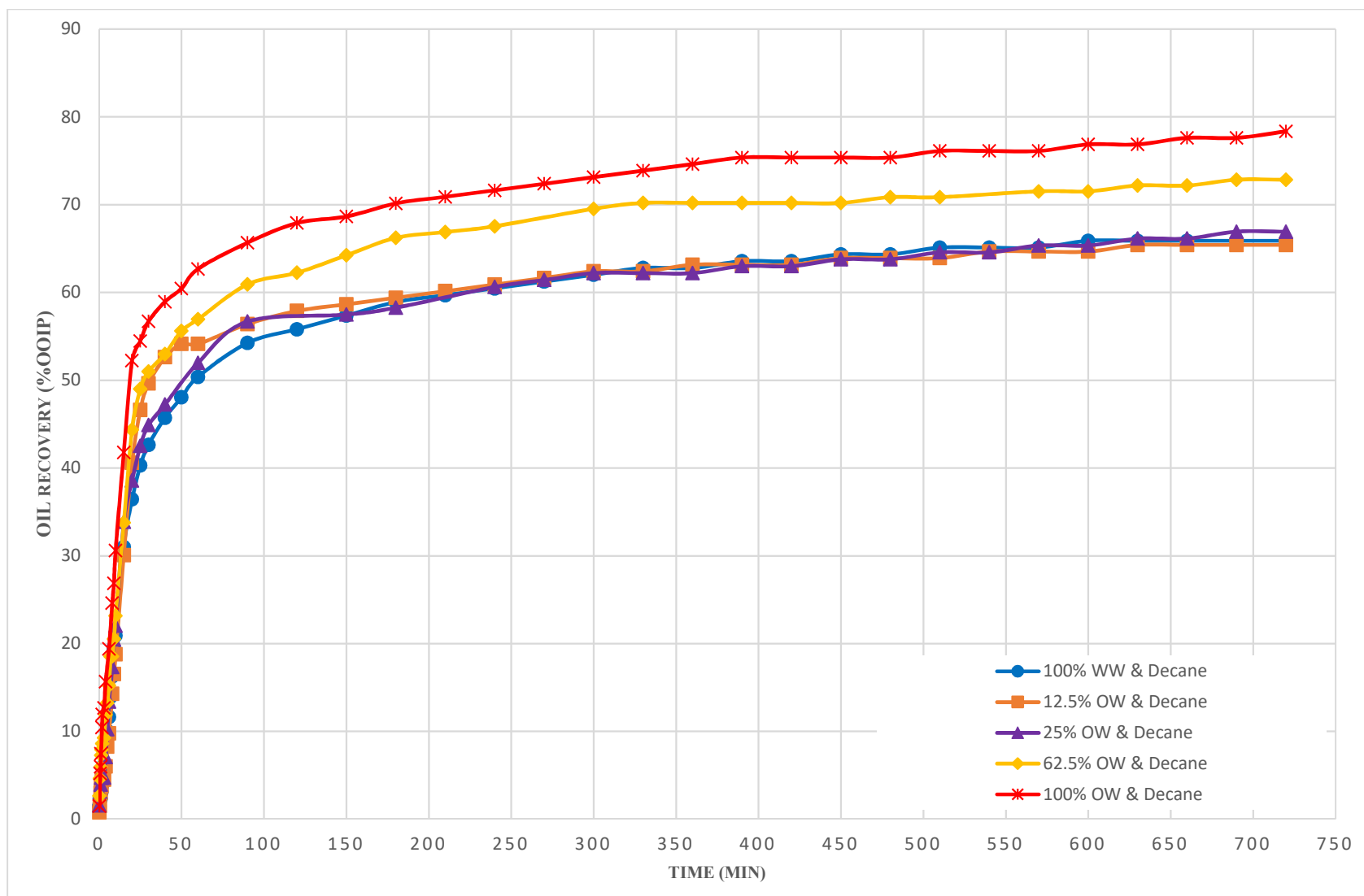


Figure 4.17. Decane (-ve) *So* system recoveries vs. time

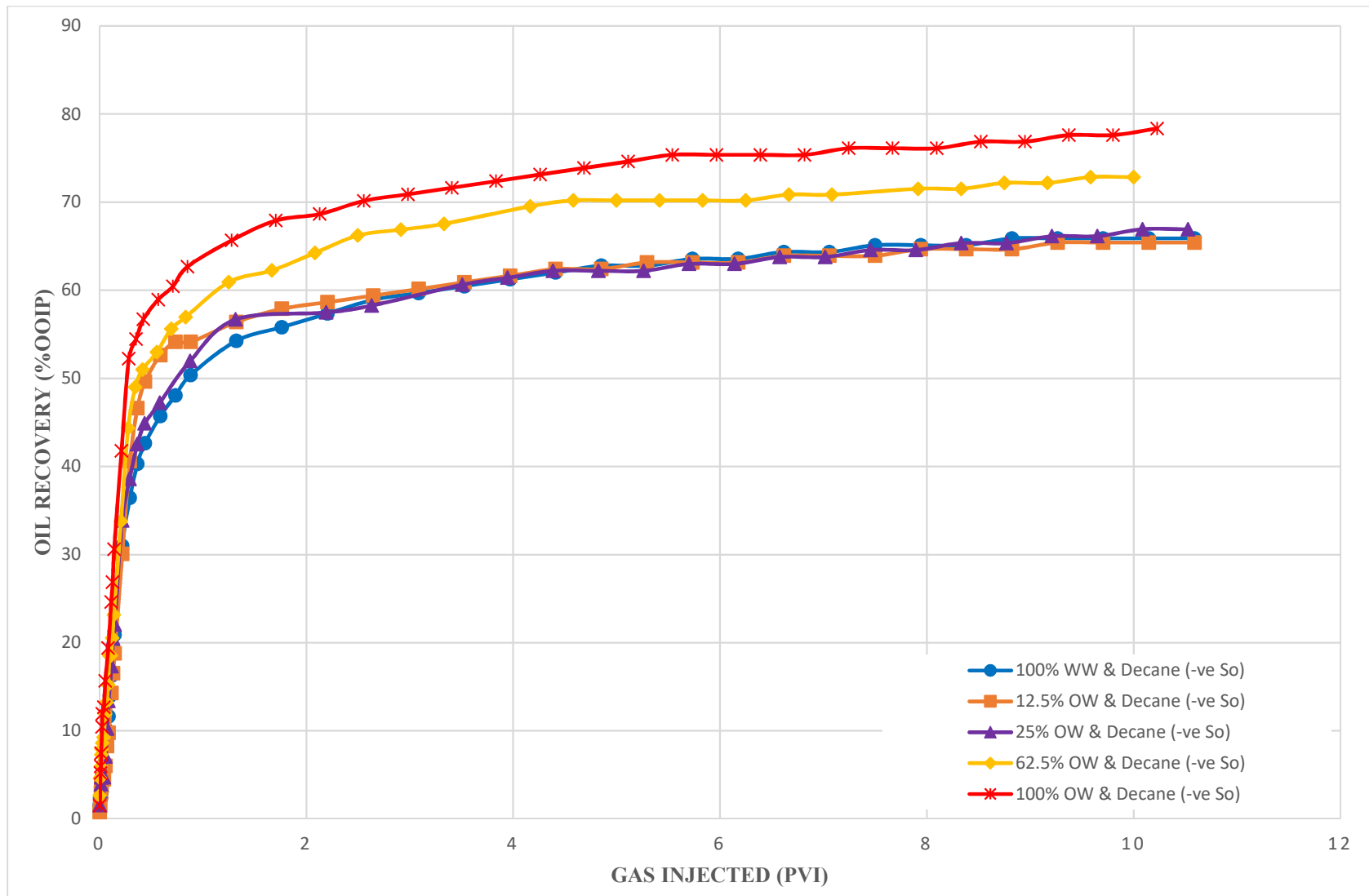


Figure 4.18. Decane (-ve)  $S_o$  system recoveries vs. PVI (pore volume injected of gas)



#### 4.2.2. Spreading system

In Soltrol (spreading) system, recovery rates are more challenging to address. Compared to a non-spreading Decane system behavior was settled after 100 minutes, with no more crossing or overlapping occurred. That is not the case for Soltrol system where curves intersections are extensive, and after 100 minutes do not determine the final behavior of oil recovery (with the exclusion of 100% OW curve, where after 100 minutes do not cross or overlap any other curve).

The sandpack with 100% WW sand was with the highest recovery; whereas the recovery of oil from the sandpack with 100% OW sand was the lowest; and in between 100% WW and 100% OW points, the other fractional-wet sandpacks ultimate recoveries are stacked together (it is of importance to notice that these recoveries closer to 100% WW sandpack ultimate recovery than to 100% OW sandpack ultimate recovery), this is shown in Figure 4.19.

Time-lapsed photographs demonstrated an irregular pattern, unlike the gas-oil interface, observed in Decane system. This behavior might play a role in the three-phase displacement and reflect the performance presented in curves. The photos illustrated a premature breakthrough of the injected gas leading into layers or areas of residuals (shown as red stained sand). This behavior was consistent in all Soltrol system experiments except 62.5%OW sandpack which was similar to Decane system behavior.

The layers or areas of oil residuals observations are evident in photographs at 30 minutes and 1 hr, shown in Figure 4.3 as a clear example. Nevertheless, photos of the end of the experiments at 12 hrs reveal a clean column of sand similar to Decane (comparing Figure 4.3 with Figure 4.4) system column which raises the point of considering these residuals appearance and effect to be temporary.

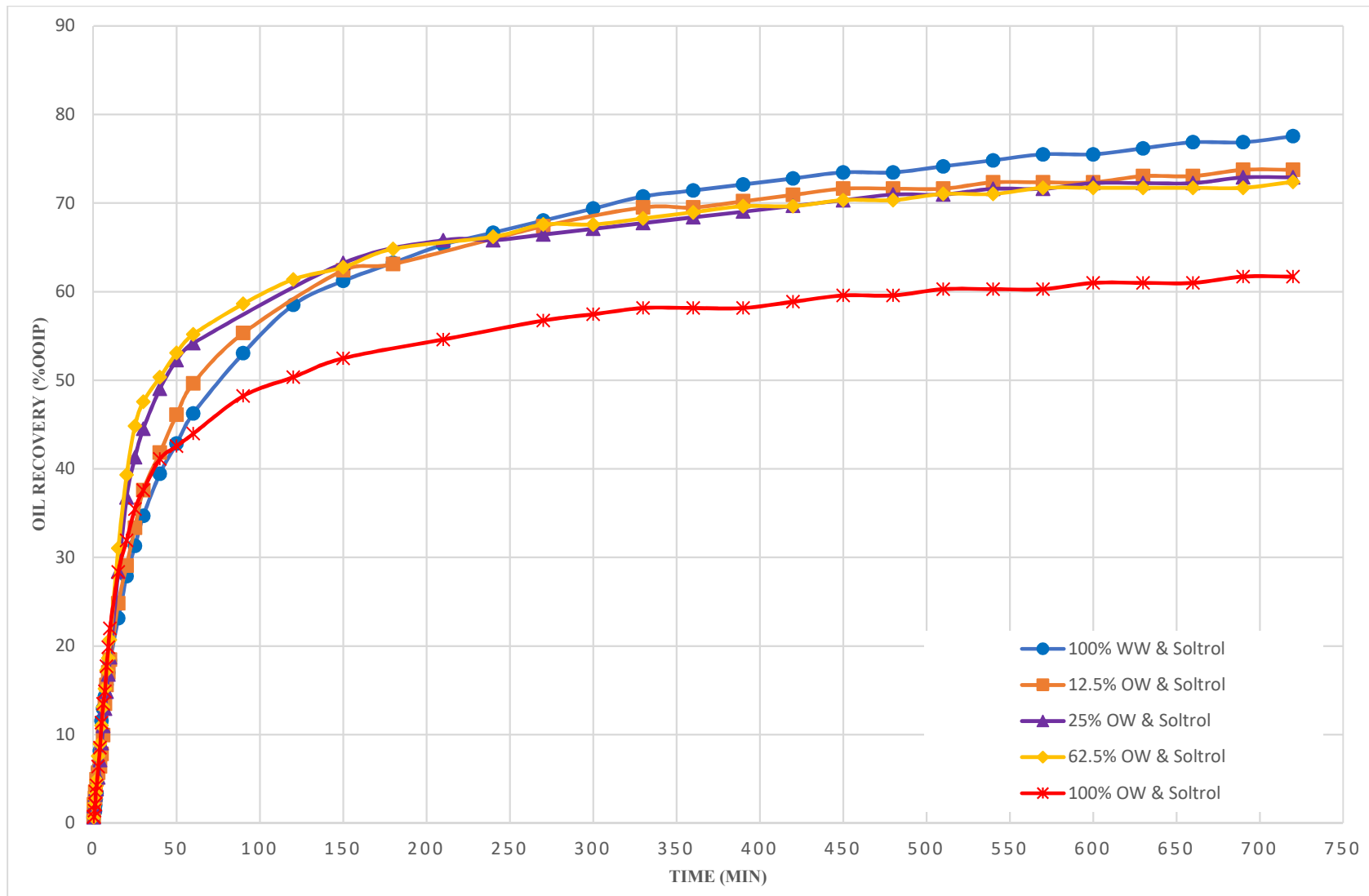


Figure 4.19. Soltrol (+ve)  $S_o$  system recoveries vs. time

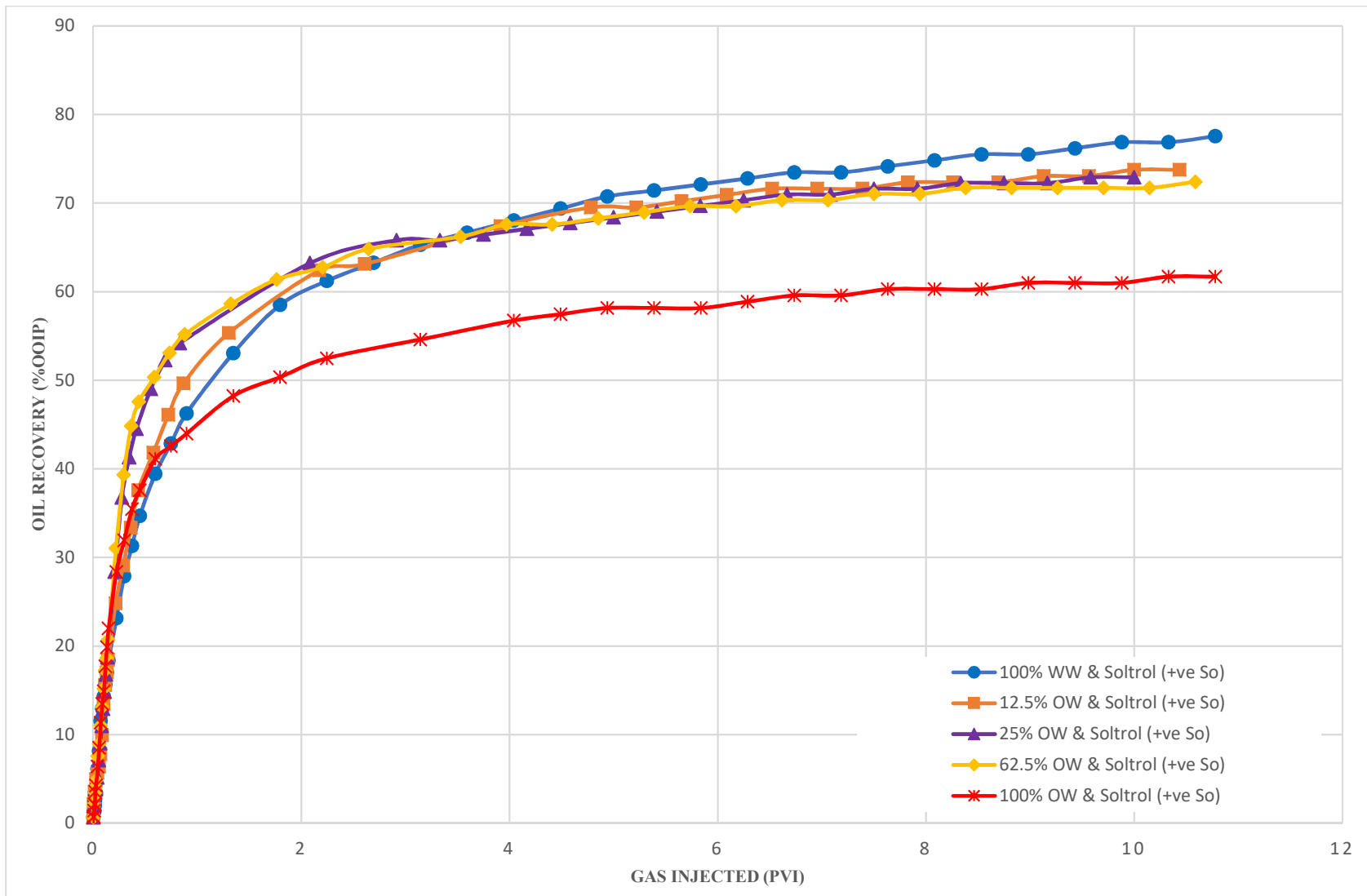


Figure 4.20. Soltrol (+ve)  $S_o$  system recoveries vs. PVI (pore volume injected of gas)

#### 4.2.3. Results Comparison with Wettability and Spreading Studies

Collective experimental results of the conducted experiments show some agreement with Dzulkarnain (2018) findings. Both this work and Dzulkarnain work indicates that the highest recovery in the water-wet sand was achieved in the positive spreading system (using Soltrol in this case), additionally in oil-wet sand experiments the highest recovery recorded in the negative spreading system (using Decane in this case).

The dissimilarities rose up with the fractional-wet sandpack results. Dzulkarnain concluded that the (50/50) WW/OW sandpack behaves similarly to a 100% OW sandpack, that is because he found that FW sandpack is with better recovery in the non-spreading system compared to spreading system recovery. However, with our experiments, this has been found to be partially acceptable since the recovery of 62.5% OW sandpack in the non-spreading system is closer to OW sandpack behavior than to WW sandpack behavior. Practically it is more accurate to consider the recovery as a midpoint between the recovery of 100% OW sandpack and the recovery of 100%WW sandpack. Non-spreading system fractional-wet 62.5, 25, 12.5 %OW experiments confirmed that the recovery is gradually increasing with the increase of OW sand percentage in the sandpack (going to the top with 100% OW sandpack).

The major difference was in the fractional-wet spreading system (with Soltrol) sandpack. Dzulkarnain considers this sandpack performance to be similar to a 100% OW sandpack. However, the 62.5, 25, 12.5 % OW experiments display a closer performance to a 100% WW sandpack, yet with a non-gradual behavior as seen with non-spreading Decane fluid system.

Recovery values obtained from our water-wet experiments are following the same trend of water-wet experiments from the work of Kantzas et al. (1988), Vizika (1993), Kalaydjian et al. (1995), Maeda and Okatsu (2008). These researchers reached a similar conclusion to what our work found that a higher recovery attained in water-wet experiments with a spreading system condition. Kantzas et al. (1998), Oren et al. (1992), and Dzulkarnain (2018) suggested that the spreading film phenomenon is connected to the higher recovery detected. In water-wet sand, the oil-phase is the intermediate phase. If the oil spreading coefficient is positive, oil forms a thin layer and spreads between the gas and water. Dicarolo et al. (2000), stated that these oil films maintain a hydraulic conductivity even at very low saturation, in his study of three-phase relative permeability. These films provided a continuous path for the bypassed oil globules behind the advancing gas front in the sandpack to be reconnected again and drained later in the experiment. Whereas in non-spreading system oil do not spreads, and no continuous layers occur leading to oil globules left behind in the corners and crevasses.

However, can non-spreading oil system form an intermediate layer? Keller et al. (1997) work answered this question that it is possible under given conditions of pore geometries and the ratio of gas-oil and oil-water capillary pressures. Later, Dzulkarnain (2018) suggested that this path not hold continuous to the production outlet. Since throughout the experiment, the network of oil-filled pores and the bottom of the sandpack were drained, and that cut off the path for the flow of oil from oil blobs in the upper position of the sandpack to the outlet, leaving these blobs suspended in the porous medium.

Our experimental work results agree partially with Oren and Pinczewski (1994) conclusion that the highest recovery recorded in oil-wet sandpack, followed by water-wet with the spreading system, and the lowest was in water-wet media with the non-spreading system (excluding the oil-wet with the non-spreading system). A major conflict of our result with the one from Oren and Pinczewski (1994) is that they considered that in oil-wet sand the sign of the spreading system was not of importance on recovery, since the oil can be drained via continuous layers of wetting phase instead of layers of spreading phase ( even through their tabulated results show difference between oil-wet negative and positive spreading systems). Our results showed that the recovery of oil-wet with spreading system oil is the absolute lower recovery recorded.

Vizika and Lombard (1996) work were similar to the findings of Oren and Pinczewski (1994) that in the oil-wet sand the spreading does not affect recovery. The disagreement was in determining the type of wettability associated with higher recovery. Vizika and Lombard (1996) highest recovery was in water-wet, and fractional-wet experiments and oil-wet recovery recorded the lowest.

It is of importance to state that Oren and Pinczewski and Vizika and Lombard studies were performed at different scales. Oren and Pinczewski worked with micromodel (pore scale), while Vizika and Lombard used nonconsolidated porous media (sandpacks/ core scale). Also, saturation history was different previous to the experiments performed: Oren and Pinczewski worked with tertiary recovery mode (at residual oil saturation) when Vizika and Lombard worked at residual water saturation.

## CHAPTER 5. CONCLUSIONS AND RECOMMENDATIONS

This chapter summarizes work accomplished, the conclusions drawn, and future recommendations.

### 5.1. Conclusions

This research accomplished the following:

1. Investigating the performance of GAGD as a secondary recovery method, using experimental procedures under spreading and non-spreading conditions in different wettability sand (water-wet, oil-wet, and different fractional-wet) mediums.
2. Plotting and analyzing the results in an attempt to understand the role of the three-phase flow mechanisms in oil recovery with gas injection.
3. Discussing and comparing the results with previous work and literature, primarily addressing the pore-scale effect on this core scale study.

In the end, into the following conclusion on oil recovery performance were made:

1. In water-wet experiments, a high recovery has been attained in the spreading system (Soltrol), whereas a low recovery has been recorded in the non-spreading system (Decane).
2. In oil-wet experiments, a high recovery has been attained in the non-spreading system (Decane), whereas a low recovery has been recorded in the spreading system (Soltrol).
3. In fractional-wet experiments, three cases have been examined:
  - i) Similar recovery rate has been detected between 12.5% OW sandpacks and 100% WW sandpacks, in both spreading and non-spreading conditions (i.e., first comparing 100% WW spreading with 12.5% OW spreading; then comparing 100% WW non-spreading comparison with 12.5% OW non-spreading).

- ii) 25% OW sandpacks in both spreading and non-spreading were also performed more similar to the 100% WW sandpack (25% OW recovery recorded a value amidst the values of 12.5%OW and 62.5%OW).
  - iii) Performance in 62.5% OW sandpacks is unique in two ways: first, in both spreading and non-spreading systems (regardless of the sign of the spreading), the recovery is identical (73% oil recovery approximately), indicating that wettability the effect of wettability outweighs that of spreading; second, the oil recovery of this sandpack in spreading system is close to that of a 100% WW sandpack, although the recovery of this sandpack in non-spreading system is close to that of a 100% OW sandpack.
  - iv) In the non-spreading system (Decane), changes in the fractional-wet sandpack result in gradual changes on ultimate oil recovery, whereas a higher percentage of OW sand in the sand column results in higher ultimate oil recovery percent. On the other hand, in the spreading system (Soltrol) the overall ultimate oil recovery in fractional wet sandpacks performs in a range (70% mean value) closer to behavior in 100% WW sandpack than to that in 100% OW. This happens because of the existence of thin oil spreading layers in spreading system sandpacks; the flow via these films might be a slow process, but eventually, it leads to higher ultimate oil recovery as is illustrated in Figure 4.1 and Figure 4.18.
4. The values of connate water saturation were particularly higher in the non-spreading fluid system compared with spreading fluid system except for sandpack containing 62.5% OW sand in which both spreading and non-spreading fluids systems have similar  $S_{wi}$ . The reason might be due to the difference in mobility ratio between the spreading and non-spreading fluid systems.



5. Pore-scale flow mechanisms affect core-scale experiments (according to this study). One of the following scenarios occurs, depending on the type of wettability and spreading:
- A. (Water-wet + spreading system) sandpack: the high recovery is attributable to the reconnection of isolated oil ganglia via the spreading layers.
  - B. (Oil-wet + non-spreading system) sandpack: the high recovery is associated with the existence of continuous (Low-viscosity) wetting layers at core-scale experiments.
  - C. (Water-wet + non-spreading system) sandpack: the low recovery is related to the absence of both wetting and spreading films.
  - D. (Oil-wet + spreading system) sandpack: the low recovery is linked to the effect of water accumulations near the bottom of porous media column; besides, the strong capillary retention of oil phase at the outlet can also cause low oil recovery. In addition, in an oil-wet media, oil is the most wetting phase, occupying the smallest pores, corners, and grooves, and this confined oil might lead to less recovery.

## 5.2. Recommendations

Suggestions for future work are: -

1. Considering using mixed wettability sandpack: these sandpacks is prepared by aging it in oil and can represent natural reservoir environments. It required an extended aging time. Then, the behavior cannot compare with fractional-wettability results.
2. Simulation of sandpack: building a model and trying to history match the experimental results. It also good to examine the relative permeability curves and try to model the most acceptable fit.
3. Using the application of CT-Scanning: the usage of such technology can reveal more about what happens inside the sandpack and can provide certain fluids saturations. Also, using the application of capillary pressure can more characterize the wettability accurately.
4. Network modeling of three-phase displacement using fractional-wet walls in order to understand more the pore-scale mechanisms that fractional-wet environment undertake.
5. The extent of the experiment procedure into a variety of formation types: with the profound understanding of both wettability and spreading in sand formation the experiments can be extended into carbonates or shale formation for unconventional reservoirs applications.
6. Transparent glass beads usage as a medium to bring more visuality into the experiment performance.

## REFERENCES

- Abdallah, W., Buckley, J. S., Carnegie, A., et al. (2007). Fundamentals of wettability. *Oilfield Review*, 19(2), 44-61.
- Agbalaka, C. C., Dandekar, A. Y., Patil, S. L., et al. (2008). *The effect of wettability on oil recovery: A review*. SPE Asia Pacific Oil and Gas Conference and Exhibition, Perth, Australia. 20-22 October. SPE-114496-MS. <https://doi.org/10.2118/114496-MS>.
- Ahmed, T. (2006). *Reservoir engineering handbook*: Elsevier.
- Al-Mudhafar, W. J., Wojtanowicz, A. K., and Rao, D. N. (2017). *Hybrid Process of Gas and Downhole Water Sink-Assisted Gravity Drainage (G&DWS-AGD) to Enhance Oil Recovery in Reservoirs with Water Coning*. Paper presented at the Carbon Management Technology Conference. Houston, Texas, 17-20 July, CMTC502487-MS. <https://doi.org/10.7122/502487-MS>.
- Baker, L. E. (1988). *Three-phase relative permeability correlations*. SPE/DOE Symposium on Enhanced Oil Recovery, Tulsa, Oklahoma, 17-20 April. SPE-17369-MS. <https://doi.org/10.2118/17369-MS>.
- Blunt, M., Fenwick, D., and Zhou, D. (1994). *What determines residual oil saturation in three phase flow?*, Paper presented at the Improved Oil Recovery Symposium. SPE 27816.
- Brown, R. J., and Fatt, I. (1956). *Measurements of fractional wettability of oil fields' rocks by the nuclear magnetic relaxation method*. Paper presented at the Fall Meeting of the Petroleum Branch of AIME. <http://doi.org/10.2118/743-G>.
- Chatzis, I. and Ayatollahi, S. (1993). *The effect of gas injection rate on the recovery of waterflood residual oil under gravity assisted inert gas injection*. Paper presented at the Technical Meeting/Petroleum Conference of The South Saskatchewan Section.
- Chatzis, I., Kantzas, A., and Dullien, F. A. L. (1988). *On the investigation of gravity-assisted inert gas injection using micromodels, long Berea sandstone cores, and computer-assisted tomography*. Paper presented at the SPE Annual Technical Conference and Exhibition.
- Craig, F. F. (1971). *The reservoir engineering aspects of waterflooding* (Vol. 3): HL Doherty Memorial Fund of AIME New York, NY.
- Crețu, A., Alexandra, P., Moldovan, M., et al. (2015). *The influence of silanized nano-SiO<sub>2</sub> on the hydration of cement paste: NMR investigations* (Vol. 1700).
- Dake, L. (1978). *Fundamentals of Reservoir Engineering*.

- Dicarlo, D. A., Sahni, A., and Blunt, M. (2000). The effect of wettability on three-phase relative permeability. *Transport in Porous Media*, 39(3), 347-366.
- Donaldson, E., and Alam, W. (2008). Wettability. Houston. Gulf Publishing Company.
- Dumore, J. M. (1964). Stability considerations in downward miscible displacements. *Society of Petroleum Engineers Journal*, 4(04), 356-362.
- Dumore, J. M., and Schols, R. S. (1974). Drainage capillary-pressure functions and the influence of connate water. *Society of Petroleum Engineers Journal*, 14(05), 437-444.
- Dzulkarnain, I. (2018) "Investigation of Flow Mechanisms in Gas-Assisted Gravity Drainage Process". LSU Doctoral Dissertations. 4699.
- Fatt, I., and Klikoff, W. A. (1959). Effect of fractional wettability on multiphase flow through porous media. *Journal of Petroleum Technology*, 11(10), 71-76.
- Green, D. W., and Willhite, G. P. (1998). *Enhanced oil recovery* (Vol. 6): Henry L. Doherty Memorial Fund of AIME, Society of Petroleum Engineers Richardson, TX.
- Herzberg, W. J. and Erwin, W. R. (1970). Gas-chromatographic study of the reaction of glass surfaces with dichlorodimethylsilane and chlorotrimethylsilane. *Journal of Colloid Interface Science*, 33(1), 172-177.
- Holbrook, O. C., and Bernard, G. G. (1958). Determination of wettability by dye adsorption. *Transactions of the AIME* 213, 261–264.
- Jerauld, G. R. (1997). Prudhoe Bay gas/oil relative permeability. *J SPE Reservoir Engineering*, 12(01), 66-73.
- Kalaydjian, F.-M., Vizika, O., Moulu, J.-C. et al. (1995). The role of wettability and spreading in gas injection processes under secondary conditions. Geological Society, London, Special Publications 84 (1), 63–71.
- Kalaydjian, F.-M. (1992). *Performance and analysis of three-phase capillary pressure curves for drainage and imbibition in porous media*. Paper presented at the SPE Annual Technical Conference and Exhibition.
- Kalaydjian, F.-M., Moulu, J., Vizika, O., et al. (1993, 3-6 October). *Three-phase flow in water-wet porous media: determination of gas/oil relative permeabilities under various spreading conditions*. Paper presented at the SPE Annual Technical Conference and Exhibition, Houston, Texas.
- Kantzas, A., Chatzis, I., and Dullien, F. A. L. (1988a). *Enhanced oil recovery by inert gas injection*. Paper presented at the SPE Enhanced Oil Recovery Symposium.

- Kantzas, A., Nikakhtar, B., and Pow, M. (1998b). Principles of three phase capillary pressures. *Journal of Canadian Petroleum Technology*, 37(07).
- Keller, A. A., Blunt, M. J., and Roberts, A. (1997). Micromodel observation of the role of oil layers in three-phase flow. *Transport in Porous Media*, 26(3), 277-297.
- Koottungal, L. (2008). worldwide EOR survey. *Oil and Gas Journal*, 106(15), 47.
- Leverett, M. (1941). Capillary behavior in porous solids. *Trans. AIME Petrol. Eng.*, 142(01), 152-169.
- Maeda, H., and Okatsu, K. (2008). *EOR using thin oil film drainage mechanism in water wet oil reservoir*. Paper presented at the SPE Asia Pacific Oil and Gas Conference and Exhibition.
- Mahmoud, T., and Rao, D. N. (2007). *Mechanisms and Performance Demonstration of the Gas-Assisted Gravity-Drainage Process Using Visual Models*. Paper presented at the SPE Annual Technical Conference and Exhibition.
- Melzer, L. S. (2012). Carbon dioxide enhanced oil recovery (CO<sub>2</sub> EOR): Factors involved in adding carbon capture, utilization and storage (CCUS) to enhanced oil recovery. *J Center for Climate*.
- Motealleh, S., Ashouripashaki, M., DiCarlo, D. A., et al. (2008). *Mechanisms of Meniscus Motion in Fractionally Wetted Porous Media*. Paper presented at the SPE Annual Technical Conference and Exhibition.
- Oak, M. J., Baker, L. E., and Thomas, D. C. (1990). Three-phase relative permeability of Berea sandstone. *J Pet Technol*, 42(08), 1,054-051,061.
- Oliviera, I. B., Demond, A. H., and Salehzadeh, A. (1996). Packing of sands for the production of homogeneous porous media. *Soil Science Society of America Journal*, 60(1), 49-53.
- Oren, P., Billiotte, J., and Pinczewski, W. V. (1992). Mobilization of waterflood residual oil by gas injection for water-wet conditions. *SPE Formation Evaluation*, 7(01), 70-78.
- Oren, P. and Pinczewski, W. V. (1994). The effect of wettability and spreading coefficients on the recovery of waterflood residual oil by miscible gasflooding. *SPE Formation Evaluation*, 9(02), 149-156.
- Øren, P., and Pinczewski, W. V. (1995). Fluid distribution and pore-scale displacement mechanisms in drainage dominated three-phase flow. In *Multiphase Flow in Porous Media* (pp. 105-133): Springer.

- Parker, J. C., and Lenhard, R. J. (1990). Determining three-phase permeability—saturation—pressure relations from two-phase system measurements. *Journal of Petroleum Science Engineering*, 4(1), 57-65.
- Rao, D. N., Ayirala, S. C., Kulkarni, M. M., et al. (2004). *Development of gas assisted gravity drainage (GAGD) process for improved light oil recovery*. Paper presented at the SPE/DOE Symposium on Improved Oil Recovery.
- Rao, D. N. (2001). Gas injection EOR-A new meaning in the new millennium. *Journal of Canadian Petroleum Technology*, 40(02).
- Sahni, A., Burger, J., and Blunt, M. (1998). *Measurement of three phase relative permeability during gravity drainage using CT*. Paper presented at the SPE/DOE Improved Oil Recovery Symposium.
- Salathiel, R. A. (1973). Oil recovery by surface film drainage in mixed-wettability rocks. *Journal of Petroleum Technology*, 25(10), 1,216-1,224.
- Seed, B. (2001). Silanizing glassware. *Current Protocols In Molecular Biology*, Appendix 3, 3B-3B.
- Sharma, A., and Rao, D. N. (2008). *Scaled physical model experiments to characterize the gas-assisted gravity drainage EOR process*. Paper presented at the SPE Symposium on Improved Oil Recovery.
- Soll, W. E., Celia, M. A., and Wilson, J. (1993). Micromodel studies of three-fluid porous media systems: Pore-scale processes relating to capillary pressure-saturation relationships. *Water resources research*, 29(9), 2963-2974.
- Stalder, A.F., Kulik, G., Sage, D., et al. (2006). A snake-based approach to accurate determination of both contact points and contact angles. *Colloids surfaces A: physicochemical Engineering aspects*, 286(1-3), 92-103.
- Stalder, A.F., Melchior, T., Müller, M., et al. (2010). Low-bond axisymmetric drop shape analysis for surface tension and contact angle measurements of sessile drops. *Colloids surfaces A: physicochemical Engineering aspects*, 364(1-3), 72-81.
- Stone, H. L. (1970). Probability model for estimating three-phase relative permeability. *Journal of Petroleum Technology*, 22(02), 214-218.
- Verma, M. K. (2015). *Fundamentals of carbon dioxide-enhanced oil recovery (CO<sub>2</sub>-EOR): A supporting document of the assessment methodology for hydrocarbon recovery using CO<sub>2</sub>-EOR associated with carbon sequestration*: US Department of the Interior, US Geological Survey Washington, DC.

- Vizika, O. (1993). *Effect of the spreading coefficient on the efficiency of oil recovery with gravity drainage*. In Proceeding of Symposium on Enhanced Oil Recovery, presented before Division of Petroleum Chemistry, Inc., American Chemical Society, Denver, CO.
- Vizika, O. and Lombard, J.-M. (1996). Wettability and spreading: two key parameters in oil recovery with three-phase gravity drainage. *SPE Reservoir Engineering*, 11(01), 54-60.
- Zahoor, M. K., Derahman, M., and Yunan, M. H. (2009). Wettability—interpreting the myth. *Nafta*, 60(6), 367-369.
- Zhou, D., and Blunt, M. (1998). Wettability effects in three-phase gravity drainage. *Journal of Petroleum Science Engineering*, 20(3-4), 203-211.
- Zhou, D., and Blunt, M. (1997). Effect of spreading coefficient on the distribution of light non-aqueous phase liquid in the subsurface. *Journal of Contaminant Hydrology*, 25(1), 1-19.

## **VITA**

Abdullah Al-Tameemi was born in Baghdad, Iraq in 1990. He graduated from the University of Baghdad, college of engineering, Mechanical Engineering department with a bachelor's degree in Engineering Science (2008 –2012).

He joined Schlumberger International Ltd. in (2012), he got assigned as Field Engineer Trainee in Drilling and Measurement segment in Basra (south of Iraq). In (2014) he got promoted to Maintenance Engineer (Process Eng.).

In (2016) he was granted in both Fulbright Foreign Student Program and Chevening the UK government's international award he chose Fulbright Program and joined as a Master of Science candidate in Craft & Hawkins Department of Petroleum Engineering at Louisiana State University. He is expected to graduate with a master's degree in petroleum engineering in May 2019.